ESTCP
Cost and Performance Report

(MR-201234)

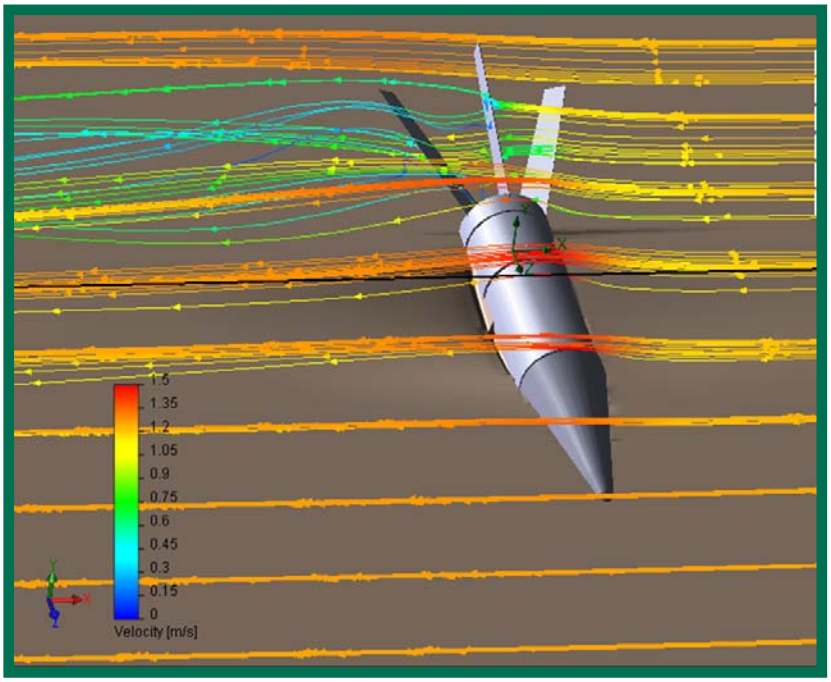

Vortex Lattice UXO Mobility Model Integration

March 2015

ENVIRONMENTAL SECURITY
TECHNOLOGY CERTIFICATION PROGRAM

U.S. Department of Defense

REPORT DOCUMENTATION PAGE

Form Approved
OMB No. 0704-0188

Public reporting burden for this collection of information is estimated to average 1 hour per response, including the time for reviewing instructions, searching existing data sources, gathering and maintaining the data needed, and completing and reviewing this collection of information. Send comments regarding this burden estimate or any other aspect of this collection of information, including suggestions for reducing this burden to Department of Defense, Washington Headquarters Services, Directorate for Information Operations and Reports (0704-0188), 1215 Jefferson Davis Highway, Suite 1204, Arlington, VA 22202-4302. Respondents should be aware that notwithstanding any other provision of law, no person shall be subject to any penalty for failing to comply with a collection of information if it does not display a currently valid OMB control number. **PLEASE DO NOT RETURN YOUR FORM TO THE ABOVE ADDRESS.**

1. REPORT DATE *(DD-MM-YYYY)*
25-02-2015

2. REPORT TYPE
Cost and Performance

3. DATES COVERED *(From - To)*
Apr 2012 – Feb 2015

4. TITLE AND SUBTITLE
Vortex Lattice UXO Mobility Model Integration

5a. CONTRACT NUMBER
W912HQ-12-C-0034

5b. GRANT NUMBER

5c. PROGRAM ELEMENT NUMBER

6. AUTHOR(S)
Jenkins, Scott A., D'Spain, Gerald L., and Wasyl, Joseph

5d. PROJECT NUMBER
MR-201234

5e. TASK NUMBER

5f. WORK UNIT NUMBER

7. PERFORMING ORGANIZATION NAME(S) AND ADDRESS(ES)
Marine Physical Laboratory, Scripps Institution Oceanography
291 Rosecrans St.
San Diego, CA 92106

8. PERFORMING ORGANIZATION REPORT NUMBER
UCSD Proposal 2011-4721 R3

9. SPONSORING / MONITORING AGENCY NAME(S) AND ADDRESS(ES)
Env. Sec. Tech. Cert. Prgm.
4800 Mark Center Dr Ste 17D08
Alexandria, VA 22350-3605

10. SPONSOR/MONITOR'S ACRONYM(S)
ESTCP

11. SPONSOR/MONITOR'S REPORT NUMBER(S)

12. DISTRIBUTION / AVAILABILITY STATEMENT
Distribution Statement A: Distribution approved for public release; distribution is unlimited.

13. SUPPLEMENTARY NOTES
none

14. ABSTRACT
The Vortex Lattice UXO Impact Mobility Model was used to predict initial impact location, burial, and orientation of UXO, and subsequent burial and migration over a 28-year period in Lake Erie Impact Areas off Camp Perry, OH. The UXO were 60 mm M49A2, 81 mm M43A1, and 106 mm M344 rounds. Impact simulations used historical range firing records, and subsequent mobility used measured wave height time series as input. Two impact types occurred, one with deep impact burials of 60-120 cm that likely prevented subsequent mobility and a second type, about 2.5% of firings, had shallow impact depths (mean 15 cm). Mobility analyses of these shallow skip-entry UXO show little movement over the 28-year period due to the fetch-limited wave heights and periods along southwest Lake Erie; mean subsequent burial depth was 27 cm, with only 4.5% becoming more than 50% exposed to allow release from burial lock-down, resulting in a mean net migration of only 15 cm. UXO have reappeared after two beach clearance efforts at Camp Perry likely because of lake water level increases and shoreline retreat. About one-quarter of shallow skip-entry rounds are predicted to become exposed over

15. SUBJECT TERMS
UXO, ballistic trajectory, impact burial, subsequent burial and migration, episodic storm/wave events, erosional zone, water level changes, shoreline retreat

16. SECURITY CLASSIFICATION OF:			17. LIMITATION OF ABSTRACT	18. NUMBER OF PAGES	19a. NAME OF RESPONSIBLE PERSON
a. REPORT	b. ABSTRACT	c. THIS PAGE			Gerald L. D'Spain
U	U	U	UU SAR	117	19b. TELEPHONE NUMBER *(include area code)* 858-534-5517

Standard Form 298 (Rev. 8-98)
Prescribed by ANSI Std. Z39.18

COST & PERFORMANCE REPORT
Project: MR-201234

TABLE OF CONTENTS

		Page
EXECUTIVE SUMMARY		1
1.0	INTRODUCTION	1
1.1	BACKGROUND	1
1.2	OBJECTIVE OF THE DEMONSTRATION	4
1.3	REGULATORY DRIVERS	6
2.0	TECHNOLOGY DESCRIPTION	7
2.1	TECHNOLOGY DEVELOPMENT	16
2.2	ADVANTAGES AND LIMITATIONS OF THE TECHNOLOGY	17
3.0	PERFORMANCE OBJECTIVES	19
4.0	SITE DESCRIPTION	21
4.1	SITE SELECTION	22
4.2	SITE HISTORY	23
4.3	SITE GEOLOGY	24
4.4	MUNITIONS CONTAMINATION	27
5.0	TEST DESIGN	31
5.1	CONCEPTUAL EXPERIMENTAL DESIGN	32
5.2	SITE PREPARATION	34
5.3	SYSTEM SPECIFICATION	35
5.4	CALIBRATION ACTIVITIES	35
5.5	VALIDATION	40
6.0	DATA ANALYSIS AND PRODUCTS	43
6.1	PREPROCESSING	45
6.2	TARGET SELECTION FOR DETECTION	52
6.3	PARAMETER ESTIMATION	53
6.4	TRAINING	53
6.5	CLASSIFICATION	54
6.6	DATA PRODUCTS	54
7.0	PERFORMANCE ASSESSMENT	67
8.0	COST ASSESSMENT	77
8.1	COST MODEL	77
8.2	COST DRIVERS	78
8.3	COST BENEFIT	81

TABLE OF CONTENTS (continued)

Page

9.0 IMPLEMENTATION ISSUES 85

10.0 REFERENCES 91

APPENDIX A POINTS OF CONTACT..... A-1
APPENDIX B HEALTH AND SAFETY PLAN B-1

LIST OF FIGURES

Page

Figure 1. ESTCP certified VORTEX UXO MM with Impact Burial Model retrofit (blue module, #12). 2
Figure 2. SCM for UXO showing the UXO MM analysis (lower left) as part of source quantification efforts (Johnson, 2002). 3
Figure 3. VORTEX UXO IMM simulation of the vortex and scour field around a 106 mm M344 round. 5
Figure 4. Mechanics of far-field burial. 9
Figure 5. Vortex lattice method. 11
Figure 6. Lattice vortex method (schematic). 12
Figure 7. Moment balance for threshold of motion condition of a UXO at rest on a sloping bottom. 14
Figure 8. The Lake Erie/Camp Perry impact range areas. 23
Figure 9. Photograph of the surface of Lake Erie taken from the University of Wyoming King Air on 25 February 2004 @ 1120 UTC. 25
Figure 10. Lake Erie ice thickness at two monitoring stations of the GLERL Great Lakes Ice Thickness Data Base, 1968-1979. 26
Figure 11. Schematic of maximum Lake Erie sheet ice and corresponding Stamukhi Zone from ice push superimposed on historic beach profile at Beach Survey Range Line #10695 on FUDS Beach, Impact Areas 1-3, Camp Perry. 27
Figure 12. 106 mm projectile on separation screen, Camp Perry UXO survey. 28
Figure 13. Examples of recovered ordnance, Camp Perry. 28
Figure 14. Shape file of M344 106 mm round on a fine sand bed used in numerical mobility model analysis. 31
Figure 15. M43A1 81mm round (left), M49A2 60 mm round (right). 32
Figure 16. Plot of density of 2,135 UXO "targets" found in 2006 magnetometer survey. 33
Figure 17. Bathymetry of western Lake Erie, OH, relative to 174.4 m mean sea level (msl). 35
Figure 18. Locations of previous studies at Lake Erie Impact Range. 36
Figure 19. UXO detected magnetically (central zone), Camp Perry. 37
Figure 20. UXO detected magnetically (east zone), Camp Perry. 38
Figure 21. UXO detected electromagnetically (large targets), Camp Perry. 38
Figure 22. UXO detected electromagnetically (small targets), Camp Perry. 39
Figure 23. Marine towed array UXO magnetometer survey, Camp Perry. 40
Figure 24. Results from the 1998 and 2006 nearshore UXO survey locations. 41
Figure 25. Grain size distribution of Lake Erie bottom sediment off Camp Perry FUDS Beach, June 1990, Range-line #10579. 45
Figure 26. Beach profile variation due to lake water level variation, Camp Perry FUDS Beach, based on low water survey at Rangeline 10579, June 1990. 46
Figure 27. Deep water wave heights (upper) and periods (lower) in western Lake Erie for entire period of record for NOAA Buoy #45005, 1980-2008. 48
Figure 28. Probability density functions of deep water wave heights (upper) and periods (lower) in western Lake Erie for entire period of record for NOAA Buoy #45005, 1980-2008. 49

LIST OF FIGURES (continued)

Page

Figure 29. Extreme event REF/DIF pattern, Camp Perry, 10 April 1998, deep water wave height = 3.58 m, period = 9.09 sec, direction = 80 degrees (true). 50
Figure 30. REF/DIF pattern due to highest 1% of Lake Erie wind waves at Camp Perry, deep water wave height = 1.5 m, period = 5 sec, direction = 45 degrees (true)..... 50
Figure 31. Historic water level variation, Lake Erie from NOAA Station 9063085, Toledo, Ohio. 52
Figure 32. Simulation of vortex and scour field from a Mode 1 simulation of the 106 mm M344 round after an oblique-skip entry mode. 55
Figure 33. Simulation of vortex and scour field from a Mode 1 simulation of the 106 mm M344 round after an oblique-skip entry mode. 56
Figure 34. Integrated ballistics/ Impact burial Vortex Lattice UXO IMM Fortran code tested end-to-end for Camp Perry Impact Areas 1, 2, and 3. 58
Figure 35. A simulation using the 6-DOF ballistics algorithms lifted from the STRIKE 35 MatLab code and transposed into Vortex Lattice UXO IMM Fortran code..... 59
Figure 36. Ballistics impact-burial simulation of a 106 mm M344 round due to javelin entry into Lake Erie clay. 60
Figure 37. Functional test of the mobility algorithms performed with the UXO IMM Fortran code for Camp Perry Impact Areas 1-3..... 60
Figure 38. UXO IMM simulation of a 106 mm M344 round entering the water column from a 60E ballistic trajectory angle with cavitation bubble (oblique-skip entry mode). 61
Figure 39a. UXO IMM simulation of a 106 mm M344 impact in Impact Area 3 as compared against known UXO target locations. 63
Figure 39b. Regression analysis of the range of trajectories from the Camp Perry firing pits to impact locations simulated by the UXO IMM versus the range distance from the firing pits to the electromagnetic contact locations discovered by the SAIC (2006) underwater magnetometer survey. 63
Figure 40. UXO IMM predicted bi-modal impact burial probability distribution for Camp Perry Impact Areas 1-3. 64
Figure 41. UXO IMM predicted spatial (range and depth) distribution of the 106 mm impacts in the Lake Erie sediment cover taken from the 2,135 simulated impact locations that give rise to the bi-modal impact burial probability distribution in Figure 40..... 65
Figure 42. UXO MM simulation of migration and burial sequence, Lake Erie, 27 March, 1998 to 05 December, 1998. 68
Figure 43. Probability density (blue) and cumulative probability (red) of UXO burial depths at Camp Perry Impact Areas 1-3 from UXO MM simulations using wave forcing, 1980-2008..... 69
Figure 44. Probability density (cyan) and cumulative probability (red) of UXO exposure at Camp Perry Impact Areas 1-3 from UXO MM simulations using wave forcing, 1980-2008..... 70

LIST OF FIGURES (continued)

Page

Figure 45. Probability density (green) and cumulative probability (red) of UXO migration distances at Camp Perry Impact Areas 1-3 from UXO IMM simulations using wave forcing, 1980-2008..... 71
Figure 46. Cumulative departure from initial impact positions for UXO in offshore Impact Areas 1-3, based on 98,613 modeled outcomes with 4,485 mobile targets using wave forcing 1980-2008..... 72
Figure 47. Regression analysis of Mode 1 versus Mode 3 predictions of UXO migration at Camp Perry, Lake Erie, OH, based on M344 106 mm rounds. 74
Figure 48. Regression analysis of Mode 2 versus Mode 3 predictions of UXO migration at Camp Perry, Lake Erie, OH, based on M344 106 mm rounds. 75
Figure 49. Regression analysis of Mode 1 versus Mode 3 predictions of UXO burial at Camp Perry, Lake Erie, OH, based on M344 106 mm rounds. 76
Figure 50. Regression analysis of Mode 1 versus Mode 3 predictions of UXO burial at Camp Perry, Lake Erie, OH, based on M344 106 mm rounds. 76
Figure 51. Beach profile change due to lake water level variation, Camp Perry FUDS Beach, based on low water survey at Range-line 10579, June 1990. 86
Figure 52. Beach Profile recession (green-dashed) computed by far-field mechanics of UXO IMM over 28 year period at Camp Perry FUDS Beach, Range-line 10579..... 87
Figure 53. Shoreline recession computed at Camp Perry (FUDS Beach) from 28 years of wave forcing (Figures 27 and 28) using far-field module of the UXO IMM. 87

LIST OF TABLES

Page

Table 1. Performance objectives. 20
Table 2. Underwater UXO Sites. 21
Table 3. Site selection scoring criteria. 22
Table 4. UXO MM far-field input parameters. 43
Table 5. UXO MM near-field input parameters. 44
Table 6. UXO MM program cost summary. 78
Table 7. Nominal cost of Mode 1 screening analysis of a single UXO site. 78
Table 8. Estimated Cost of Mode 2 detailed analysis. 80
Table 9. Mode 3 Enhanced Analysis Cost Estimate. 81

ACRONYMS AND ABBREVIATIONS

3-D	three-dimensional
6-DOF	six-degree of freedom
cm	centimeter
CNO	Chief of Naval Operations
dem/val	demonstration/validation
EM	electromagnetic
EOD	Explosive Ordnance Disposal
ESTCP	Environmental Security Technology Certification Program
FRF	Field Research Facility
FUDS	Formerly Used Defense Site
GLERL	Great Lakes Environmental Research Laboratory
IMM	Impact/Mobility Model
km	kilometer
kPa	kilopascal
LIDAR	Light Detection and Ranging
LWD	International Great Lakes Low Water Datum, LWD = 174 m MSL
m	meter
MBES	Mine Burial Expert System
mm	millimeter
MM	mobility model
msl	mean sea level
NAD	Navy Ammunition Depot
NAVFAC	Naval Facilities Engineering Command
NAVFAC ESC	Naval Facilities Engineering Center
NAWC/WD	Naval Air Warfare Center, Weapons Division
NESDI	Navy Environmental Sustainability Development to Integration
NFESC	Naval Facilities Engineering Service Center
NGDC	National Geophysical Data Center
NOAA	National Oceanographic and Atmospheric Administration
NOS	National Ocean Survey
NWS	Naval Weapons Station
ONR	Office of Naval Research

PMRF	Pacific Missile Range Facility
REF/DIF	refraction/diffraction
ROI	return on investment
ROV	remotely operated vehicle
SAIC	Science Applications International Corporation
SST	Sound and Sea Technology
UnMES	Underwater Munitions Expert System
USACE	U.S. Army Corps of Engineers
USAESCH	U.S. Army Engineering and Support Center
USGS	United States Geological Survey
USEPA	United States Environmental Protection Agency
UXO	unexploded ordnance
UXO IMM	UXO Impact Mobility Model
UXO MM	UXO Mobility Model
VORTEX	Vortex Lattice Model
WES	Waterways Experiment Station

ACKNOWLEDGEMENTS

The work discussed in this cost and performance report builds on extensive previous work in model development and field validation. In 2003, the Naval Facilities Engineering Service Center (NAVFAC ESC) Point Hueneme began a Unexploded Ordnance (UXO) Mobility Model program effort that leveraged model development started under the Office of Naval Research's (ONR) Mine Burial Program. NAVFAC ESC proceeded to fund new algorithm development for the Vortex Lattice Model (one of three models to emerge from the Mine Burial Program) and the new software was called the UXO Mobility Model (UXO MM). The UXO MM was developed under the Chief of Naval Operations (CNO) Navy Environmental Sustainability Development to Integration (NESDI) program. The NESDI program is managed for CNO-N45 by the Naval Facilities Engineering Command (NAVFAC).

Subsequently, NAVFAC ESC was awarded a 3-year project by the Environmental Security Technology Certification Program (ESTCP) called "The Unexploded Ordnance (UXO) Mobility Model Demonstration/Validation Program" (DeVisser, 2004). Ms. Barbara Sugiyama and Ms. Alexandra DeVisser, with NAVFAC ESC, were the co-principal investigators for this effort with support from Sound and Sea Technology, Inc. (SST). The SST program was led by Mr. Jeffrey Wilson. The UXO MM was developed by Dr. Scott Jenkins and Mr. Joe Wasyl of the Scripps Institution of Oceanography. The model was tested and evaluated by Mr. Dennis Garrood, Mrs. Chanda Daly, and Mr. Eugene Keam of SST. The model was subsequently upgraded for reef-range environments under ESTCP Project MR-201003.

Technical material contained in this report has been approved for public release.
Mention of trade names or commercial products in this report is for informational purposes only;
no endorsement or recommendation is implied.

This page left blank intentionally.

EXECUTIVE SUMMARY

The overall conclusion from this project is that for those sites containing unexploded ordnance (UXO) that meet certain environmental conditions, the UXO presently underwater will remain underwater and, therefore, will not pose a threat to future land-based activities. In addition, the UXO presently buried in unconsolidated bottom sediments will remain buried in many cases. Therefore, no remedial action needs to be taken in these situations; rather, environmental conditions should be monitored over time to verify that no changes that might lead to underwater sediment removal or erosion occur. At these sites, the only UXO of potential concern are those objects residing in intrinsically erosional areas, typically the land/sea interface (shore-zone), where they may become uncovered in the future. Therefore, any future remedial actions at these types of UXO sites need only include land-based methods.

The conclusion of this project differs from the conclusions of the Strategic Environmental Research and Development Program (SERDP)/Office of Naval Research (ONR)-sponsored Workshop on Acoustic Detection and Classification of UXO in the Underwater Environment in July 2013. An important distinction between the mine countermeasure and UXO problems is that buried UXO pose no danger until uncovered, in contrast to the threat posed by buried mines. Therefore, only underwater UXO that is exposed (including UXO that was formerly buried) needs to be regularly monitored, particularly after major storms and other significant erosional events. Surveys for buried UXO only need to be conducted if dredging and/or offshore construction projects are to be undertaken in the area.

The Vortex Lattice (VORTEX) UXO Impact Mobility Model (UXO IMM) was used to predict migration and burial behavior of UXO rounds in Lake Erie impact areas off Camp Perry, OH. The UXO rounds considered include: 60 millimeter (mm) M49A2, 81 mm M43A1, and 106 mm M344 rounds (Figures 1a and b). Trajectories and impact burials were re-constructed by the UXO IMM from historical range firing records that provided: date, firing pit (firing location), weapon type, ammunition type, number of rounds fired, and azimuth and inclination angles for each firing. Range distances from firing pits to 2,135 electromagnetic contacts identified as UXO by the 2006 magnetometer surveys by Science Applications International Corporation (SAIC) (2006) were reproduced by UXO IMM impact simulations from firing logs, with a coefficient of determination of R-squared = 0.868.

The ballistic impact simulations identified two basic types of impact that produce significantly different impact burial characteristics and round orientation. These differences result from the obliquity of the ballistic trajectory as the round enters the water column. The project team refers to these as “javelin entry mode” and the “oblique-skip entry mode.” The impact burial probability distribution was found to be bi-modal, with the majority being deep impacts on the order of 60 centimeters (cm) to 120 cm resulting from high apex trajectories with javelin water entry modes. The UXO rounds associated with these deep impacts are likely not subject to subsequent mobility due to the fetch limited wave heights and wave periods along the southwest shores of Lake Erie. However, a smaller peak in the bi-modal impact distribution is attributable to shallow impacts associated with oblique trajectories and oblique-skip water entries. These shallow impacts (burial depths about 15 cm) amount to 2.53% of the firings in the Camp Perry firing logs, and account for

about 98,613 of the UXO targets in Impact Areas 1-3. Due to these shallow burial depths, the targets from oblique skip entries become the focus of our subsequent UXO mobility analysis.

The subsequent mobility analysis was performed to answer two questions posed by the ESTCP review panel at the spring 2013 In-Progress Review: 1) For projectiles deposited in Lake Erie in a variety of initial conditions (fully buried on impact, partially buried, on the surface); "How many years does it take for the effects of the initial conditions to be washed out?;" and 2) "Does the position and orientation of the projectiles only become randomized during severe storms or are the normal seasonal weather patterns sufficient?"

The skill factor, R, predicted by the UXO IMM at Camp Perry was calculated at $R_h = 0.86$ for impact burial and $R_> = 0.95$ for subsequent migration. Ninety-seven percent of 98,613 modeled daily outcomes of shallow oblique-skip impacts predicted fully buried UXO during some portion of the 28-year long simulation period. Thirty-nine percent (%) of the modeled outcomes predicted subsequent burial depths (burial occurring after impact) in the range of 5 cm to 24 cm, which was the range observed in the U.S. Army Corps of Engineers (USACE) ordnance migration field tests conducted at Camp Perry Formerly Used Defense Site (FUDS) Beach in 2001-2003. The mean depth of subsequent burial from model predictions was found to be 27 cm and the maximum subsequent burial depth was calculated at 79 cm. Any UXO buried deeper than 79 cm are not subjected to dynamic burial and exposure, and remain permanently entombed below the variable beach profile critical mass as a consequence of impact burial.

Exposure is a critical mechanism in the UXO mobility problem, as only those rounds that become sufficiently exposed to be released from burial lock-down are subject to migration. Exposure consequently sets an upper bound on the quantifiable risk assessment. The project team found that 98.6% of the shallow oblique-skip impacts of UXO in the offshore impact areas at Camp Perry (or about 97,000 rounds) will exhibit some degree of exposure during some portion of the 28-year simulation period. However, the UXO IMM calculations show that only 4.5% of the shallow oblique-skip impacts of UXO will become sufficiently exposed (more than 50% exposed) to be released from burial lock-down and have a potential to move. This result means that out of 3.9 million buried UXO rounds in the three offshore impact areas at Camp Perry, of which 98,613 UXO are shallow impacts due to oblique-skip entries, only 4,485 UXO rounds have the potential to migrate from their point of impact due to storms and lake water level changes nearly all of those are in the erosional nearshore area between the beach and the -3.35 meters (m) International Great Lakes Low Water Datum (LWD) depth contour (extending about 700 m offshore of the beach berm). Moreover, only 1% of shallow impacts (about 1000 rounds) will become exposed 80% or more, and thus, have likelihood of significant gross movement.

The project team found that 70% of the 4,485 exposed UXO will move less than 19 cm over a 28 year period. In fact, the mean net migration distance is only 15 cm. Only 10% of the exposed UXO (about 450 rounds) move a net distance of 0.5 m, and only 5% (about 225 rounds) exhibit a net movement of more than 1 m away from their point of impact; 0.1% (5 rounds) have a net migration of 2.9 m or more, while the largest net movement of any of the 4,485 exposed rounds was 3.7 m. These results are consistent with the 2001-2003 ordnance migration studies at Camp Perry conducted by the USACE.

The charge questions above were answered by tracking the gross movement over time of the 4,485 UXO in the Camp Perry Impact Areas 1-3 that are sufficiently exposed (50% exposed or more) to be released from burial lockdown. The metric used for gross movement is the cumulative departure from initial impact position due to subsequent migration. The project team found that the combined gross movement of the 4,485 potentially mobile UXO is 2700 m to 3000 m over a 28 year period of wave forcing, or an average gross movement of 0.6 m to 0.66 m for each mobile target. Thus, the UXO do not appear to be very mobile in the near-shore of Camp Perry. However, of greater importance to the long term monitoring of this site is the time response of the cumulative residual calculation. It shows that gross movement of UXO in the offshore waters of Impact Areas 1-3 is episodic, occurring in response to a handful of large storm wave events (six severe weather events over 28 years) and is not continuous or gradual in response to seasonal changes. The cumulative residual calculation also shows that very little gross movement of the UXO occurs after 9,000 to 10,000 days, and consequently the UXO field can be considered stable after periods of time on the order of 25 to 30 years. If this is so, then why, after two separate beach clearance efforts at Camp Perry, are UXO reappearing in the cleared areas? This project team submits that two large scale mechanisms in the western basin of Lake Erie and the Toussaint River/FUDS Beach Littoral Cell cause UXO to reappear in cleared areas. These large scale mechanisms involve lake water level variations and shoreline retreat.

Lake Erie water levels change slowly over seasonal and multi-decadal cycles (varying as much as 2 m over the past 100 years). Wave action superimposed on a persistent high water level can cause the equilibrium beach profile to re-adjust both upward and landward. Such broad scale changes in the equilibrium beach profiles (in response to high lake water levels) will dig up some of the more deeply impacted UXO in regions of the beach and shoreline that normally (or only rarely) do not erode. Hence, the UXO did not reappear by moving upslope and onto the beach from offshore, but rather, they were always there, just out of sight, buried in portions of the sediment cover that were outside of the critical mass at lower lake water levels.

The second explanation for the reappearance of UXO on FUDS Beach at Camp Perry is somewhat similar to the high water level theory, but involves long term shoreline retreat. It is an historic fact that the shoreline south east of the Toussaint River has been progressively retreating landward since at least 1877. The shoreline retreats because of the wave shoaling pattern set up by the sheltering effects of the Catawaba and Bass Island complexes to the northeast. This shoaling pattern causes wave-driven longshore currents flowing away from FUDS Beach towards the south east to be stronger than those flowing towards the beach from the Toussaint River to the northwest, resulting in a net outflow of littoral sediment from the beach. That net outflow of beach sand causes the equilibrium beach profile to retreat landward. While the beach profile retreats landward, the critical mass progressively grows at an average annual rate of dV_c/dt = 19.6 m^3 per meter of beach per year. A UXO population density of 1 round per 100 m^3, implies that progressive shoreline recession at Camp Perry will expose about 1 new round every 5 years per meter of beach. Along the 5 kilometer (km) reach of FUDS Beach, shoreline recession would expose about 980 rounds per year (both above and below the waterline), or about 27,000 rounds over the entire 28 year-long simulation. Thus, about one-quarter of the 98,613 rounds predicted to become exposed in 28 years by the UXO IMM simulation are due to shoreline retreat. The fundamental distinction here, however, is that shoreline retreat is progressive, not episodic like extreme storm events or lake water level variation and not periodic like seasonal beach profile variation. Therefore, those 980

rounds per year exposed by shoreline retreat are new rounds, not previously subjected to visual detection or beach clean-up. That number will continue to grow over time until shoreline recession exhumes all of the deepest impact burials

OBJECTIVE OF THE DEMONSTRATION

There were two primary technical objectives for this project: 1) integrate a ballistics impact model after Chu and Ray, (2006), Hale, (2009) and Chu et. al., (2010) with the presently configured VORTEX UXO Mobility Model (MM), and subsequently validate with UXO survey data; and 2) use the integrated MM (referred to as UXO MM) to answer two charge questions posed by the ESTCP review panel at the spring 2013 IPR:

1. For projectiles deposited in Lake Eire in a variety of initial conditions (fully buried on impact, partially buried, on the surface), how many years does it take for the effects of the initial conditions to be washed out?
2. Does the position and orientation of the projectiles only become randomized during severe storms or are the normal seasonal weather patterns sufficient?

These primary objectives were met.

TECHNOLOGY DESCRIPTION

The UXO MM is a processes-based model that uses VORTEX computational methods to generate three-dimensional (3-D) simulations of subsequent burial, exposure and migration of complex UXO shapes. In these simulations, the model accounts for effects of large scale erosion or accretion of the seabed (far-field processes) and fine scale vortex shedding, scour and bedform evolution around the UXO shape (nearfield processes). Farfield processes are those that alter the seabed elevation over length scales that are comparatively large with respect to the size of an individual UXO round. Nearfield processes are due to the flow disturbance caused by the UXO and affect the seabed elevation by local scour as well as induce hydrodynamic forces that cause the UXO to move. The present MM software was validated in two ESTCP funded field tests, where it correctly predicted all the basic behaviors of UXO test surrogates with high quantitative predictive skill factors.

The ballistic impact burial model that was embedded into the MM architecture (Figure 1, Module #12) is STRIKE35, a six-degree of freedom (6-DOF) ballistics model developed by Chu, et. al., 2010. STRIKE35 is a derivative of the Navy's well proven mine impact burial model IMPACT35 (Chu and Fan, 2007). STRIKE35 is written in MatLab and was transposed to FORTRAN and integrated in the MM flow chart as a separate module designated #12 in Figure 1 to result in the integrated UXO MM. STRIKE35 has physics for the three basic processes of impact burial mechanics: 1) aerodynamic trajectory through the atmosphere after Hume (2007) and Hale (2009); 2) impact with the air-water interface after Chu and Ray (2006); 3) free-fall through the water column after Chu and Ray (2006); and 4) impact with a sedimentary seabed after Chu and Fan (2007). The computational sequence proceeds round by round and the model output includes both depth of impact burial and orientation of the round on impact with the seabed.

STRIKE 35 was validated during controlled impact studies in two test ponds at the Naval Air Warefare Center, Weapons Division (NAWC/WD), Indian Wells, CA (Chu et. al., 2010). STRIKE35 is an evolution from the mine impact burial model IMPACT35 that was validated during ONR's Mine Burial Program (Chu and Fan, 2007). The MBES (predecessor expert system to the Underwater Munitions Expert System [UnMES]) was validated during ONR's Mine Burial Program, Rennie et al. (2007).

DEMONSTRATION RESULTS

From the Camp Perry firing logs, the likely range activity gives an estimate that 3.9 million UXO targets have impacted the offshore regions of Impact Areas 1-3. Direct comparisons of UXO "targets" found by underwater magnetometer survey conducted by SAIC (2006) versus an UXO IMM simulated impacts were good, with a coefficient of determination for range distance to impact of R-squared = 0.868 out to distances of 12 km from the firing pits; and a skill factors, R_h, calculated at $R_h = 0.86$ for impact burial. In the main range fan, 92% of the targets checked by the SAIC divers were actually UXO, while the remaining 8% were other metal objects. The size of the UXO varies from small caliber bullets to as large as the 106 mm rounds. There also was at least one 250 lb bomb found near West Sister Island, but by far the dominant UXO types are the Army 106 mm M344 round artillery shells, the 60mm M49A2, and 81 mm M43A1 mortars. A probability distribution of the impact burial depth of these 1.3 million impacts simulated from the firing logs, is clearly bi-model, with the majority being deep impacts on the order of 60 cm to 120 cm resulting from high apex trajectories with javelin entry modes. The UXO rounds associated with these deep impacts are likely not subject to subsequent mobility due to the fetch limited wave heights and wave periods along the south west shores of Lake Erie. However, the smaller peak in the bi-modal distribution is attributable to shallow impacts associated with oblique trajectories and oblique skip entries. These shallow impacts (burial depths ~ 15 cm) amount to 2.53 % of the firings in the Camp Perry firing logs, and account for about 98,613 of the UXO targets in Impact Areas 1-3. Due to these shallow burial depths, 98.6% of targets from oblique skip entries become exposed (97,000 exposed rounds); and these UXO become the focus of our UXO mobility analysis.

During 28-year UXO IMM simulations, only 4,485 UXO rounds become exposed more than 50% and subsequently have the potential to migrate from their point of impact due to natural causes; nearly all of those rounds are in a near-shore area between the beach berm and the -3.35 m LWD depth contour (extending offshore about 700 m away from the beach berm). While the net movement of these mobile UXO is small, ranging from tens of centimeters to several meters, the gross movement can be large, as much as several thousand meters. If the shorezone off Camp Perry were to remain stable, it might take as long as 25 years for these mobile UXO to reach a final steady state distribution. However, the shorezone is not stable and has historically been erosional with progressive shoreline retreat. It is this long term erosional trend that threatens to expose UXO along the shoreline for the indefinite future, where human interaction may become problematic.

IMPLEMENTATION ISSUES

The UXO IMM is extremely data intensive with its input and gridding requirements, and requires relatively long run times for any given UXO scenario involving a particular munitions type, initial burial state, bottom type and environmental forcing. Regardless, the successful implementation of this model at Camp Perry, OH, revealed several important issues that may require further use of

this model at this site in the event of occurrence of another extreme event Lake Erie storm. Presently, about one-quarter of the 97,000 rounds predicted to become exposed in 28 years by the UXO IMM simulation are due to shoreline retreat. The fundamental distinction here, however, is that shoreline retreat is progressive, not episodic like extreme storm events or lake water level variation, and not periodic like seasonal beach profile variation. Consequently, an average of about 980 rounds per year could be exposed by shoreline retreat, and these are new rounds, not previously subject to visual detection or beach clean-up. That number will continue to grow over time until shoreline recession exhumes all of the deepest nearshore and beach dune impact burials off FUDS Beach at Camp Perry. This finding indicates that future UXO surveys and monitoring efforts should focus on the erosional nearshore zone, beginning on the barrier dune where land-based detection assets can be used, and extending offshore to the -4 m LWD depth contour where high resolution electromagnetic and acoustic detection systems. Offshore of this erosional nearshore region, the UXO field is stable and the majority of UXO will remain permanently entombed their initial ballistic impacts.

1.0 INTRODUCTION

Knowledge of the process and time scales for the scour, burial, re-exposure, migration and subsequent re-burial of unexploded ordnance (UXO) that remain in and on the seafloor in coastal environments are key to the planning of the future use of these sites, including possible remediation. Because these processes are intrinsically chaotic, predictions of the fate and transport of a broad-field UXO population are extremely sensitive to the initial state of that population, specifically: the numbers of UXO per cubic meter of seabed sediments, the distribution in the depth of impact burial, and the initial horizontal distribution of the UXO population. We address predictive uncertainties related to not knowing the initial population state of the UXO by integrating an existing ballistics impact burial model with the ESTCP funded Vortex Lattice (VORTEX) UXO Mobility Model (UXO MM) (see Figure 1) in order to compute the initial state of the UXO population based on range firing records. The integrated UXO Impact/Mobility Model (UXO IMM) was validated using the range firing records from Camp Perry, Ohio, as inputs along with the results of six separate UXO survey and target recovery efforts between 1992 and 2006, as ground truth for the resulting UXO IMM fate assessment predictions.

The UXO MM is a processes-based software model that uses VORTEX computational methods to generate three-dimensional (3-D) simulations of subsequent burial, exposure, and migration of complex UXO shapes (Figure 1). These simulations account for effects of large scale erosion or accretion of the seabed (far-field processes) and fine scale vortex shedding, scour and bedform evolution around the UXO shape (near-field processes).

1.1 BACKGROUND

In January 2002, the Navy, through its Pollution Abatement Ashore Program (now referred to as the Navy Environmental Sustainability Development to Integration Program [NESDI]), published a study "Environmental effects of underwater ordnance" (Johnson et al., 2002). A site conceptual model (SCM) was developed under this program and is shown schematically in Figure 2. After evaluating the SCM against existing scientific data and models, various data gaps were identified. One of these data gaps was the inability to predict the mobility and burial of UXO underwater. To meet this need, the Naval Facilities Engineering Service Center (NAVFAC ESC) Point Hueneme began a UXO MM program effort that was based on the schematic outlined in dark blue on the lower left side of Figure 2. The initial focus of this effort was to explore the feasibility of leveraging model development begun under the Office of Naval Research's (ONR) Mine Burial Program. In October 2002, Professor Douglas Inman and Dr. Scott Jenkins gave a briefing at NAVFAC ESC Point Hueneme, Code ESC51, on the VORTEX Mine Burial Model, one of three predictive models being developed and field validated under the Mine Burial Program (Inman and Jenkins, 2002; Jenkins and Inman, 2002; Jenkins et al., 2007). The other two were a simple rational parameterized model formulated by Professor Carl T. Friedrichs, Virginia Institute of Marine Science (Friedrichs, 2001 and 2007; Richardson et al., 2004; Elmore et al., 2005; Trembalis et al., 2007) and a probabilistic Mine Burial Expert System (MBES) being developed by Dr. Alan Brandt and Dr. Sarah E. Rennie at Johns Hopkins University Applied Physics Laboratory (Rennie and Brandt, 2002; Rennie et al., 2007; Almquist et al., 2007).

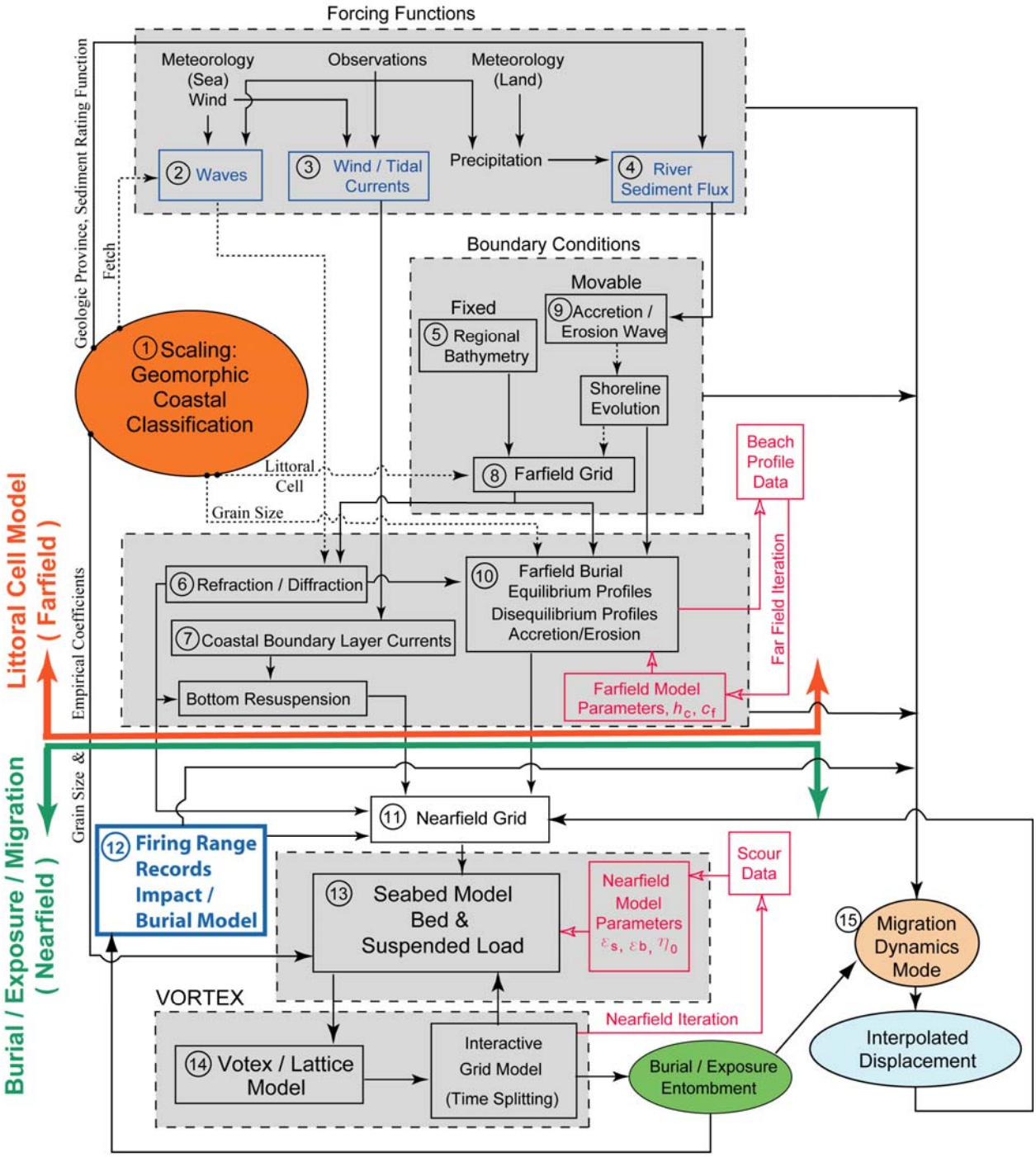

Figure 1. ESTCP certified VORTEX UXO MM with Impact Burial Model retrofit (blue module, #12).

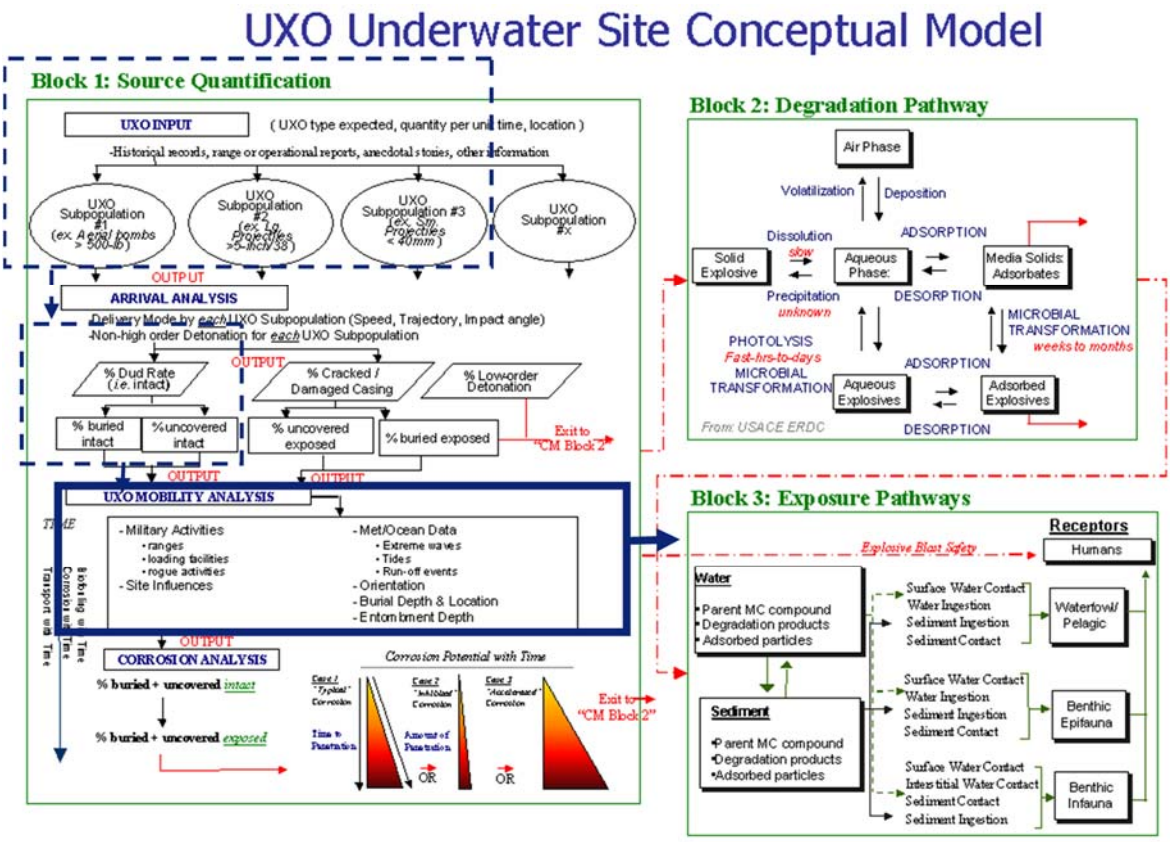

Figure 2. SCM for UXO showing the UXO MM analysis (lower left) as part of source quantification efforts (Johnson, 2002).

While the mine burial models were well advanced in predicting the scour and burial processes and the general vertical movement of mines on a sedimentary seabed, there were a number of aspects of underwater UXO behaviors that these models could not account for, notably UXO mobility associated with horizontal displacement of the UXO target. In addition, the prediction of UXO mobility often begins with an initial state of complete burial due to high velocity ballistic impact, in contrast to the mine burial prediction problem that generally begins with an initial state of partial burial due to relatively low velocity impacts with the seabed during the mine planting operations. Many UXO targets are considerably smaller and lighter than mines with tapered and often complex shapes due to fragmentation of the UXO round on impact. Therefore, it was apparent at the outset that evolving a UXO MM from the existing mine burial models would require additional algorithm development and validation. NAVFAC ESC proceeded to fund new algorithm development for the VORTEX and the new software was called the UXO MM. The UXO MM was developed under the Chief of Naval Operations (CNO) NESDI program. The NESDI program is managed for CNO-N45 by the Naval Facilities Engineering Command (NAVFAC).

The UXO MM was initially field validated using 20 millimeter (mm) UXO surrogates at Point Mugu, CA (Wilson, 2004) and 5”/38 naval round surrogates at Pacific Beach, WA (Wilson and Jenkins, 2005). Subsequently, NAVFAC ESC was awarded a 3-year project by the ESTCP called “The Unexploded Ordnance (UXO) Mobility Model Demonstration/Validation Program” (DeVisser, 2004). This program was managed by Ms. Barbara Sugiyama and Ms. Alex DeVisser, of NAVFAC ESC, with support from Sound and Sea Technology, Inc. (SST). The SST effort was

lead by Mr. Jeffrey Wilson. The ESTCP funded certification program developed a detailed software User's Manual for the UXO MM (Garood, 2008) and attempted to test the UXO MM in a greater range of coastal environments than had been attempted previously, and environments that were specifically selected to be proxies for known UXO sites.

Recently, under ESTCP Project MR-201003, UXO MM software was up-graded to allow the model to predict UXO migration and burial in reef environments without reliance on dense Light Detection and Ranging (LIDAR) bathymetric grids that limit the model's computational domain. This revised model software was built on the concept of interconnected geomorphic control cells consisting of a reef platform bounded by awa channels, which when assembled together, form a digital representation of the fringing reef system around an island.

1.2 OBJECTIVE OF THE DEMONSTRATION

This project had two primary technical objectives. The first objective was to integrate a ballistic impact model after Chu and Ray (2006), Hale (2009), and Chu et al. (2010) with the presently ESTCP certified VORTEX UXO MM. The integration involved adding a new module labeled #12 in Figure 1 to the existing UXO MM architecture. Whereas present UXO MM simulations and predictions are based on an assumption of a prone initial state of the UXO round as in Figure 3 upper, the addition of ballistic impact burial physics to the model allows the initial state to be quantified in terms of the depth of impact burial, orientation of the round and the overall population density and distribution when combined with inputs from firing range records (types and numbers of rounds, firing angles, dates, etc). In this project, it was hypothesized that the ballistic impact burial algorithms will remove considerable uncertainty from the UXO MM predictions because the governing processes of scour, burial, re-exposure, migration, and subsequent re-burial are intrinsically chaotic; therefore, they are sensitive to the initial state condition. This point is demonstrated by Figure 3 (lower) where considerable differences can be noticed relative to Figure 3 (upper) in the vortex scour field around a UXO round that is in an initial state more representative of a ballistic impact with the seabed.

The second technical objective was to subject the integrated UXO IMM to a demonstration/validation (Dem/Val) exercise, using UXO ground truth data from six separate UXO survey and target recovery efforts between 1992 and 2006 from the three offshore impact ranges at Camp Perry, on Lake Erie, OH. (Camp Perry is probably the best understood and most data rich of all live underwater UXO sites). By comparing the results of this Dem/Val exercise to the results of a previous Dem/Val of the UXO MM at Camp Perry that were based on assumptions of a uniform distribution of UXO in the prone position (Wilson et al., 2008e), the project team was able to quantify the sensitivity of UXO fate and transport assessments to the initial state assumption.

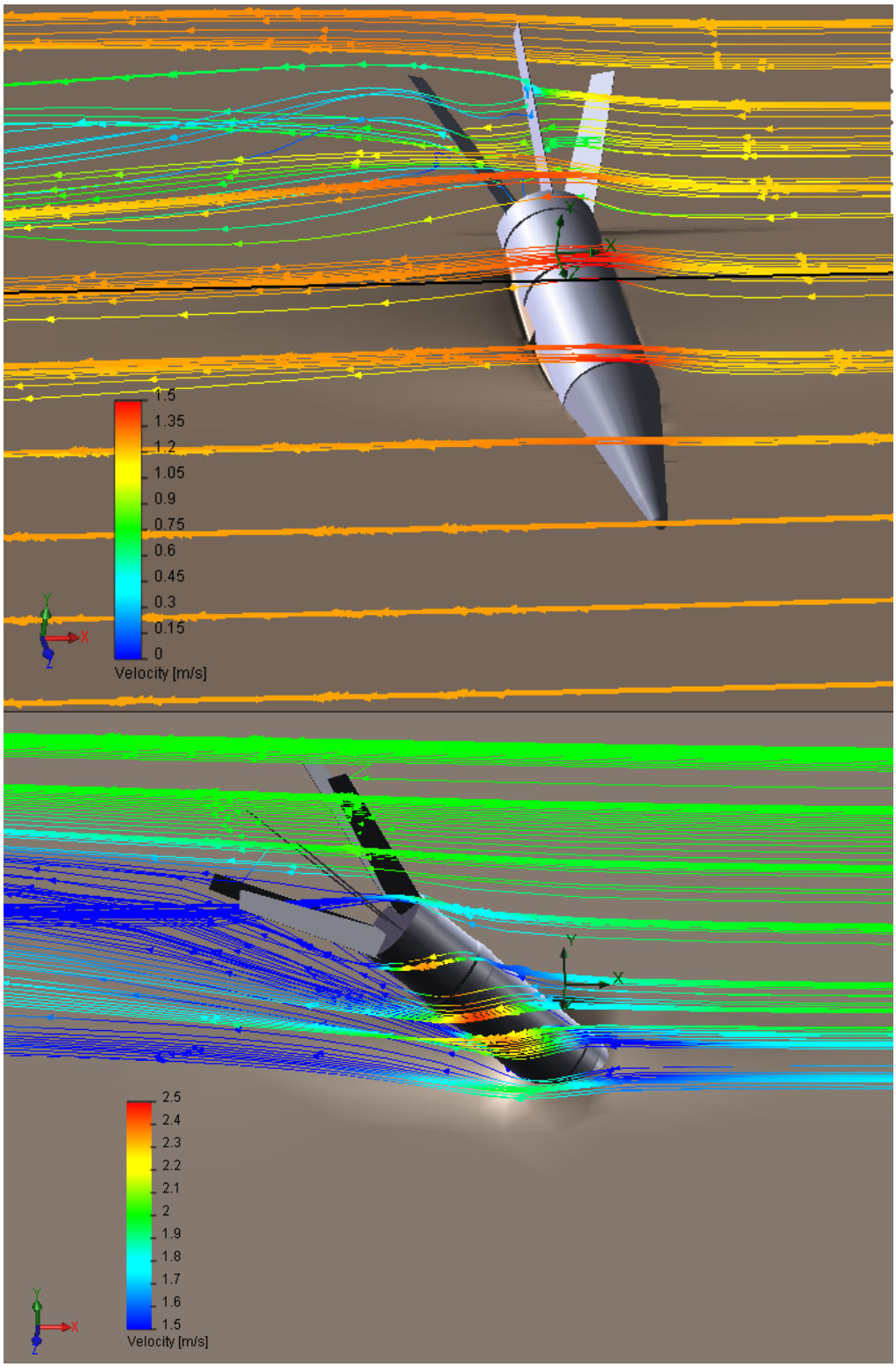

Figure 3. VORTEX UXO IMM simulation of the vortex and scour field around a 106 mm M344 round.

Upper: lying proud on the bottom, buried 52% in a medium-coarse sand bottom under a wave crest propagating from right to left. Lower: impacted obliquely in a medium-coarse sand bottom under a wave crest propagating from right to left.

1.3 REGULATORY DRIVERS

Navy requirements: 1.I.2.b *Improved Marine Sediment/Dredge Spoil Remediation and Decontamination*; 1.I.1.g *Improved Methods for Removal of Unexploded Ordnance (UXO);* and 1.III.2.n *Improved Characterization and Monitoring Techniques for Sediments*.

Army requirements: A(1.6.a) *Unexploded Ordnance (UXO) Screening, Detection and Discrimination*, and A(1.6.b) *Soil/Sediment Unexploded Ordnance (UXO) Neutralization/ Removal/Remediation*.

2.0 TECHNOLOGY DESCRIPTION

The UXO MM is a processes-based model that uses vortex lattice computational methods to generate 3-D simulations of subsequent burial, exposure, and migration of complex UXO shapes. It accounts for effects of large scale erosion or accretion of the seabed (far-field processes) and fine scale vortex shedding, scour and bedform evolution around the UXO shape (near-field processes). Far-field processes are those that alter the seabed elevation over length scales that are comparatively large with respect to the size of an individual UXO round. Near-field processes are due to the flow disturbance caused by the UXO and affect the seabed elevation by local scour as well as induce hydrodynamic forces that cause the UXO to move. The present UXO MM software was validated in two ESTCP funded field tests, where it correctly predicted all the basic behaviors of UXO test surrogates with high quantitative predictive skill factors.

Migration and burial processes consist of two distinct types: near field and far field (Jenkins et al., 2007). These processes operate on significantly different length and time scales. Near-field processes occur over length scales, the order of the body dimensions, and on time scales of a wave period, primarily governed by scour mechanics. In contrast, far-field processes involve changes in the elevation of the seabed with cross-shore distances of hundreds of meters that may extend along the coast for kilometers. Far-field time scales are typically seasonal with longer periods due to variations in climate and travel time of longshore sediment fluxes associated with accretion/erosion waves. These processes are coupled together in an architecture diagrammed by the flow chart shown in Figure 1 and referred to as the *Vortex Lattice (VORTEX) Scour and Burial Model* (Jenkins et al., 2007). The far-field processes and inputs are found above the orange line in Figure 1 while the near-field processes and inputs are below the green line.

As with any boundary value problem, the solution follows from specifying initial conditions, forcing functions, and boundary conditions, from which the response is computed using a set of process-based algorithms. This computational sequence proceeds in Figure 1 from the top down, with the set of forcing functions and initial conditions bundled together in a *module* shown by the pink shaded box at the top of the flow chart, while boundary conditions (beige box) and response (blue box) modules of the far field are found in the pathways below that. The far-field response modules are upstream of the near-field modules in the computational flow chart because the far-field processes determine the fluid forcing and elevation of the sand bed around the object, essential to specifying the near-field boundary value problem.

Far-field processes can cause buried UXOs to become exhumed, rendering them mobile to subsequent migration and re-burial. These processes provide the broad-scale forcing leading to the general bed erosion that exhumes buried UXO and can also cause general bed accretion, insuring perpetual entombment of buried UXO or accelerating the subsequent burial of exhumed UXO. These far-field processes involve changes in the elevation of the seabed with cross-shore distances of hundreds of meters that may extend along the coast for kilometers. The domain of such regional scale variation is the littoral cell. Far-field time scales are typically seasonal with longer periods due to variations in climate. Far-field exhumation and burial mechanics are associated with large scale processes including changes in beach profile, deposition from rivers, sediment loss by turbidity currents, and bottom modification by ice push. These processes vary with many time scales, including diurnal oscillations associated with tides and sea breeze; inter-annual oscillations

associated with summer/winter seasonal change; multi-annual variability associated with short-term global climate oscillations such as the El Nino-Southern Oscillation; and multi-decadal differences due to long term climate variability associated with the Pacific Decadal and North Atlantic Oscillations. Because the far-field processes determine the elevation and slope of the seabed on which the near-field processes operate, the far field exerts a controlling influence on the near field. Hence, far-field processes form the basis of the model and are shown as the top half of the UXO MM architecture in Figure 1.

Far-field processes are controlled by the balance between the amount of sediment entering the far field and the amount leaving it. This balance, known as the sediment budget, requires the identification of sediment sources and sinks, which will vary with the type of coastline. Some basic types of coastlines have been identified. The Geomorphic Coastal Classification module in Figure 1 (highlighted in red) is used to select the relative scaling and assigns the sediment sources and sinks to which a particular UXO site belongs. The classification includes three general tectonic types of coasts with their morphologic equivalents and two types associated with latitudinal extremes: 1) collision coasts with narrow shelves and steep coastal topography resulting from collisions between two or more tectonic plates; 2) trailing edge coasts that are on the stable, passive margins of continents with broad shelves and low inland relief; 3) marginal sea coasts that are semi-enclosed by island arcs and thereby fetch limited; and 4) biogenic coasts that are formed by fringing coral reefs or mangroves.

Although the relative importance of transport processes varies among coastal type, two processes are always important to UXO exhumation and burial. These are seasonal changes in the beach profile (Figure 4a) and fluxes of sediment into and out of the UXO environment by accretion/erosion waves.

The forcing functions that drive the far field processes are developed by the module indicated by the pink box in Figure 1, and provide time series of waves (#2), currents (#3) and sediment flux (#4). Waves and currents are derived from direct observations from Datawell directional wave buoys and Acoustic Doppler Current Profilers (ADCP), to validate model velocity algorithms. Fluxes of river sediment from the Toussaint River are input as explicit boundary conditions via sediment rating curves applied to annual flow volumes that are monitored by the United States Geological Survey (USGS). The wave and current forcing provides excitation applied to the deep water boundary of the far-field computational domain. These boundaries are specified in the boundary conditions module (beige box) in Figure 1, where the far-field computational domain is assembled from a series of boundary-conforming control cells, using a combination of bathymetric data obtained from National Ocean Survey (NOS) and by the National Geophysical Data Center.

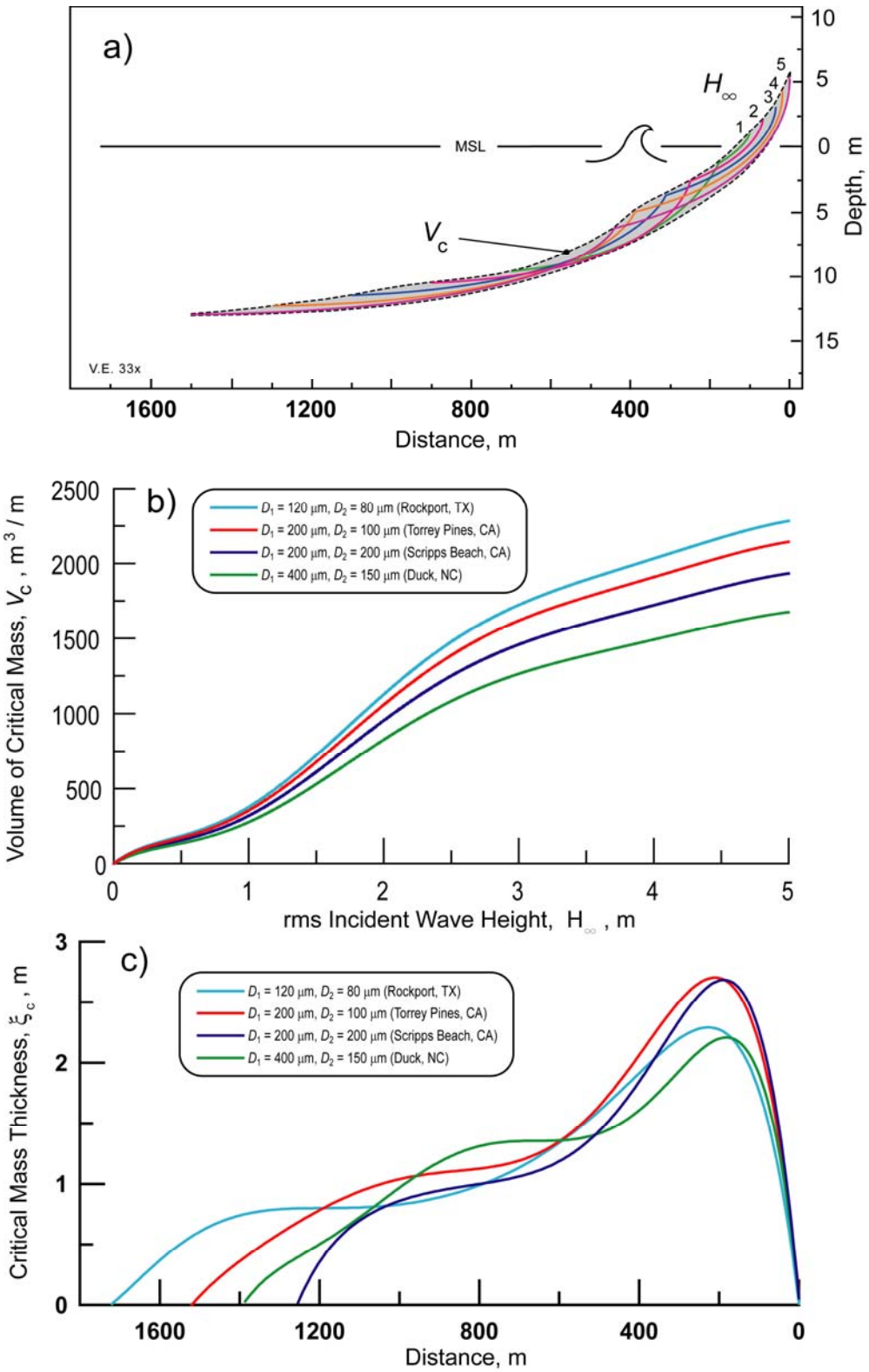

Figure 4. Mechanics of far-field burial.
a) envelope of profile change gives critical mass;
b) volume of critical mass from elliptical cycloids;
c) cross-shore variation in thickness.

With these forcing functions and boundary conditions, the far-field response module (blue box) computes the spatial and temporal evolution of the fluid forcing and bottom elevation along cross-shore profiles of a control cell representing the gross morphology of a UXO field. The bathymetry of a UXO field can be specified by profiles having three matching segments: 1) the stationary profile that extends from the deep water boundary inshore to closure depth h_c, where profile changes become vanishingly small; 2) the shore-rise profile that continues from closure depth to the wave break point; and, 3) the bar-berm profile that begins at the break point and ends at the berm crest. The stationary profile is invariant with time and is given by the regional bathymetry. Bottom elevation changes along the non-stationary profiles of the shore rise and bar-berm (Figure 4a) are computed by (#10) in the far-field response module (blue box) using equilibrium profile algorithms Jenkins and Inman (2006). The stationary and non-stationary profiles are interpolated to create a Cartesian depth grid within each control cell on which simultaneous refraction and diffraction (REF/DIF) patterns are computed by (#6) using algorithms from Kirby (1986) and Dalrymple et al. (1984 to specify fluid forcing by shoaling waves. Fluid forcing by currents in the far field are computed in (#7) where wave induced streaming and mass transport are based on algorithms after Longuet-Higgins (1953) and shallow water tidal currents follow from algorithms after Longuet-Higgins (1970).

Fluid forcing time series and bottom elevations computed in the far-field response module are through-put to the near-field response modules shown below the green line in Figure 1. Near-field processes occur over length scales on the order of the UXO dimensions and on time scales of a few seconds to hours, primarily governed by local hydrodynamic forces and scour mechanics arising from the disturbance, which the UXO creates in the flow.

The UXO and adjacent seabed is subdivided into a set of panels to form a lattice (Figure 5a). The vortex field induced by the UXO is constructed from an assemblage of horseshoe vortices, with a horseshoe vortex prescribed for each panel. This computational technique is known as the vortex lattice method and has been widely used in aerodynamics and naval architecture. The strength of the vortices is derived from the pressure change over each panel associated with the local wave and current velocity. The release of trailing vortex filaments from each panel causes scour of the neighboring seabed. This action is portrayed in Nature in Figure 5b and schematically in Figure 6. When viewed in any cross-wake plane (Figure 6b), each pair of filaments induces a flow across the seabed that results in scour proportional to the cube of the vortex strength and inversely proportional to the cube of the sediment grain size. This sensitivity of scour to grain size selectively removes the finer grained fraction of the bed material and leaves behind the coarser grained fraction in the scour depression. The coarse material that remains in the scour hole armors the bed against further scour thereby slowing the rate of scour burial.

a)

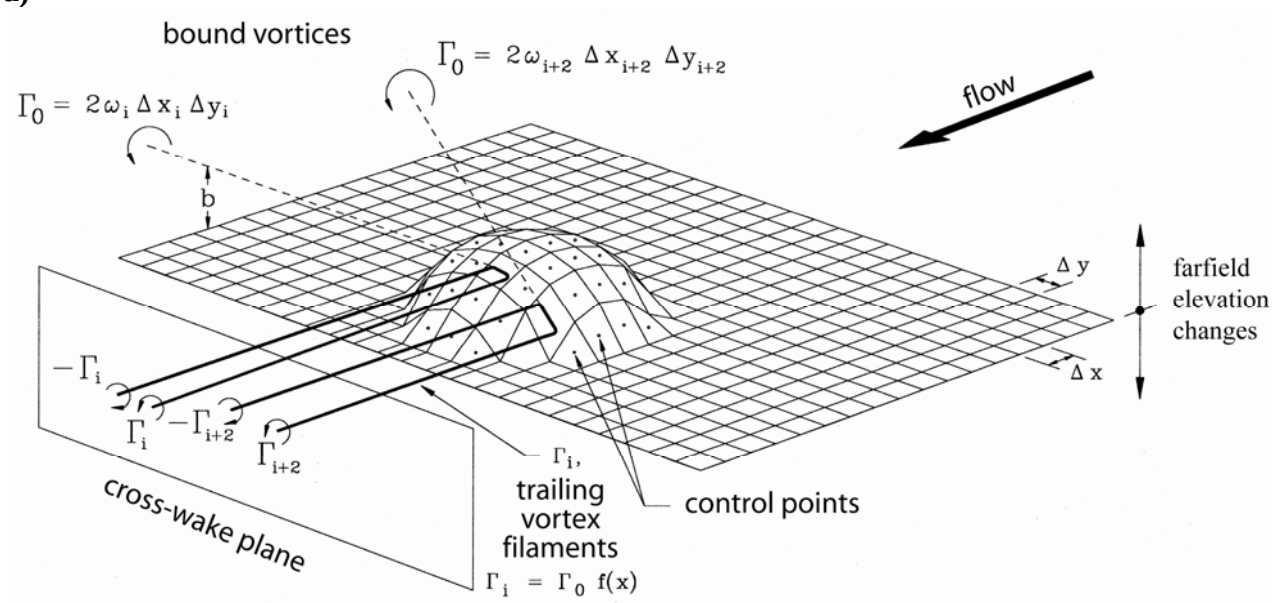

b)

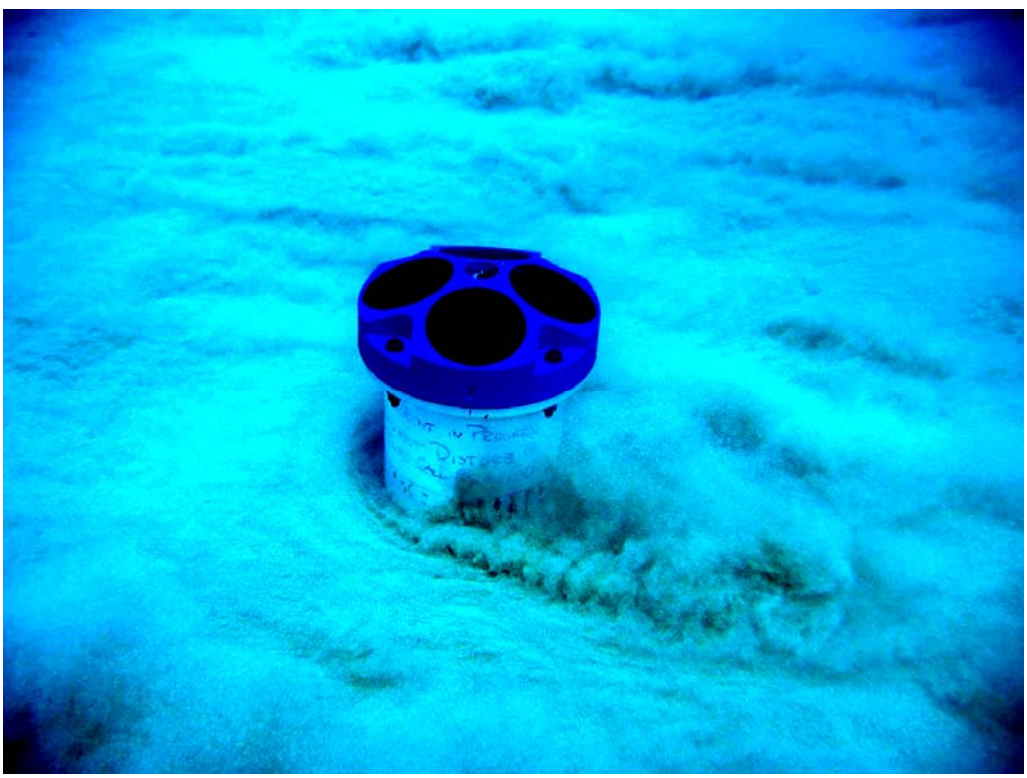

Figure 5. Vortex lattice method.
a) lattice and horseshoe vortex system;
b) horseshoe vortices inducing sediment transport in nature.
(photo courtesy of Kimball Millikan)

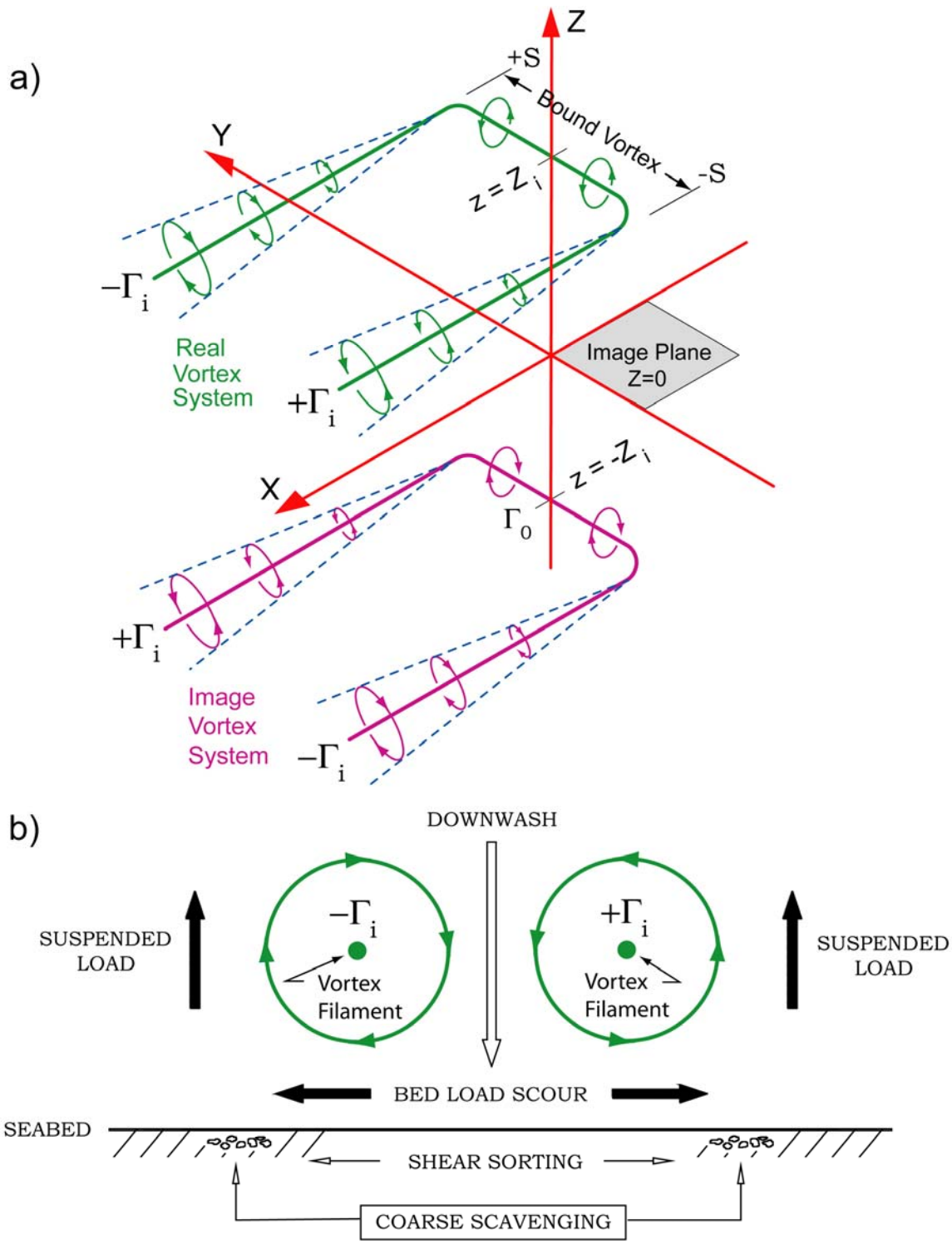

Figure 6. Lattice vortex method (schematic).
a) Image method for vortex induced velocity at any point near the bed (image plane) due to the horseshoe vortex system of an arbitrary lattice panel (Figure 5a). The real vortex of the lattice panel is diagrammed in magenta; the image vortex is in green. b) Schematic in the cross-wake plane of a pair of vortex filaments trailing out of the page (Figure 5a).

The far-field throughput to the near-field process modules is initially applied to the local seabed boundary conditions module (gray box in Figure 1). These local boundary conditions include two types: 1) the slope and elevation of the seabed plane around the object base derived by (#11) from location in the far-field control cell; and 2) the shape file of the body in question (#12). These two local boundary conditions are used to generate lattice panels by (#13) that define the object and bedform of the surrounding seabed (Figure 5a). The lattice is the computational domain of the near-field scour-burial processes where the method of embedded vortex singularities (vortex lattice method) is applied in (#14) using algorithms after Jenkins and Wasyl (1990) and Jenkins et al., 2007. This method employs horseshoe vortices embedded in the near-bottom potential wave oscillation to drive local sediment transport in (#13) based on ideal granular bed load and suspended load equations after Bagnold (1956 and 1963). A horseshoe vortex is specified by (#14) for each lattice panel during every half-cycle of the wave oscillation as shown schematically in Figure 5a. The horseshoe vortices release trailing pairs of vortex filaments into the local potential flow field that induce downwash on the neighboring seabed (Figure 6b), causing scour with associated bed and suspended load transport as computed by (#13). This scour action by trailing vortex filaments can be seen occurring in nature in Figure 5b.

The trailing vortex filaments also produce reaction forces on the UXO, that induce movement at the instant the moments from these forces balance the moments of gravity associated with the immersed weight of the UXO, as shown schematically in Figure 7. UXO migration is governed by Newton's second law and the controlling relations are formulated by balancing the forces due to acceleration *dU/dt* against the hydrodynamic and gravitational forces acting on it, according to:

$$\rho_m \frac{dU}{dt} V_0 = \rho c_f A_0 (u - U)\left|u - U\right| + \rho\, c_a V_0 \frac{d(u-U)}{dt} + \rho\, c_m V_0 \frac{du}{dt} + \rho_m V_0 g \sin\beta \qquad (1)$$

where ρ_m is the density of the UXO, ρ is the fluid density, V_o is the volume of the UXO, and A_o is the cross-sectional area of the UXO. The rate of change of momentum of the UXO is the result of four distinct forces: 1) profile drag, that is non-linear in terms of the relative velocity between the UXO and the water (u - U), where c_f is the coefficient of drag and u is the water velocity; 2) added mass forces that vary with the relative acceleration between the UXO and the water, where c_a is the added mass inertia coefficient; 3) virtual mass forces that are the resultant of the wave pressure acting on the UXO *vis-à-vis* the local diffraction solution (c_m is the coefficient of wave diffraction); and 4) downslope gravity forces due to the bottom profile slope and the local slope, β, of the bedform around the UXO. The project team utilized an advanced set of physics for the specification of each of these terms, including: the higher harmonics of the non-linear drag; the added mass of the trailing vortex filaments in specifying total added mass forces; the effects of acoustic thrust from streaming induced by end effects in oscillating flow, and torques induced by circulation streaming around the unburied portion of the UXO. These considerations lead to the formulation of the resultant hydrodynamic forces, F_x, acting to move the UXO having the shallow water form (Jenkins and Inman, 1985),

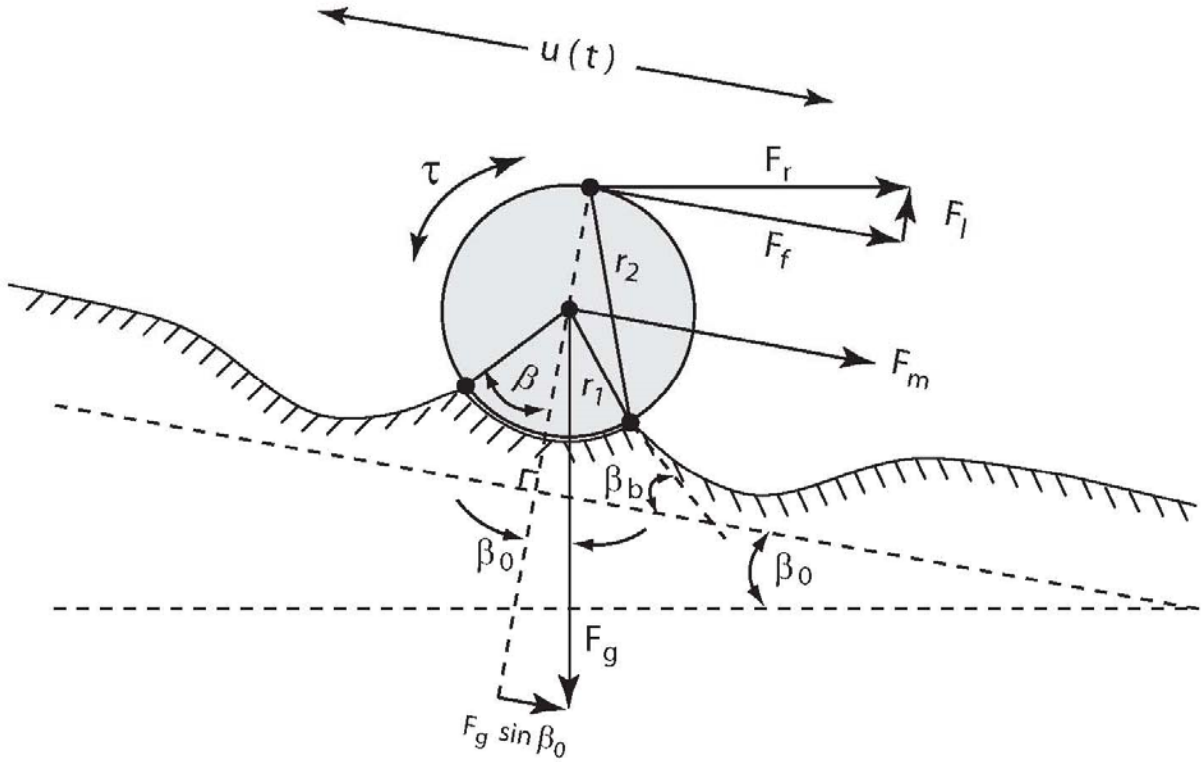

Figure 7. Moment balance for threshold of motion condition of a UXO at rest on a sloping bottom.

Threshold of migration criterion: sum of moments = 0

$$\vec{F}_g \times \vec{r}_1 = \vec{F}_m \times \vec{r}_1 + \vec{F}_r \times \vec{r}_2 + \vec{\tau}$$

$$F_f = F_f(\sigma t) + F_f(2\sigma t)$$

$$\tau = \tau_0 + \tau_3$$

F_m : added mass force

$F_f(\sigma\, \mathrm{t})$: drag + acoustic thrust

$F_f(2\sigma t)$: 2nd harmonic drag

F_l : lift from circulation streaming

τ_0 : steady torque from circulation streaming

τ_3 : 3rd harmonic torque from acoustic streaming

$$
\begin{aligned}
F_x(\sigma t) &= -\rho\frac{4}{3}\pi a^3\sigma u_m\left[\frac{3}{2}+\frac{9\delta}{4a}-\frac{d_0^2}{D^2}\left(\frac{27}{8}-0.15820R_e+0.8736\frac{\delta}{a}\right)\right]\sin\sigma t \\
&+\rho\pi a^2 u_m^2\left[3\sqrt{\frac{2}{R_e}}\left(1+\frac{\delta}{a}\right)-\frac{d_0}{D}\left(\frac{3}{4}+0.32939R_e-14.582\frac{\delta}{a}\right)\right]\cos\sigma t \\
&+\rho\frac{d_0}{D}\frac{\delta}{a}\pi a^2 u_m^2\frac{162}{5}\left(\frac{1}{\sqrt{2}}-\frac{1}{2}\right)\left(\cos 3\sigma t-\sin 3\sigma t\right)
\end{aligned}
\tag{2}
$$

where the torques acting to roll the UXO in the moment balance of Figure 7 have the form:

$$
\bar{\tau} = \rho\,\pi a^3 u_m^2 \tanh k(h-b)\left\{\begin{aligned}&\frac{\delta}{a}\frac{15}{8}+\frac{\delta\, d_0^2}{aD^2}\frac{81}{16}\left(1-\tanh^2 k(h-b)\right)\\&+\frac{\delta d_0^2}{aD^2}\frac{2187}{128}\left(\frac{1}{\sqrt{2}}-\frac{1}{2}\right)\left(\cos 2\sigma t-\sin 2\sigma t\right)\end{aligned}\right\}
\tag{3}
$$

In these equations, u_m is the orbital velocity, a is the UXO radius, D is the UXO diameter, $\sigma = 2\pi/T$ is the wave radian frequency, $d_0 = u_m/\sigma$ is the orbital amplitude, h is the water depth, b is the height of the UXO above the seabed, k is the wave number, δ is the boundary layer thickness, and $R_e = u_m d_0/v$ is the wave Reynolds number.

The lattice generation in (#14), horseshoe vortex generation in (#14), and sediment transport computations in (#13), and UXO threshold movement and migration (#15) are implemented as a leap-frog iteration in a time-stepped loop shown by the red and blue pathway arrows at the bottom of Figure 1. The leading time step (red arrow) computes the strength of the horseshoe vortex filaments generated by the pressure gradients and shear setup over the lattice panels of the combined body-bedform geometry of the previous (lagging) time step. The bed and suspended load transport induced by these filaments results in an erosion flux from certain neighboring lattice panels on the seabed and a deposition flux on others, based on image lifting line theory (Figure 6a) as first applied in Jenkins and Wasyl (1990) to a mobile sedimentary boundary. The erosion and deposition fluxes of the leading time step are returned in the computational loop to the lattice generator (blue arrow) where those fluxes are superimposed on the lattice geometry of the lagging time step. That superposition produces a new lattice geometry for implementing the next leading time step. By this leap-frog iterative technique, an interactive bedform response is achieved whereby the flow field of the leading time step modifies the bedform of the lagging time step; and that modified bedform in turn alters the flow field of the next leading time step. This lead and lag arrangement is based on the fact that the inertial forces of granular bed near incipient motion are large compared to those of the fluid, hence the flow field responds faster to a change in bedform than the bedform can respond to a change in flow field.

Because most UXO are bodies of revolution, the burial mechanism proceeds by a series of scour and roll events on a fine sand bottom, whereby the UXO successively scours a depression and then rolls into that depression. In contrast, a flat bottom mine-like objects (e.g., MANTA, ROCKAN, etc.) or UXO resting flat-side down bury by scour and slip sequences involving episodic shear

failures (avalanches) of the slopes of the scoured depression, Jenkins and Inman, (2002). During these shear failures, the UXO is in a state of sliding friction with the bed and is easily moved by the hydrodynamic forces of waves and currents.

Both of these mechanisms (scour and roll or scour and slip) may be arrested by large scale changes in the bed elevation due to either seasonal profile changes or influx of material by accretion/erosion waves. Both of these mechanisms (scour and roll, and scour and slip) involve movement of the UXO during the burial sequence. Over erosion-resistant beds, waves and currents may cause UXOs to migrate large distances before scour and burial arrests further UXO migration. During lower energy summer condition, sand moves onshore from the shore rise, shifting the bottom profile shoreward, exposing the UXOs and inducing migration. On muddy seabeds during storms, both the UXO and seabed may move as a unit.

The ballistic impact burial model that was embedded into the UXO MM architecture (Figure 1, Module #12) is STRIKE35, a six-degree of freedom (6-DOF) ballistics model developed by Chu et al. (2010). STRIKE35 is a derivative of the Navy's well proven mine impact burial model IMPACT35 (Chu and Fan, 2007). STRIKE35 is written in MatLab and was transposed to FORTRAN and integrated in the UXO MM flow chart as a separate module designated #12 in Figure 1 to result in the integrated UXO IMM. STRIKE35 has physics for the three basic processes of impact burial mechanics: 1) aerodynamic trajectory through the atmosphere after Hume (2007) and Hale (2009); 2) impact with the air-water interface after Chu and Ray (2006); 3) free-fall through the water column after Chu and Ray (2006); and 4) impact with a sedimentary seabed after Chu and Fan, 2007. The computational sequence proceeds round by round and the model output includes both depth of impact burial and orientation of the round on impact with the seabed.

STRIKE 35 was validated during controlled impact studies in two test ponds at the Naval Air Warfare Center, Weapons Division (NAWC/WD), Indian Wells, CA (Chu et al., 2010). STRIKE35 is an evolution from the mine impact burial model IMPACT35 that was validated during ONR's Mine Burial Program (Chu and Fan, 2007). The MBES (predecessor expert system to the Underwater Munitions Expert System UnMES) was validated during ONR's Mine Burial Program, Rennie et al. (2007).

2.1 TECHNOLOGY DEVELOPMENT

The UXO MM is adapted from a modification of the Vortex Lattice UXO Scour/Burial Model originally developed under ONR's Mine Burial Program (Jenkins et al., 2007). Several important modifications to the previous basic VORTEX were made:

- Algorithms for calculating the near-field effects on UXO were modified to address the complex and tapered shapes of small size (relative to mines).
- The overall algorithm for calculating the far-field effects that drive sediment movement was modified. The far-field sediment movement determines when the UXO is and is not buried, which has a major impact on overall UXO migration. The algorithm for calculating the total shape and size of the critical volume of sediment that is active along a given beach was re-created using thermodynamic balance as the basis rather than the past methods based on Dean's models.

- To support the critical volume analysis, an improved method of calculating the closure depth (the depth beyond in which there is no net movement of sediment) was developed and incorporated in the UXO MM.

Under the present project, the UXO MM has been upgraded to more efficiently compute fate and transport of UXO in a wide variety of coastal environments. We have integrated STRIKE 35 and developed code revisions to Module #8 in the architecture of the UXO IMM (Figure 1) in order to model the Camp Perry UXO fields.

2.2 ADVANTAGES AND LIMITATIONS OF THE TECHNOLOGY

The advantages of using the UXO IMM to assess the fate of UXO are discussed below. Areas where UXO are buried and will remain so can be positively identified, which can substantially reduce areas of required remediation. In areas of intermittent or sustained exposure, it is possible to predict the percent of the time that UXO are exposed to human contact, or to other hazardous processes such as corrosion, damage, etc. Where UXO are exposed, it is possible to predict the rate and direction of net movement as a function of weather and other local conditions. These calculations help to determine the probability of UXO appearing in adjacent areas outside of initial impact zones. After obtaining in situ survey of UXO, the UXO IMM allows munitions response managers to determine whether the UXO will remain where originally found, and thereby guide the speed of remediation efforts.

The primary limitations of the UXO IMM, as with all high-fidelity computer models, are the quantity and quality of the input data. In general, the UXO IMM output statistics are driven by the statistics of (a) the estimates of original UXO distributions (type, location, burial depth), and (b) the data on past weather conditions (waves, currents). Data on the sediment type and local bathymetry are also critical to the UXO IMM accuracy, but they tend to be better known.

The UXO IMM only deals with intact rounds (not fragments). Fragments are sharp and cannot roll, so in general they tend to move much less than the smoothly contoured and intact projectiles. The UXO IMM does not specifically address UXO populations consisting of boxes or intact pallets, although it could be modified to do so. The UXO IMM does not take into account the degradation of UXO rounds by corrosion, dispersion of dissolved chemicals. Explosives are unique environmental contaminants, solid at room temperature and subject to slow dissolution in an aqueous medium. Explosives have slower degradation rates and tend to be less mobile than other anthropogenic water contaminants such as oil and metals. However, since the UXO IMM does predict the time sequence of burial, exposure, movement, and reburial, that information is an important input to other software programs that estimate corrosion rates and the release of chemicals.

This page left blank intentionally.

3.0 PERFORMANCE OBJECTIVES

The approach to quantitatively evaluate performance in this project is to calibrate and validate changes in the predictive skill of the UXO IMM by matching predicted UXO impacts and subsequent migrations with UXO survey results from a control site chosen through a site selection processes (Jenkins and D'Spain, 2013). Two approaches were applied to the validation. By the first approach, the project team constructed probability density functions of impact, migration, and burial magnitudes predicted by the UXO IMM and compared them with the probability density functions assembled from the observed outcomes of the UXO surveys. Because the survey outcomes involved small ensemble statistics, the project team merged the results of a number of surveys over a long period of time.

In the second approach, the project team computed a predictive skill factor R from the mean squared error between the UXO IMM prediction and measured outcomes for impact location, burial depth h, and subsequent migration distance, ξ. For burial depth, the skill factor has the following form (adapted from Jenkins et al., 2007):

$$R_h = 1 - \frac{1}{N\hat{\sigma}_i}\left\{\sum_{1}^{i=N}\left[\hat{h}(i) - h(i)\right]^2\right\}^{1/2} \tag{4}$$

where $\hat{h}(i)$ is the measured burial depth for i = 1, 2..., N observations, $h(i)$ is the predicted burial depth for the ith observation, and $\hat{\sigma}_i$ is the standard deviation of all observations over the period of record. For migration distance, the skill factor has a similar form:

$$R_\xi = 1 - \frac{1}{N\hat{\sigma}_i}\left\{\sum_{1}^{i=N}\left[\hat{\xi}(i) - \xi(i)\right]^2\right\}^{1/2} \tag{5}$$

where $\hat{\xi}(i)$ is the measured migration distance for i = 1, 2..., N observations, and $\xi(i)$ is the predicted migration distance for the ith observation. The performance objectives shown in Table 1 provide the basis for evaluating the performance and costs of using the modified UXO IMM. To apply the criteria in Table 1, the UXO survey locations must be accurate within about 1 meter. That level of accuracy is consistent with the expected error bounds on the basic environmental parameter measurements (sediment grain size, wave velocities, etc.) used as inputs to the UXO IMM. When the predictions of the calibrated UXO IMM were compared to the measured UXO surrogate movements using the basic least-squares skill evaluations criterion, it was found with the un-modified UXO IMM that $R_\xi = 0.88$ for movement, and $R_h = 0.90$ for burial. Anything greater than $R = 0.8$ is considered very good for ocean modeling (Gallagher et al., 1998).

Table 1. Performance objectives.

Performance Objective	Metric	Data Required	Success Criteria
UXO IMM provides credible prediction of movement in support of test planning, ops.	Predictions check against general engineering theory and observations at similar sites.	Graphic presentations of predicted and measured movement of surrogates from the field demo site.	Differences between predicted values and measurements are consistent, and can be reduced to within 20% or less by calibration.
Field Demonstration collection of sufficient quality data to allow validation of UXO IMM.	Tracking movement of surrogates with accuracy consistent with input data and UXO IMM computational resolution.	Measured position of the surrogates v. time at the field test (location and depth of burial).	> 50% of surrogates are tracked successfully at the test site. Movements are measured within +/- 10%.
Match between predictions and measurements, with coefficients correctable to positive match.	Model skill factor (ability to correctly predict surrogate movements and burial).	Measured position of the surrogates v. time at the field test (location and depth of burial).	R > 0.8

4.0 SITE DESCRIPTION

The initial phase of the Navy UXO MM program (Johnson et al., 2002), funded an extensive literature and web search, in addition to gathering field information. Additional UXO site data are contained in reports by the U.S. Environmental Protection Agency (U.S.EPA) (2000), Tucker (2003), Jarrah (2001), and the U.S. Army Engineering and Support Center (USAESCH) (2009). These sources have identified 25 sites where underwater UXO are highly likely to exist and are listed in Table 2.

Table 2. Underwater UXO Sites.

Coastal Ammunition Loading Sites
NAD Indian Island, WA
NAD Seal Beach, CA
NAD Detachment Concord, CA
NAD Detachment North Island, CA
Ex-Naval Ship Yard Mare Island, CA
NWS Yorktown, VA
NWS Charleston, SC
NWS Mayport, FL
Ex-NAD, Jackson Park, WA (former NAD with continuing UXO problems)
Coastal Live Firing Ranges
San Clemente, Island, CA (heavy past usage and still active at reduced levels)
San Nicholas Island, CA (old gunnery range now used for missile testing)
Camp Perry, OH (heavy past usage and still active at reduced levels)
Formerly Used Live Firing Ranges
Kaho'olawe, HI (heavily used naval gunnery, bombing, and ordnance test site)
Vieques Island, PR (heavily used naval gunnery, bombing and amphibious exercise site)
Culebra Island, PR (40 years of use as gunnery and bombing range)
Normans Island, MA (WW II gunnery and bombing)
Hingham Island, MA (WW II gunnery and bombing)
Panama Canal Zone (multiple formerly used defense sites)
Mare Island, CA (former Navy firing range)
Salton Sea Test Range, CA (former navy inland sea small caliber firing range)
Ex-Naval Station Adak, AK (extensive UXO of all types)
Operational Bases with Potential Underwater UXO
Marine Corps Base Hawaii (Kaneohe)
NWS Dahlgren, VA
NWS San Diego, CA
NAD Earle, NJ

NAD=Navy Ammunition Depot NWS= Naval Weapons Station

Table 2 is predominantly comprised of Navy sites, though it is not all-inclusive. However, it is typical of the shallow and very shallow water regions necessary for establishing representative coastal scenarios for comprehensive UXO IMM modeling of subsurface UXO impact burial and subsequent exposure and movement. While the UXO IMM is capable of simulating impact burial from UXO that fell to the seabed during loading mishaps, there is generally no chronology available on when those mishaps occurred at the various operational bases, NADs and NWSs listed in Table 2. Furthermore, U.S.EPA (2000) points out that only a small fraction of those loading mishaps have precise location information (principally station markings on pilot charts). In

addition, ordnance involved in loading mishaps is generally bulk palletized, typically in some unknown configuration; whereas the UXO IMM is coded to simulate seabed impacts of individual ordnance. Therefore, we will limit our demonstration/validation (dem/val) site selection to only the live and formerly live firing ranges listed in Table 1, where impact burial is due to ballistic flight of single ordnance.

4.1 SITE SELECTION

In evaluating the dem/val suitability of the UXO sites in Table 2, a site scoring criteria based on the data requirements of the UXO IMM was applied. Input data requirements include all 40 parameters, which may be divided into four generic types of data bases: 1) bathymetry, beach profiles and sediment data; 2) wind, wave, and current forcing, water level data, and stream flow data; 3) firing records including chronology, weapons type, azimuth and inclination angles; and 4) UXO surveys providing location, classification, and burial depth data. The project team scored the quality of these four types of data bases at each UXO site based on the traditional A,B,C,D,F grading system, in which: A = Highly Detailed Data; B = Detailed Data with some data gaps; C = Sparse Data with many data gaps, but with some detailed data; D = Sparse Data of Marginal to Poor Detail; F = No Usable Data. The data sources for these scorings include: Johnson et al. (2002); EPA (2000); Tucker (2003), Jarrah (2001); the USAESCH (2009); American Technologies, Inc. (2002); EOD Technology, Inc. (1992); Evans-Hamilton, Inc. (2003); Naval Facilities Engineering Service Center (NFESC) (2008); Pope, Lewis, and Welp (1996); Science Applications International Corporation (SAIC) (2006); Baj (2008); National Oceanographic and Atmospheric Administration (NOAA) (2012); Coastal Data Information Program (CDIP) (2013); USGS (2008); National Geophysical Data Center (2008); and Stauble (1992). The scores derived from these sources for the data base quality at the twelve live and formerly firing ranges in Table 2 are listed in Table 3.

Table 3. Site selection scoring criteria.

UXO Site	Bathymetry @ 1-3 arc-seconds Beach Profiles & Sediment Data	Wind, Wave & Current Forcing, Water Level Data, & Stream Flow Data	Firing Records w. Chronology, Weapons Type, Azimuths & Inclinations	UXO Surveys w. Location & Classification & Burial Data
San Clemente, Island	A	A	C	F
San Nicholas Island	A	A	C	F
Camp Perry	**A**	**A**	**B**	**A**
Kaho'olawe	A	A	D	C
Vieques Island	A	A	D	C
Culebra Island	A	A	F	F
Normans Island	A	A	D	C
Hingham Island	A	A	D	C
Panama Canal Zone	A	B	F	F
Mare Island	A	A	D	A
Salton Sea Test Range	A	C	A	F
Adak, Andrew Bay	A	B	F	D

Data Quality Scores:
A = Highly Detailed Data
B = Detailed Data with Gaps
C = Sparse with Some Detailed Data
D = Sparse with Marginal to Poor Detailed Data
F = None
Red = Highest Score

Inspection of Table 3 reveals that Camp Perry achieved the highest score (by a wide margin over the other candidate sites) as a suitable dem/val site. The principal discriminators in this site suitability scoring were the availability of firing records and UXO surveys that established location and classification of UXO rounds that had been fired. Usable firing records were found for only two sites, Camp Perry and Salton Sea Test Range. The firing records for the Salton Sea Test Range were complete, while the Camp Perry firing records contain gaps, primarily the earlier periods of usage prior to 1966. However, no UXO survey data with locations and classifications are available at Salton Sea Test Range, while six separate UXO survey and target recovery efforts have occurred at Camp Perry on Lake Erie, Ohio, between 1992 and 2006, from three well-defined offshore impact ranges. Water levels are highly variable on an inter-annual basis at both sites, but water level data in Lake Erie is well-studied and monitored at the Great Lakes Environmental Research Laboratory.

4.2 SITE HISTORY

The Lake Erie Impact Range is shown in Figure 8. The site has been classified by the United States Government as a Formerly Used Defense Site (FUDS) because it fronts the former Erie Proving Grounds at the Erie Army Depot, Camp Perry. For almost half a century (1918-1966) the site was used by the Department of the Army for testing and proof-firing of artillery, aerial bombardment, and small arms fire. The "formerly used" impact areas were used for both artillery and aerial bombardment testing through the early 1960s. Active live fire still occurs in the reduced area shaded in red on Figure 8.

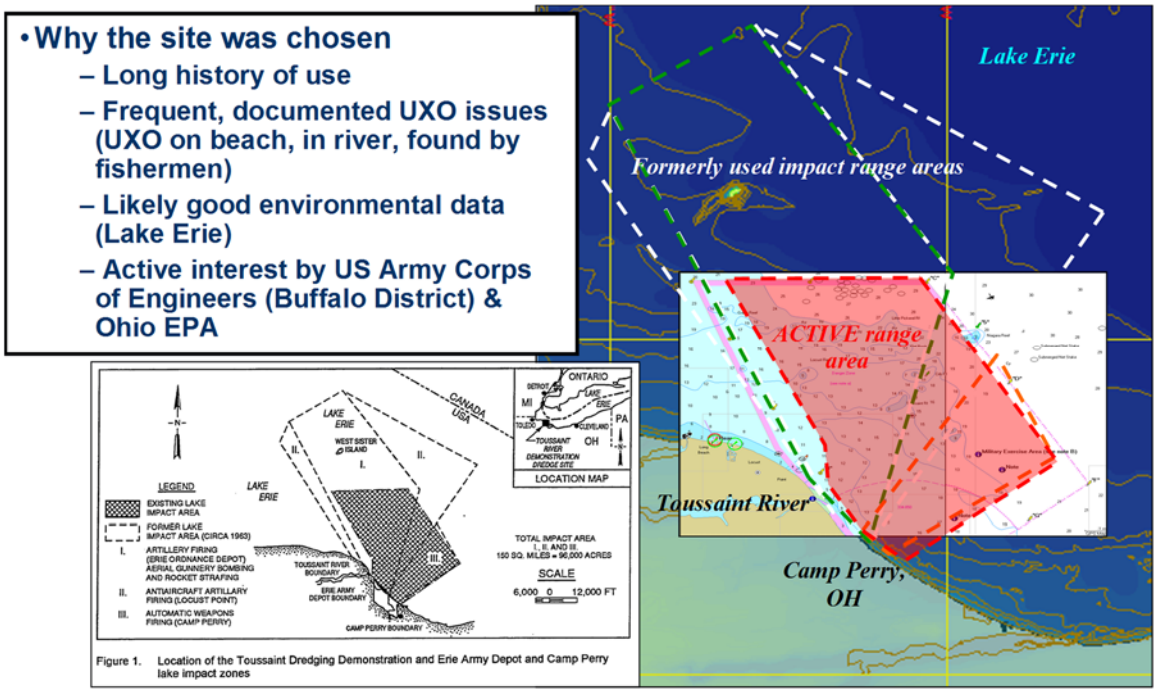

Figure 8. The Lake Erie/Camp Perry impact range areas.

The Lake Erie site was selected for the dem/val because of several important factors:

- The site has an extensive history of UXO interaction with human activities.
- The site environmental data were readily available, at least at the desk-top level.
- Multiple quantitative sampling studies of the underwater UXO distribution at the site have been completed, including remote sensing, test excavations, and beach clearances (a rare condition).
- A rare controlled field test of the burial/mobility of surrogate UXO items was conducted at key locations within the nearshore area.
- The site includes occasional ice rafting effects, which makes it representative of Arctic beaches not previously studied in the ESTCP program.
- Substantial local and Congressional interest exists for developing a long-term solution to the management of UXO at the site.

The three major types of human interaction with UXO in the Lake Erie area are:

a. *Commercial and sport fishing.* There are extensive commercial trap net fisheries conducted around the perimeter of the present active firing range. Fishing is no longer allowed inside the active range, but the fisheries do intersect virtually all of the previously used firing areas. There have been many reports of fishermen finding UXO in their nets, although those reports have become less frequent in the past 5 years as the fishery itself has declined. In some cases, the UXO were reportedly transported back to the Toussaint River marinas and dropped overboard there during unloading. Also, a large sport fishery is present, which is known as the "Walleye Capitol of the World." The walleye fishermen troll with 10-12 lb "cannonball" shaped sinkers on the bottom.

b. *Toussaint River Channel.* The 2100 ft x 250 ft channel has been dredged through a sand spit to a depth of 4-5 feet every few years over the past 15 years to provide a route for the sport fishermen from the Toussaint River marinas out to the offshore fishing grounds and reefs. A 106 mm UXO jammed in the dredge just before the first dredge operations were completed in the channel in 1992. A controlled experiment was conducted in 1995 that recovered 37 items in the single pass through the channel.

c. *Camp Perry Beach.* Although the beach is not open to the public, there are military personnel who do use the beach and it is accessible to boaters as well. Beach clearance operations have found several thousand UXO items.

4.3 SITE GEOLOGY

The beach and bathymetry show a very shallow slope offshore. The bottom is generally flat, with a thin layer of sediment cover, but there are occasional rock outcrops. A general transport of sediment occurs from the northwest along the shore to the southeast. However, the dredged channel of the Toussaint River acts as a sediment trap, so the main beaches between there and Camp Perry are steadily eroding and receding.

The lake level rises and falls 1-2 meters annually as a result of both natural and man-made forces. The lake level also can change by as much as a meter in a day or two under the effects of strong local winds.

The coastline is ice-bound for 1-3 months each winter. In some areas, the wind becomes so powerful that it can drive the ice onto the shore. See Section 4 for further discussion. The typical waves are from the northeast and are relatively low-energy, with heights of 1-2 meters (m) and periods of 5-7 seconds. Extreme storms can produce 3-4 meter waves. The conditions can be very difficult for small craft, but the water motion that is the forcing function for sediment transport (or UXO movement) on the lake bed is relatively low.

Review comments on this project express concern that ice processes on Lake Erie during winter may affect UXO fate and transport in the three impact areas of Camp Perry, and that the UXO IMM does not possess the process physics to account for such UXO/ice interactions. The mechanism for such interactions would be associated with ice keels gouging the lake bottom and pushing the UXO around as the ice keels drift. This is known to occur in the Arctic with rocks and boulders, and the processes are referred to as "ice gouging" when ice keels become grounded on the bottom and subsequently move, while the process of ice keels moving under the influence of wind stress is referred to as "ice push" (Inman and Jenkins, 2004). The question of whether this occurs with UXO at Camp Perry depends on the thickness of the Lake Erie ice sheet in winter (Figure 9); and whether that thickness is sufficient to cause ice gouging over lake water depths where UXO reside.

Figure 9. Photograph of the surface of Lake Erie taken from the University of Wyoming King Air on 25 February 2004 @ 1120 UTC.
(Photo courtesy of Michael Spinar)

Figure 10 plots the historic Lake Erie ice thickness at two monitoring stations of the Great Lakes Environmental Research Laboratory (GLERL) Great Lakes Ice Thickness Data Base, 1968-1979. The historic maximum ice thickness was on the order of 70 centimeters (cm) (0.7 m) during the epic cold La-Nina winters of 1977 and 1978. Figure 11 gives a schematic showing this maximum Lake Erie sheet ice and its corresponding Stamukhi Zone from ice push superimposed on historic beach profile at Beach Survey Range Line # 10695 on FUDS Beach, Impact Areas 3, Camp Perry. As the northwesterly post-frontal winter winds across the southwestern shores of Lake Erie push this maximum-thickness ice sheet onshore, the leading edges of the ice sheet crumple against the shoreline, forming ice keels in an inshore region known as the "Stamukhi Zone." The depth of ice keels in the Stamukhi Zone is typically twice the thickness of the converging ice sheet (Inman and Jenkins, 2004). When these ice features are superimposed on the beach profile at Camp Perry in Figure 11, it was found that ice push displacement of UXO is only possible within 100 m of the shoreline of Impact Area 3, where water depths are less than 1.5 m International Great Lakes Low Water Datum (LWD). However, Figure 11 shows that the preponderance of UXO targets are concentrated in the offshore domain of Impact Area 3 where water depths are typically -4 m to -8 m LWD. Therefore, if we selectively focus the dem/val simulations of the UXO IMM to UXO impacts beyond 100 m of the shoreline, aliasing of the results by ice processes can be avoided.

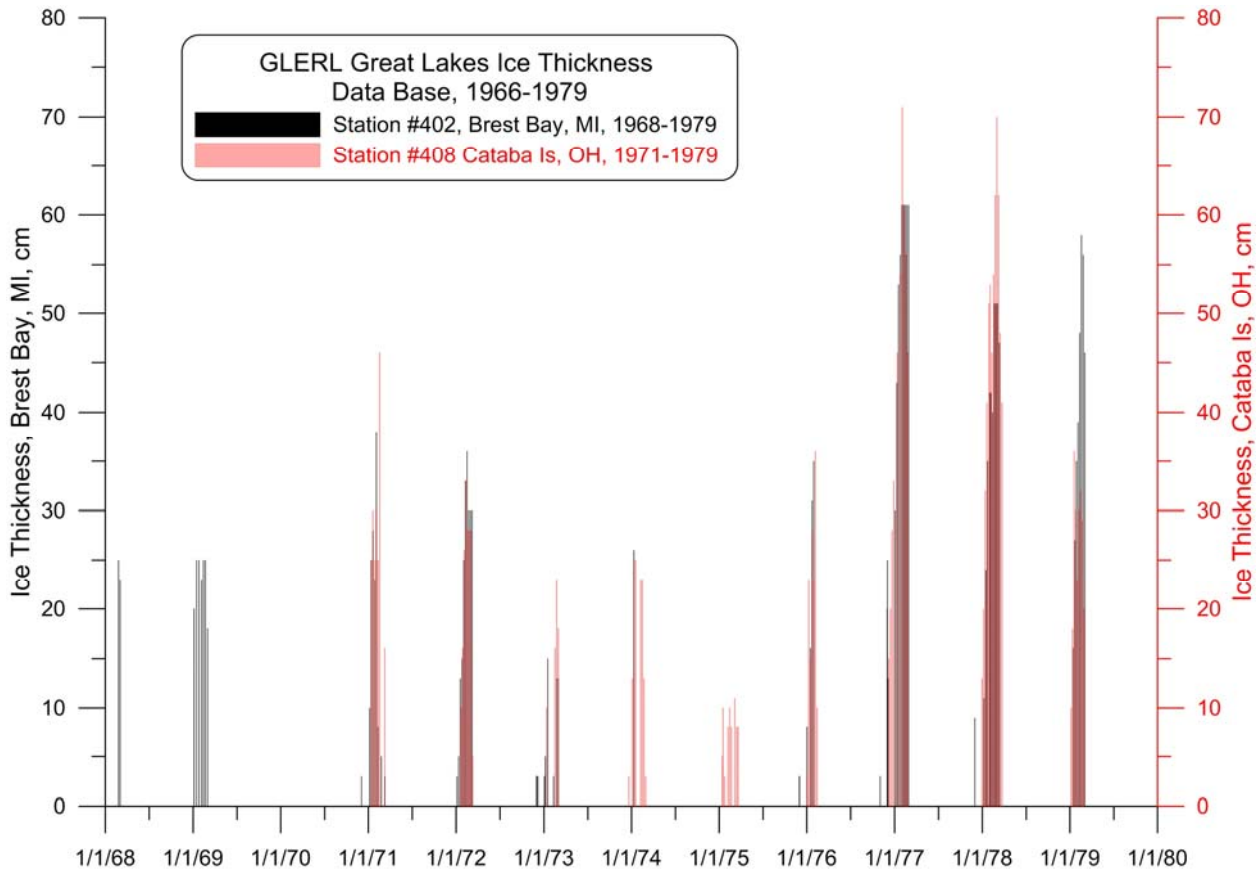

Figure 10. Lake Erie ice thickness at two monitoring stations of the GLERL Great Lakes Ice Thickness Data Base, 1968-1979.

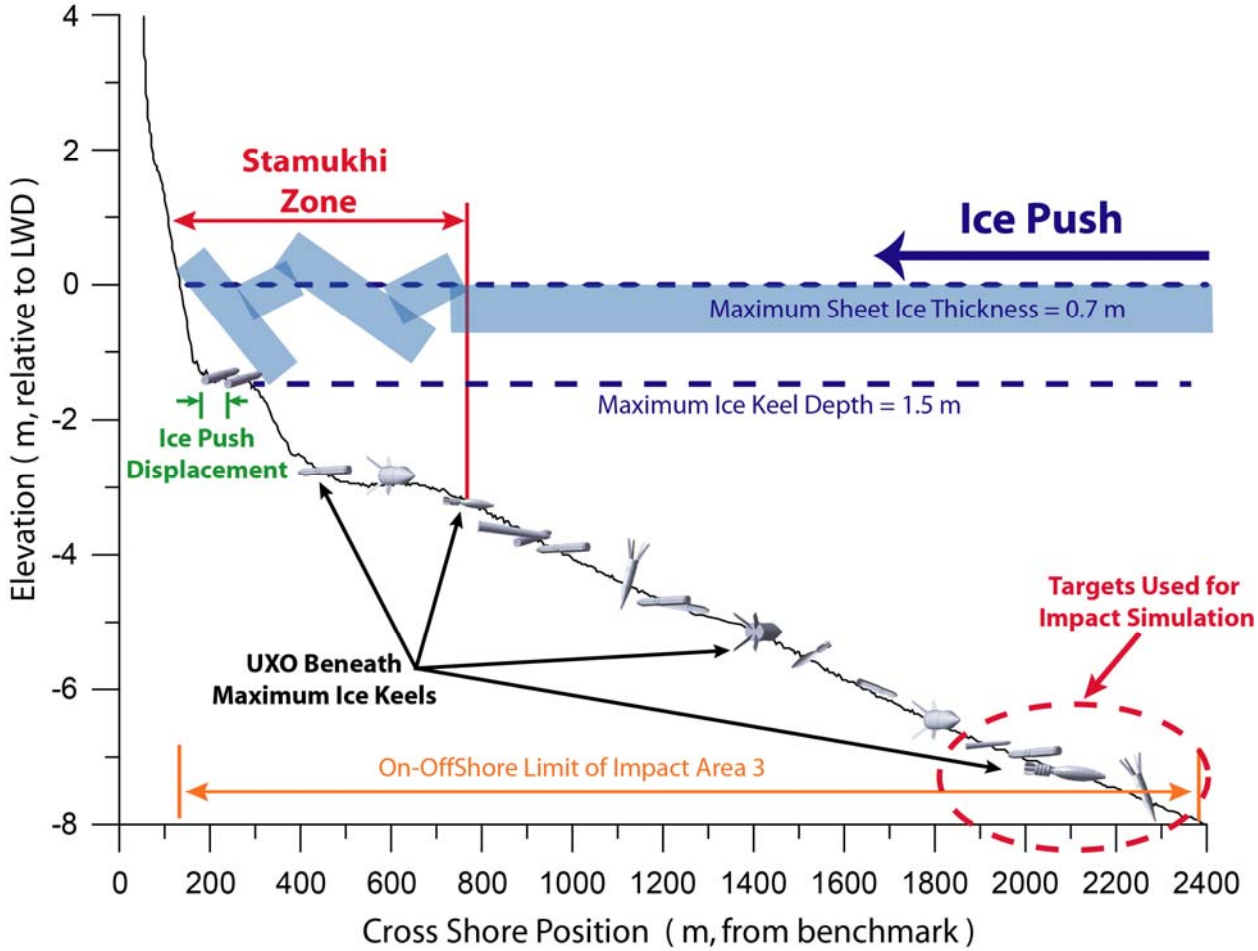

Figure 11. Schematic of maximum Lake Erie sheet ice and corresponding Stamukhi Zone from ice push superimposed on historic beach profile at Beach Survey Range Line #10695 on FUDS Beach, Impact Areas 1-3, Camp Perry.

4.4 MUNITIONS CONTAMINATION

During the period 19 July through 26 October 1995, the U.S. Army Corps of Engineers (USACE) Buffalo District Office conducted a demonstration dredging project that was designed to safely separate the ordnance from the dredged material (Welp and Clausner, 1998). All equipment was specially modified with armor plating to ensure the safety of the operators and observers. The channel was dredged with a modified clamshell bucket dredge that deposited the material on separation screens placed over the hoppers of bottom-dump scows. The sediment passed through the screens and retained UXO by a combination of gravity flow and jet fluidization. The screen was visually monitored via a remote control camera, with ordnance disposed of separately when discovered. A 106 mm projectile on the separation screen is shown in Figure 12, with additional examples of recovered ordnance shown in Figure 13 (Welp and Clausner, 1998). During the demonstration project, 19,300 cubic yards of material were removed from the authorized channel limits. The operation removed less than half of the estimated 45,000 cubic yards available. A total of 37 pieces of ordnance was recovered (568 lb. scrap metal), of which 31 pieces were classified as inert ordnance.

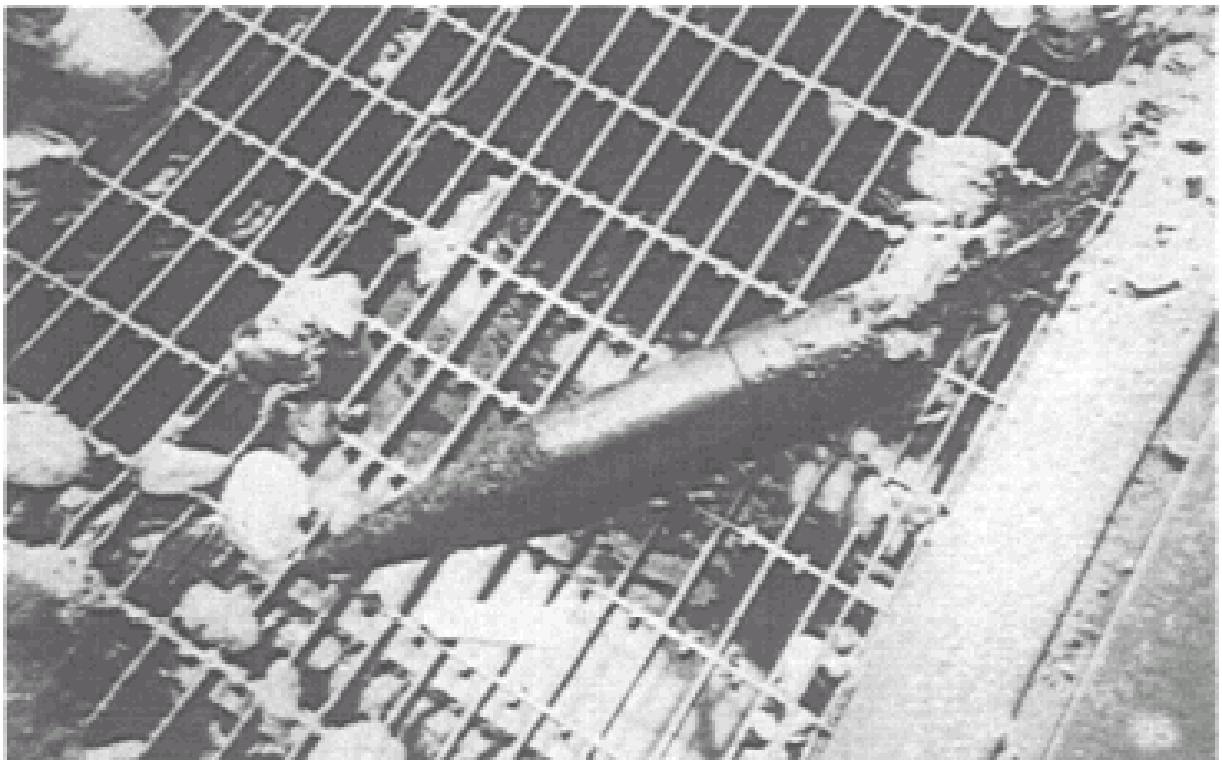

Figure 12. 106 mm projectile on separation screen, Camp Perry UXO survey.

Figure 13. Examples of recovered ordnance, Camp Perry.

In 1999, a clamshell dredge with operator protection (similar to the 1995 project) was used to dredge the channel. However, no screens were used to separate ordnance. If ordnance was observed in the barge, Explosive Ordnance Disposal (EOD) personnel were to be called in to conduct removal and disposal efforts. The dredge material was transported to the open-lake disposal area and released by a barge operator who was situated behind a protective barrier. During this dredging episode, no ordnance was observed. However, only the outer pile on the barge was observed, therefore, personnel were not actively screening for ordnance and, as only the outer surface of the above-water spoil pile could be observed, the absence of ordnance could not be fully substantiated (Welp and Clausner, 1998).

This page left blank intentionally.

5.0 TEST DESIGN

The project team utilizes the UXO IMM to predict the initial impact burial and subsequent exposure, migration and burial behavior of UXO rounds in Lake Erie impact areas off Camp Perry. The UXO rounds considered include: 60 mm M49A2; 81 mm M43A1; and 106 mm M344 rounds (Figures 14 and 15). These U.S. Army projectiles present a new set of modeling challenges for the VORTEX because they are significantly more complex geometries than the U.S. Navy projectiles considered in previous studies. The most complex of these new geometries is the 106 mm M344 round that features six aerodynamic stabilizer fins and has very small radii of curvature associated with the nose section of the round (Figure 14).

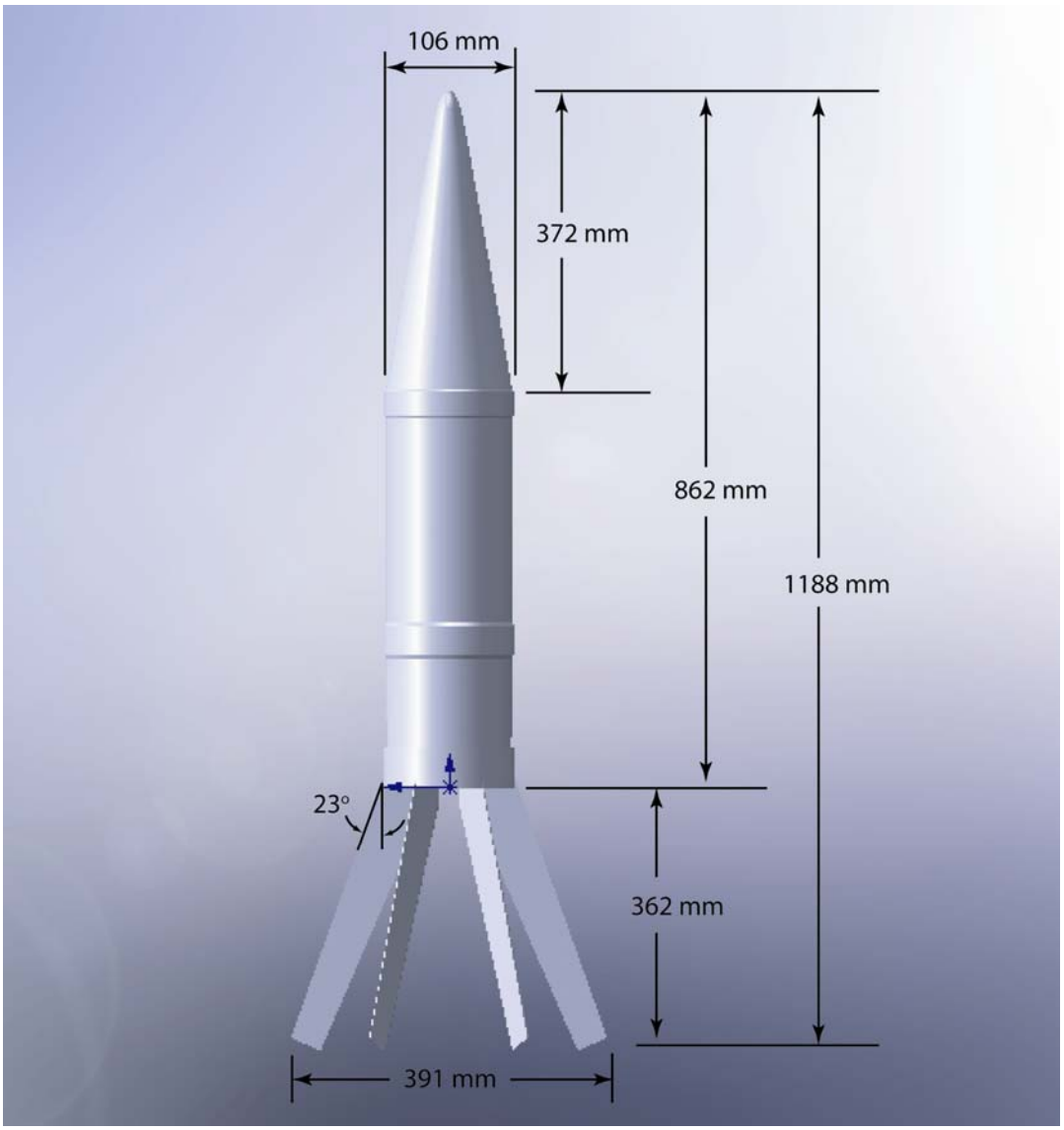

Figure 14. Shape file of M344 106 mm round on a fine sand bed used in numerical mobility model analysis.

Figure 15. M43A1 81mm round (left), M49A2 60 mm round (right).

5.1 CONCEPTUAL EXPERIMENTAL DESIGN

The project team calibrated the UXO IMM to reproduce the impact pattern shown in Figure 16. Figure 16 gives a plot of the density of the UXO "targets" found by underwater magnetometer surveys conducted by SAIC in 2006 (SAIC, 2006). The distribution in Figure 16 shows that the preponderance of UXO targets are concentrated in the offshore domain of Impact Area 3 where water depths are typically -4 m to -8 m LWD. There is a smaller population that resides in the near-beach domain of Impact Area 3, where water depths are typically 0 m to -2 m LWD.

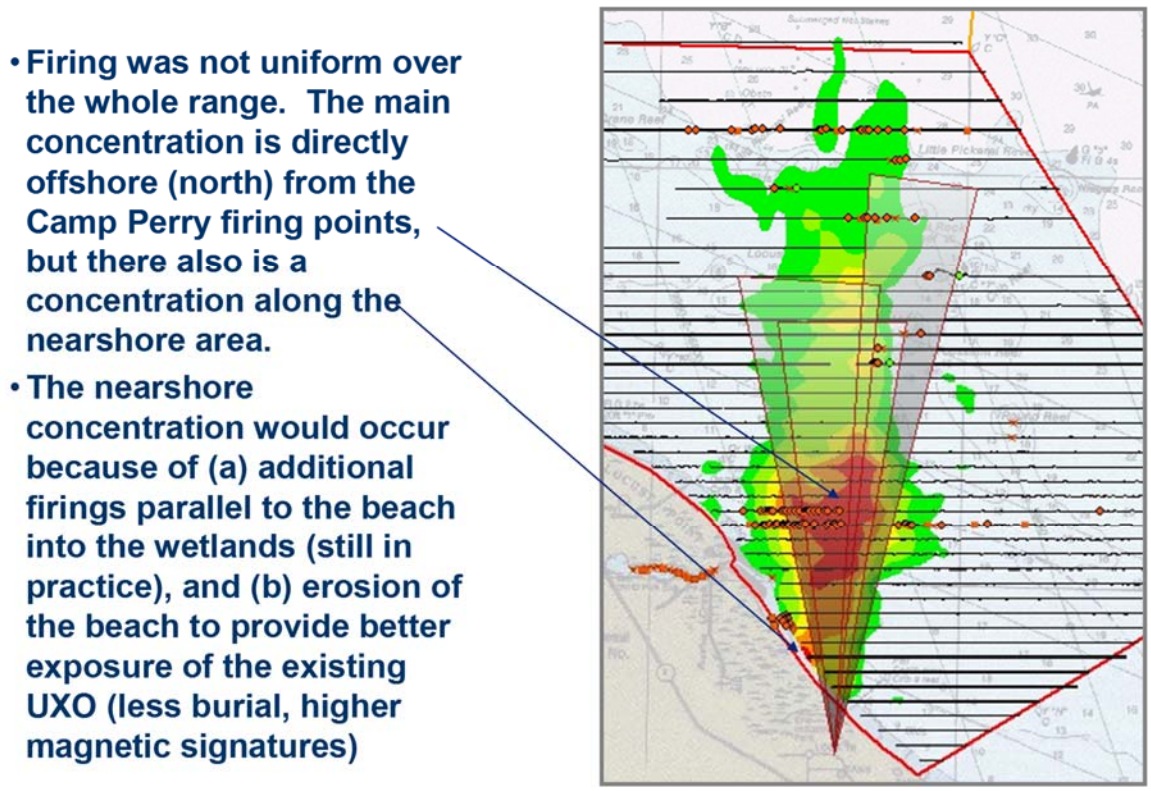

Figure 16. Plot of density of 2,135 UXO "targets" found in 2006 magnetometer survey.

The magnetometer surveys identified and located 2,135 suspected UXO targets. The small red colored dots represent targets that were checked by divers. In the main range fan, 92% of the targets checked were actually UXO, while the remaining 8% were other metal objects. The size of the UXO varies from small caliber bullets to as large as the 106 mm rounds. There also was at least one 250 lb bomb found near West Sister Island, but by far the dominant UXO types are the Army artillery shells and mortars, which are typically 0.3 to 0.4 m long.

After calibrating the UXO IMM for the impact pattern and burial depths from Figure 16, the model will be run forward in time using historic wave and water-level forcing functions to examine potential dispersal of the UXO from presently known locations in Figure 16. The objective of this analysis is to answer two charge questions issued to us in the Spring In-Progress Review of 2013:

1) For projectiles deposited in Lake Erie in a variety of initial conditions (fully buried on impact, partially buried, on the surface), how many years does it take for the effects of the initial conditions to be washed out?
2) Does the position and orientation of the projectiles only become randomized during severe storms or are the normal seasonal weather patterns sufficient?

The model can be operated in three distinct modes depending on the data that is available for making a migration/burial prediction and the user's desire to make site specific adaptations to the model's configuration. When little more than the general coastal setting and the time frame of the UXO field are known, the model is run in ***Mode 1***. Mode 1 predictions use pre-configured gridding

systems, forcing functions, boundary conditions and calibration factors based on the coastal classification system (#1 in Figure 1). Seven input parameters are required for Mode 1 operation and are discussed in greater detail in Wilson and Jenkins (2005).

When information is known about the gross site-specific details of a suspected UXO field, then the model can be run in ***Mode 2***. Mode 2 operation makes migration/burial predictions using pre-configured gridding systems and calibration parameters with user supplied bathymetry, wave, and sediment data. The 20 Mode 2 input parameters are listed in Jenkins and Wasyl (2008).

The model is run in its most detail intensive configuration as ***UXO IMM***. This operational mode is for applications in which contemporary, high resolution site specific information is known about the UXO field. UXO IMM input parameters include 40 parameters as listed in Wilson et al (2008) (see also Section 6.0). In the following portions of this report, the details of setting up the model for UXO IMM operations at the Camp Perry site shall be explored. In Section 6, the project team shall perform UXO IMM simulations of fate and transport of UXO in Camp Perry impact areas.

5.2 SITE PREPARATION

Far-field initialization involves data base constructions and model parameterizations for model inputs above the orange line in Figure 1. A detailed listing of these inputs can be found in Wilson et al. (2008). They are reviewed here in context specific or unique to the Camp Perry/FUDS Beach site.

The stationary far-field bathymetry was derived from the NOS digital database compiled by the National Geophysical Data Center (NGDC) (2008), and was subsequently assembled in a far field grid as contoured by the white lines in Figure 17 (10m depth contour indicated in gold). Depth contours are labeled in meters relative to the LWD. LWD for Lake Erie is at 174 m relative to the International Great Lakes Datum, 1985 (NOAA, 2008). The far-field grid in Figure 17 includes a sufficient portion of the west basin of Lake Erie to account for the island sheltering effects along the Toussaint River/FUDS Beach Littoral Cell due to the Catawaba and Bass Island complexes. The system of barrier islands and sand spits that control the beach and shoreline dynamics of this highly variable littoral system are defined by the 0 m LWD contour in Figure 17. The far field grid is assembled from a 1201 x 1201 point array (1,442,401 grid points) formatted by latitude and longitude using 3 x 3 arc second grid cell resolution and yielding a computational domain of 84.2 km along the x-axis (longitude) and 111.2 km along the y-axis (latitude). This is one of the larger grids on which the VORTEX has computed UXO transport and burial to date, and was necessitated by the broad-scale features of the Catawaba and Bass Island complexes and their influence on longshore fluxes of sediment and mass exchange occurring along the reach of the Toussaint River/FUDS Beach Littoral Cell. The small amount of grid distortion between x- and y- length scales in the far-field grid is compensated internally during a transformation to Cartesian coordinates using a Mercator projection centered on Camp Perry.

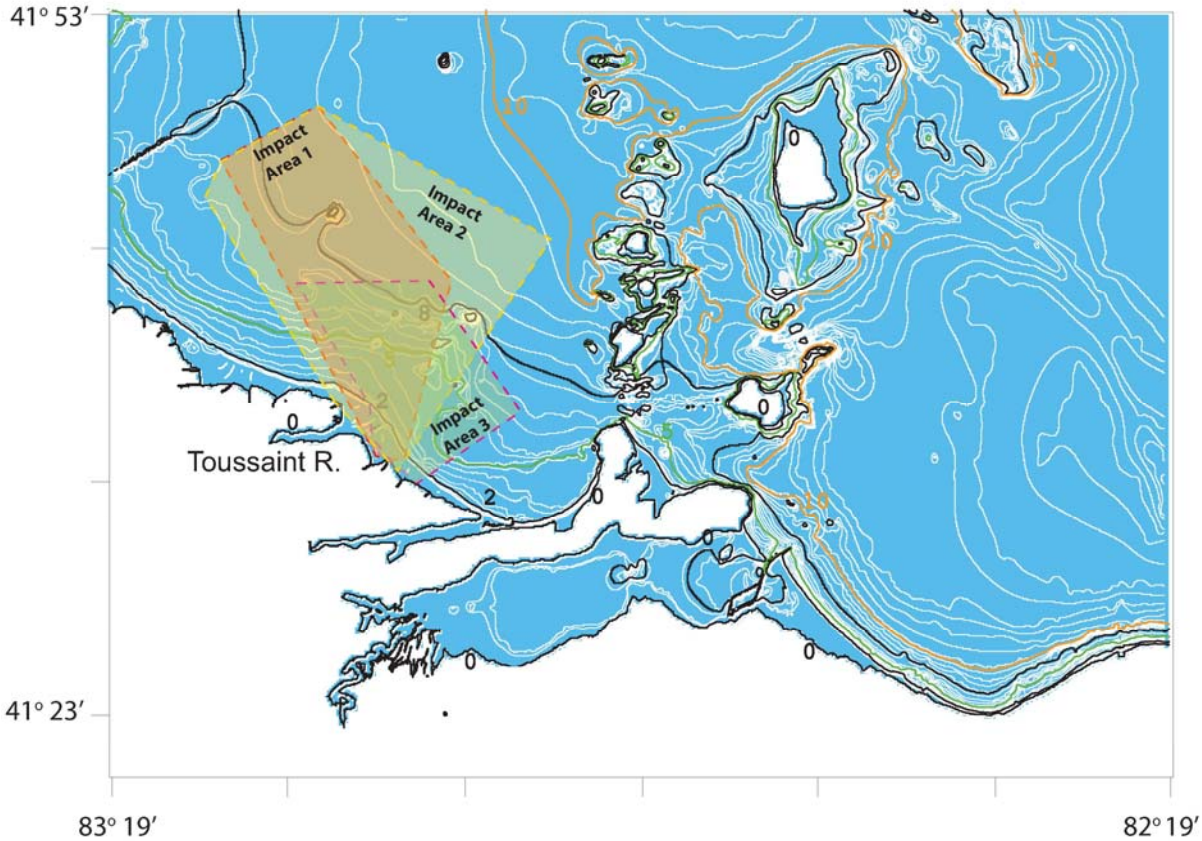

Figure 17. Bathymetry of western Lake Erie, OH, relative to 174.4 m mean sea level (msl). Camp Perry impact areas shown in shading. Bathymetry contours at 0, 2, 5, 8, and 10 m depth are labeled in the figure – those at 0, 2, and 8 m are plotted as black curves; the 5-m contour is plotted in green; and the 10-m contour is plotted in pink. The white bathymetry contours occur at 0.5-m depth increments.

5.3 SYSTEM SPECIFICATION

The concentrations of suspected ordnance and explosive waste (OEW) lakeward of the FUDS beach, on the beach, and in the entrance channel of the Toussaint River were documented relative to geomorphic features, sediment type, and the geography of Erie Army Depot. All data collection was positioned using a differential global positioning system (DGPS). Data sets collected to document ordnance concentrations and site geology included land and underwater magnetometer, ground-penetrating radar (GPR), electromagnetic, side-scan sonar (SSS), a remotely operated vehicle (ROV), site narratives, historical information, and coastal process data (Pope, Lewis, and Welp, 1996).

5.4 CALIBRATION ACTIVITIES

Calibration procedures for the sensor systems used in the Camp Perry UXO surveys identified in Section 5.5 are discussed in detail in EOD Technology, Inc. (1992; 2002); American Technologies, Inc. (2002); Pope, Lewis, and Welp (1996); Welp and Clausner (1998); Evans-Hamilton, Inc. (2003); and SAIC, Inc. (2006).

The dem/val exercise for this project uses archival field data collected by previous UXO surveys at Camp Perry. There have been six major quantitative studies of the UXO. The general areas of the studies are shown in Figure 18. These include:

- Beach clearances in 1992 (EOD Technology, Inc., 1992) and 2002 (American Technologies, Inc., 2002). A clearance also took place in May 2008, but no data are available;
- UXO in situ surveys in 1993 by USACE Waterways Experiment Station (WES) (Pope et al 1996);
- Dredging demonstration in the Toussaint River Channel by WES in 1995 (Welp and Clausner, 1998);
- UXO migration study at sites near Toussaint River and Camp Perry beach by WES in 2001-2003 (Evans-Hamilton, Inc., 2003); and
- UXO survey and target recovery by SAIC in 2006 (SAIC, Inc., 2006).

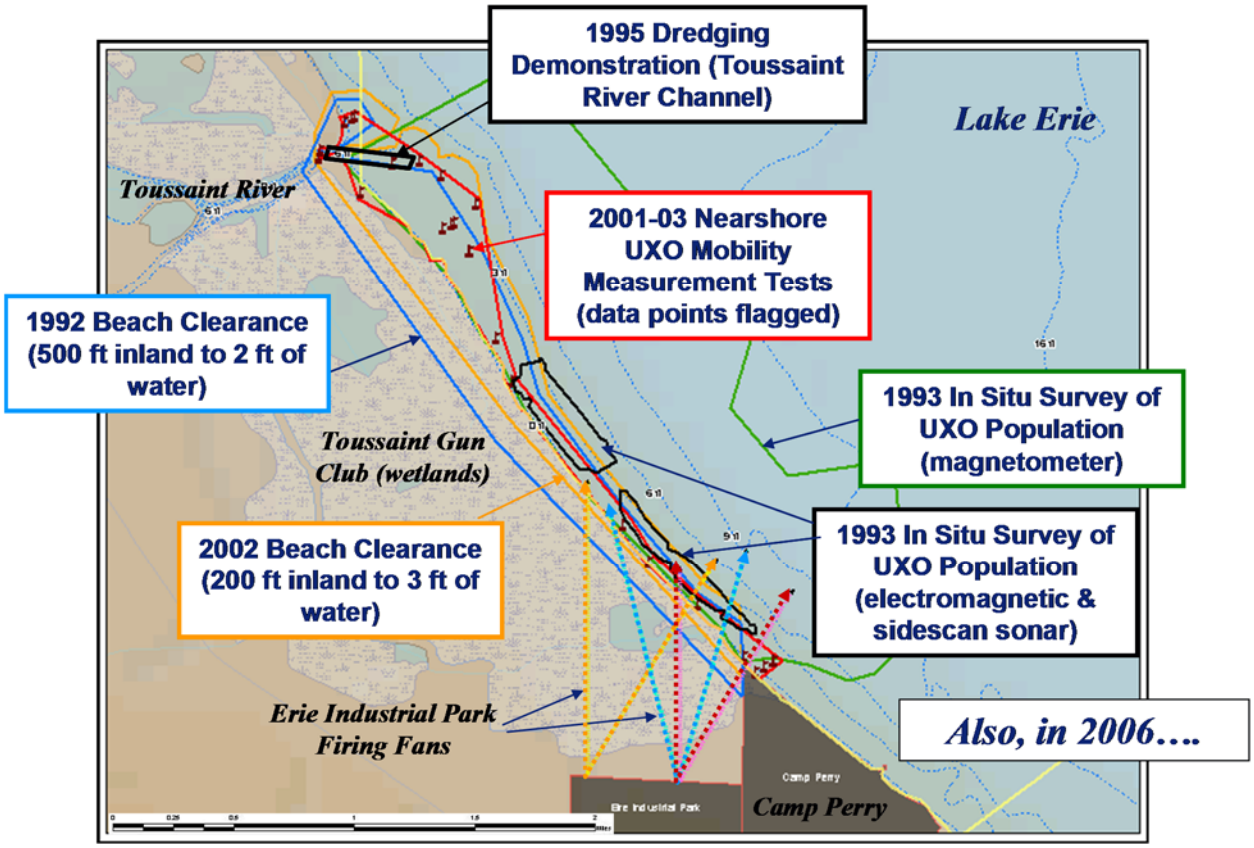

Figure 18. Locations of previous studies at Lake Erie Impact Range.

Beach Clearances (1992, 2002)

In the fall of 1992, a contractor removed or exploded in place all visible ordnance as well as ordnance buried up to 0.3m (1ft), from the still water surface to 152 m (500 ft) inland. A total of 5,438 ordnance items, from small caliber cartridges to large pieces such as 160 mm projectiles,

were identified and removed. The largest populations of ordnance were 20 mm (24%); 60 mm (23%); 106 mm (15%); and 105 mm (14%). Approximately 20% of the ordnance was classified as UXO (EOD Technology, Inc., 1992). In 2002, a similar clearance was conducted where 3,193 items were recovered, however, only 22 of the objects were classified as intact UXO items (American Technologies, Inc., 2002). Another clearance operation was conducted in May 2008, but as of the writing of this report, data are not yet available. There are plans in place to repeat the beach clearance every 3 years until 2057, or until no more UXO appears on the beach.

UXO Surveys by WES (1993)

During September 1993, the USACE WES, with site assistance from the Huntsville Division and the Buffalo District and several contractors, conducted a multi-instrumented geophysical and oceanographic field investigation to document site geological conditions, the influences of various coastal processes, and OEW distribution patterns. The surveys focused on two nearshore sections of the beach adding up to approximately 38% of the total area. Figure 19 and Figure 20 show the results of the magnetometer survey; Figure 21 and Figure 22 show the results of the electric field survey.

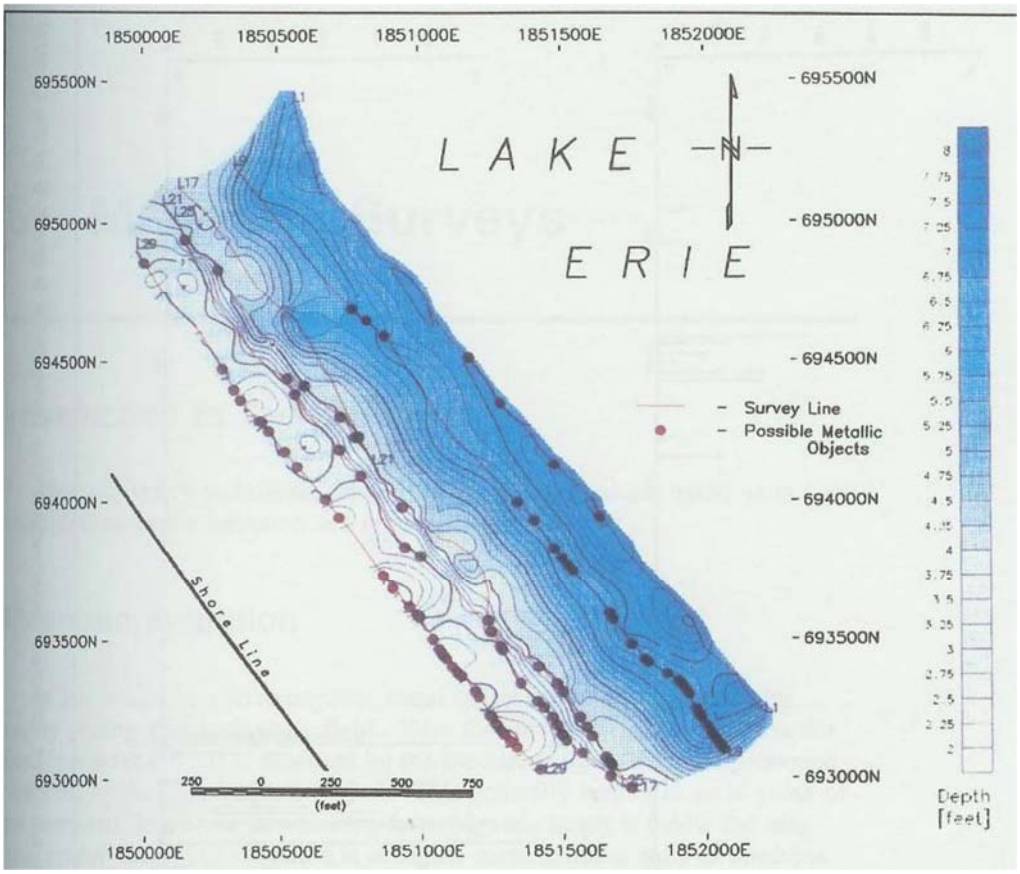

Figure 19. UXO detected magnetically (central zone), Camp Perry.

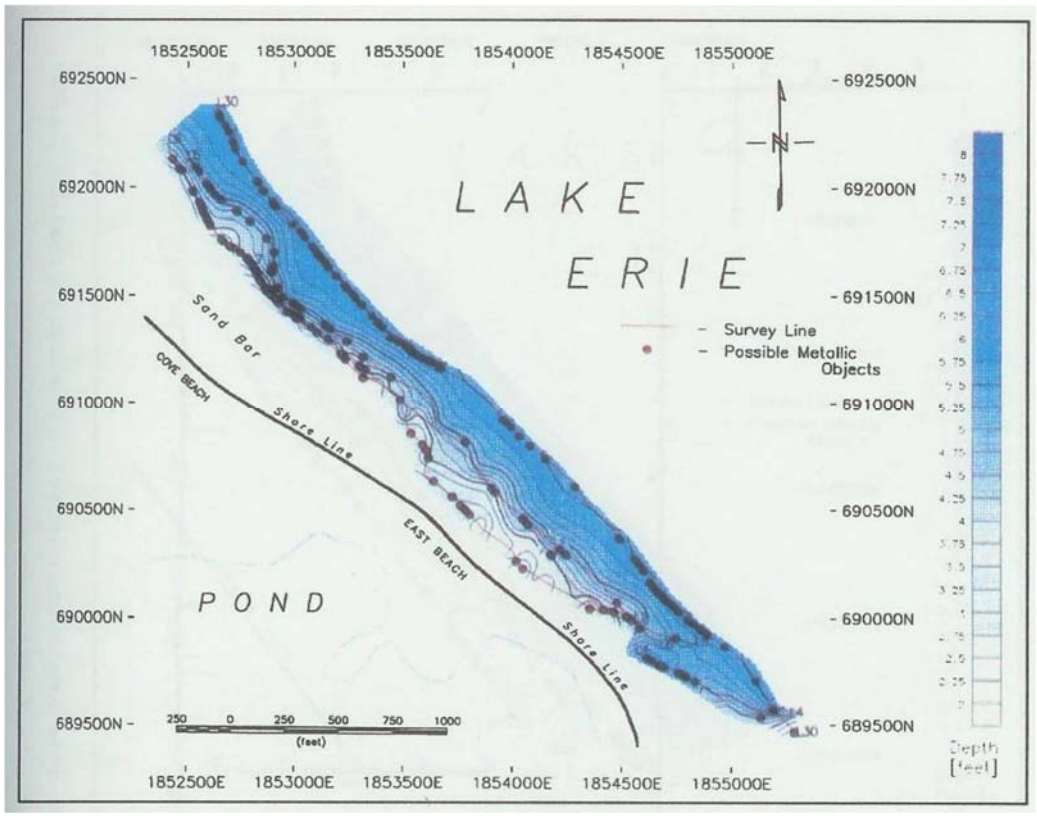

Figure 20. UXO detected magnetically (east zone), Camp Perry.

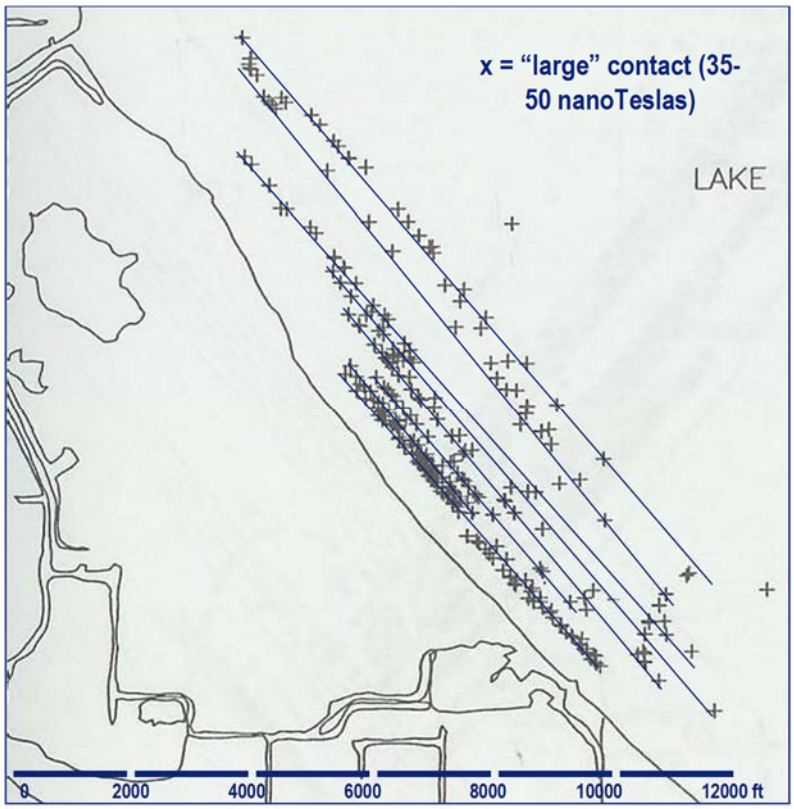

Figure 21. UXO detected electromagnetically (large targets), Camp Perry.

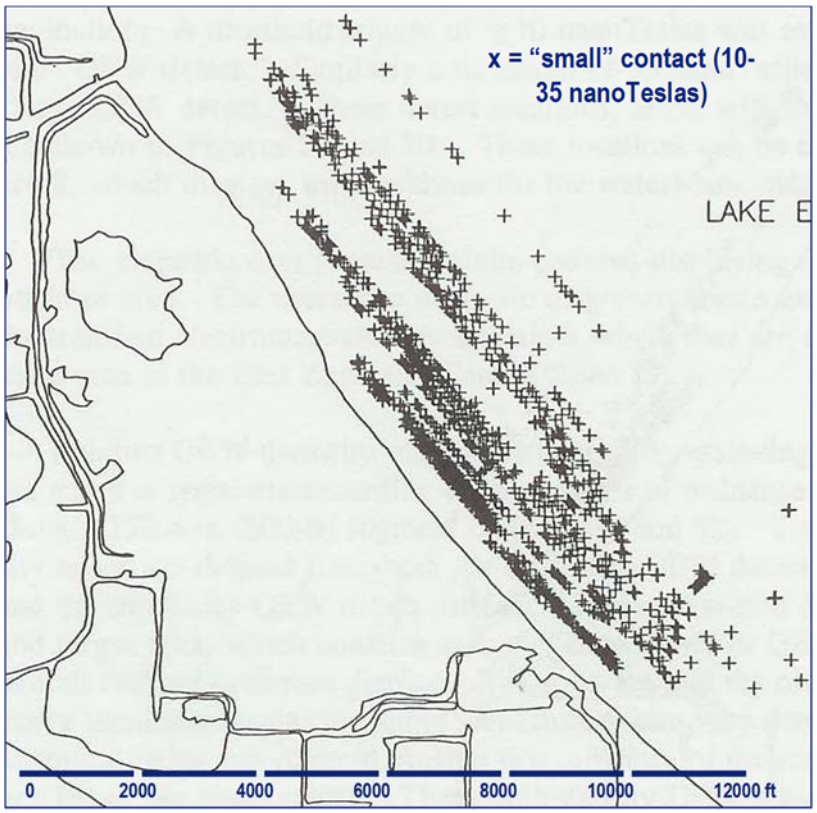

Figure 22. UXO detected electromagnetically (small targets), Camp Perry.

UXO Migration Study (2001-2003)

This study was undertaken to investigate the movement of realistic ordnance surrogates under wave and current conditions in a natural and significant setting. In addition, the potential for movement resulting from the action of lake ice was investigated. The ordnance-like objects that were deployed in this study were realistic simulations of ordnance that are known to have been fired at the Erie Proving Grounds. They were simulations of the following ordnance:

- 60-HE M49A3;
- 81-HE M56;
- 81-M43A1;
- 90-APT; and
- 106-HE M344.

The surrogates were deployed in nearshore areas (depths less than 6 ft) centered around the Toussaint River navigation channel, where they could potentially be moved into the channel; and alongshore southeast of the Toussaint River in documented impact areas, where they could potentially be transported toward the river. These locations were chosen to provide information on movement as it relates to the potential of encountering UXO during future dredging operations. Surveys to relocate and map the locations of the surrogates were conducted over a 2-year period,

during which a full range of actual wave, current, and ice conditions were experienced (Evans-Hamilton, Inc., 2003).

Evans-Hamilton indicated that the majority of the drogues placed in the study area exhibited mobility limited to approximately 1 ft. horizontal. These authors note that a few of the drogues traveled 5 to 6 ft. and one drogue, which was placed in the ice during deployment #2, traveled a distance of 49.919 ft. (Evans-Hamilton, Inc., 2003). Additionally, nearly all of the drogues eventually buried, with some under more than 1 ft. of sediment (Evans-Hamilton, Inc., 2003).

UXO Magnetometer Surveys (SAIC, 2006)

A magnetometer survey using both boat and helicopter platforms was conducted by SAIC in 2006 (SAIC, Inc., 2006). Figure 23 shows both the scan lines and the targets identified by these surveys. Because these surveys were conducted by the state-of-art magnetometer systems and subsequently validated by human observations, these data are the primary data set used in the validation exercises of the UXO IMM.

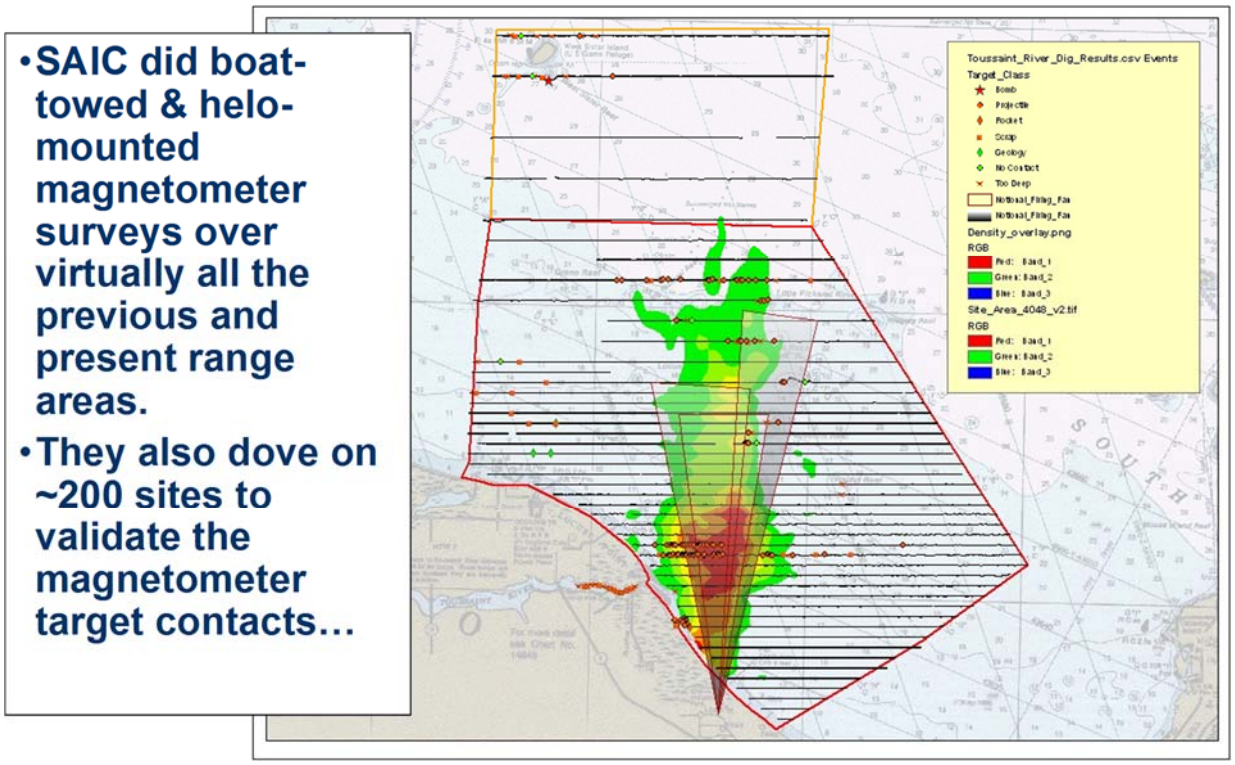

Figure 23. Marine towed array UXO magnetometer survey, Camp Perry.
(SAIC, Inc., 2006)
The small colored dots represent targets that were checked by divers.

5.5 VALIDATION

The magnetometer surveys were validated by diver observations for the UXO targets identified by the red dots in Figure 23. Figure 24 show the general distribution of the UXO in the near-shore of

FUDS beach. Selected magnetometer "targets" from Figures 23 and 24 were investigated by divers to confirm that targets were UXO, rather than other metal objects. The results revealed that the distribution was very consistent with the most recent firing fans.

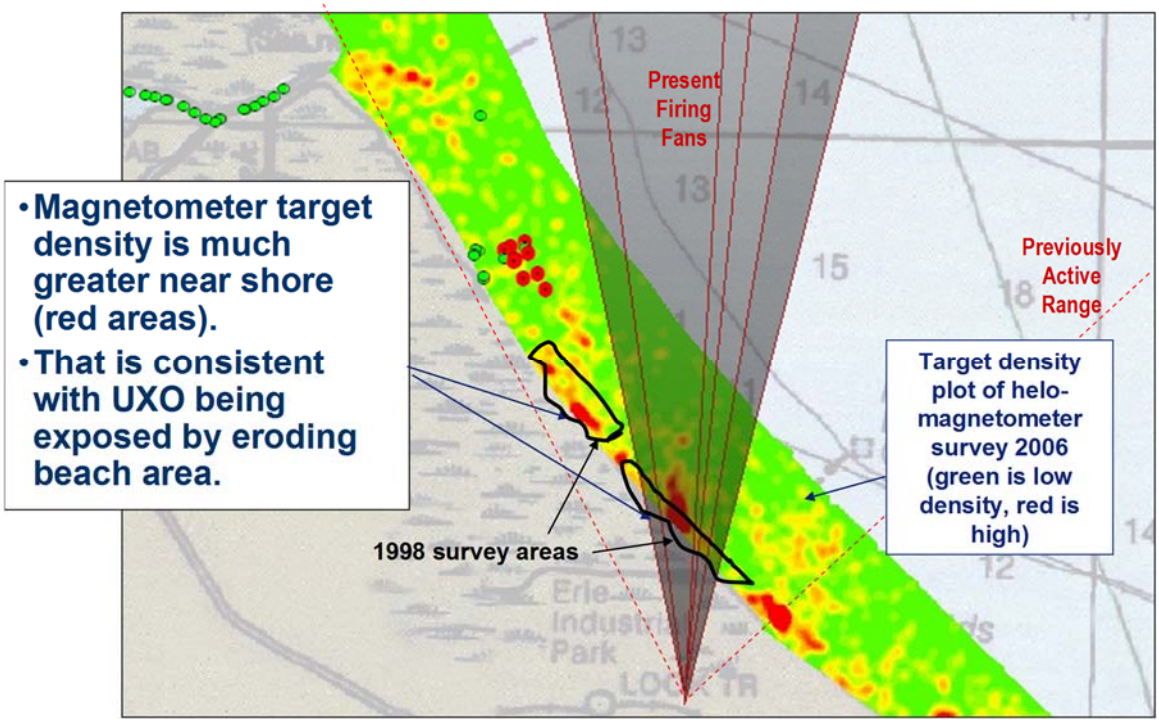

Figure 24. Results from the 1998 and 2006 nearshore UXO survey locations.
Red dots indicate targets validated by diver observations, Camp Perry (SAIC, Inc., 2006).

This page left blank intentionally.

6.0 DATA ANALYSIS AND PRODUCTS

The UXO IMM can be operated in three distinct modes depending on the data that are available for making a burial prediction and the user's desire to make site specific adaptations to the model's configuration. When little more than the general coastal setting and the time frame of UXO introduction and initial depth are known, the UXO IMM is run in Mode 1. Mode 1 predictions use pre-configured gridding systems, forcing functions, boundary conditions and calibration factors based on the coastal classification system. The seven input parameters required for Mode 1 operation are indicated by the *italicized* entries in Tables 4 and 5.

Table 4. UXO MM far-field input parameters.

Far-field Littoral Cell Model Parameters	
1	*Coastal Type: Collision, Trailing Edge, Marginal Sea/Narrow-Shelf Mountainous, Marginal Sea/Wide-Shelf Plains, Marginal Sea/Deltaic-Tideless, Marginal Sea/Deltaic-Tidal, Arctic Form of Cryogenic, Coral Reef Form of Biogenic*
2	*Estimated time when UXO entered the environment*
3	*Time period of prediction*
4	Deep water directional wave spectra or discrete height, period and direction estimates of principal band
5	Deep water wave height of antecedent extreme event
6	Wind speed
7	Precipitation or river flow rate data (Q)
8	Coefficients (a, b) of sediment rating curve (R = aQb)
9	Grid cell dimension x-axis (Longitude)
10	Grid cell dimension y-axis (Latitude)
11	Number of grid cells along the x-axis (Longitude)
12	Number of grid cells along the y-axis (Latitude)
13	Latitude/longitude of upper left hand corner of far-field grid (Raster formatted grid)
14	Stationary bathymetry file at start of simulation
15	Position of mean shoreline (0.0 m msl) at start of simulation
16	Distance offshore to closure depth
17	Median grain size of shelf sediments (seaward of closure depth)
18	Grain size distribution of shore rise and bar-berm sediments (as many as 9 size bins)
19	Volume concentration of seabed sediment
20	Tidal harmonic constituents
21	Longshore transport efficiency coefficient
22	Shore rise bottom friction coefficient
23	Breaker dissipation coefficient
24	Angle of internal friction

Table 5. UXO MM near-field input parameters.

Near-field Scour and Burial Model Parameters	
25	*Ordance type*
26	User selected grid cell(s) from far-field grid corresponding to UXO sweep area
27	*Coordinates of firing pit*
28	*Time of firing*
29	*Azimuth and inclination angles*
30	Grain size distribution of seabed sediments (as many as 9 size bins)
31	Local seabed elevation and slope from user selected grid cell of far-field model
32	Local orbital velocity from user selected grid cell of far-field model
33	Local tidal velocity from user selected grid cell of far-field model
34	Bed roughness
35	Seabed drag coefficient
36	Bedload transport efficiency
37	Suspended local transport efficiency
38	Angle of internal friction
39	Volume concentration of seabed sediment
40	User selected grid cell dimension for unregistered UXO type

When information is known about the gross site specific details of a suspected UXO field, then the UXO IMM can be run in Mode 2. Mode 2 operation makes burial predictions using pre-configured gridding systems and calibration parameters with user supplied bathymetry, wave and sediment data. The Mode 2 input parameters are the seven *italicized* and 13 underlined entries for parameters listed in Tables 4 and 5.

The UXO IMM is run in its most detail intensive configuration as Mode 3. This operational mode is for applications in which contemporary, high-resolution, site-specific information is known about the UXO field. This operational mode was used in field experiments at Ocean Shores in August 2003 and for both of the ESTCP field tests. Mode 3 is intended for experienced modelers, and allows for customized configurations of all gridding systems, calibration factors and file structures of forcing functions and boundary conditions. Mode 3 input parameters include all 40 parameters listed in Tables 4 and 5.

Note that these parameters are all measurable by, or derivable from, conventional ocean environmental measurement technology. The following are all sources for data needed for the Mode 3 UXO IMM operation: existing Defense Mapping Agency; charts; commercial surveys with multi-beam bathymetry/imagery; sub-bottom profiles; a series of core samples; and hindcast coastal wave, tide, and current measurements. The UXO IMM is very complete in the parameters it considers, but does not demand new technology or great expense to collect the required data. The inputs allow deterministic simulations of UXO behavior. The UXO IMM simulations then allow long-range predictions based on stochastic application of site-specific climatic conditions. The accuracy of the UXO IMM predictions is limited almost entirely by the statistics of the inputs.

6.1 PREPROCESSING

The model was gridded, as described in Section 5.2, for a fine to medium-coarse sand bottom that was parameterized by 20 grain size bins according to the grain size distribution shown in Figure 25. The cumulative distribution in Figure 25 (blue line) reveals that the FUDS Beach sand at Camp Perry is moderately well sorted by the wave action, but also includes some coarse sands and gravels overlying lacustrine clays. Mineral analysis indicates it is predominately quartz of glacial origin with a moderate organic content (approx. 3 to 7%) associated with the underlying peat deposits and organic rich silts and clays that are occasional exposed by erosion of beach profiles due to storms and rises in lake water levels. The median grain size is 485 microns, and 70% of the sediment is comprised of medium-coarse sand between 305 microns and 820 microns. These sediment characteristics are well suited for the ideal granular relations used in the VORTEX (Jenkins et al., 2006).

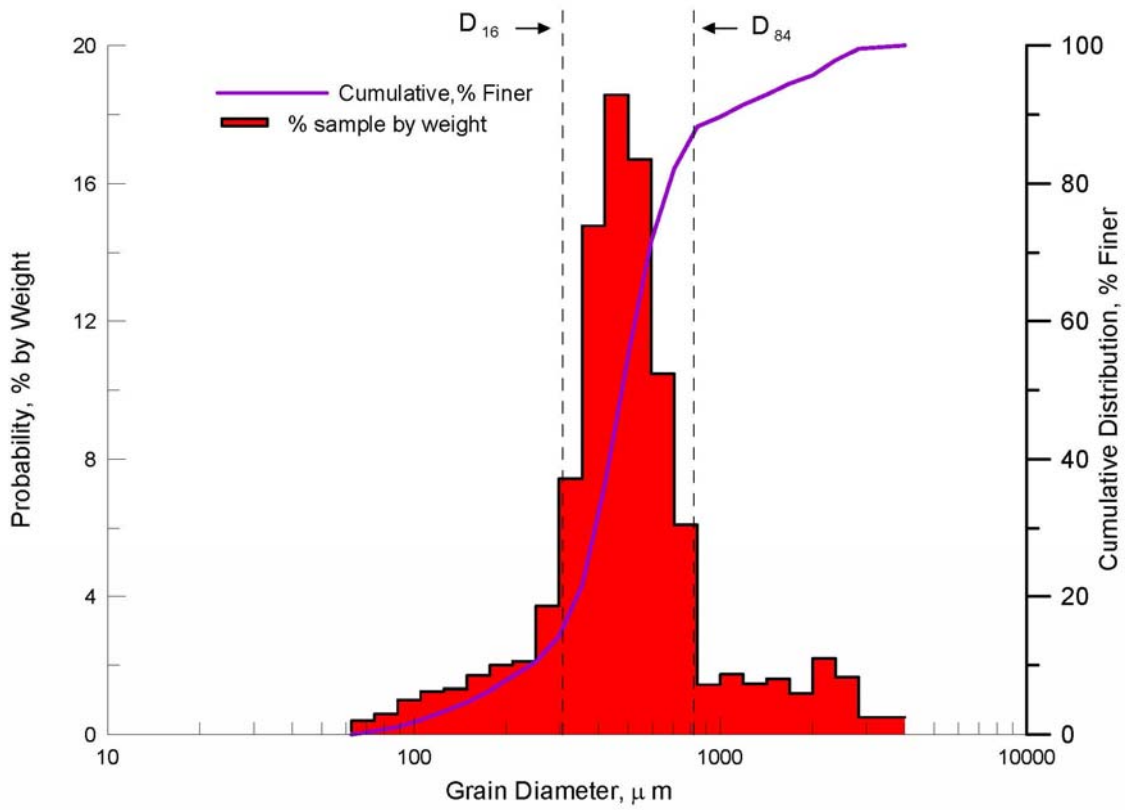

Figure 25. Grain size distribution of Lake Erie bottom sediment off Camp Perry FUDS Beach, June 1990, Range-line #10579.

For the non-stationary bathymetry data inshore of closure depth (less than -3.35 m LWD), the project team used the equilibrium beach algorithms from Jenkins and Inman (2006). Depth contours generated from these algorithms vary with wave height, period, and grain size, and are calibrated from beach profile surveys at FUDS Beach (Figure 26). These surveys were used to calibrate the elliptic cycloid algorithms of the model to predict profile evolution over the 28-year duration of the simulation. Unfortunately, only two sets of beach profile surveys have been identified for the FUDS Beach site (see Pope et al., 1996)—one performed by the USACE in 1973

and the other in 1990). The type-b cycloid algorithms in the VORTEX were found to give the best fit to the measured profiles. The type-b cycloid has been built into the G-95/field research facility (FRF) version of the VORTEX code and the algorithms are detailed in NFESC (2008). These profile algorithms use a general solution of the form:

$$h = \frac{\pi \varepsilon x}{2I_e^{(1)}}\left(\frac{1 - cos\theta}{\theta - sin\theta}\right) = r(1 - cos\theta) \tag{6}$$

Here, h is the local depth; ε is a stretching factor proportional to the Airy wave mild slope factor (Jenkins and Inman, 2006); x is the on-off shore position; r is the radius vector measured from the center of the cycloid ellipse whose semi-major and semi-minor axes are a, b; e is the eccentricity of the cycloid ellipse given by $e = \sqrt{1 - b^2/a^2}$; $I_e^{(1)}$ is the elliptic integral of the first kind; and θ is the angle of rotation of the cycloid (for more details, see Jenkins and Inman, 2006). The cycloids are given by the trajectory of a point on the circumference of an ellipse that rolls seaward in the cross-shore direction under the plane of $h = 0$. This trajectory defines the elliptic cycloid and the segment traced by the first half of a rotation cycle $(0 < \theta < \pi)$ of the rolling ellipse is the equilibrium beach profile.

The depth of water at the seaward end of the profile $(\theta = \pi)$ is $h = 2b$ for the type-b cycloid. The length of the profile X is equal to the semi-circumference of the ellipse:

$$X = \frac{2bI_e^{(1)}}{\varepsilon} \cong \frac{\pi b}{\varepsilon}\sqrt{\frac{2 - e^2}{2(1 - e^2)}} \qquad \text{at } \theta = \pi \qquad \text{(type-b cycloid)} \tag{7}$$

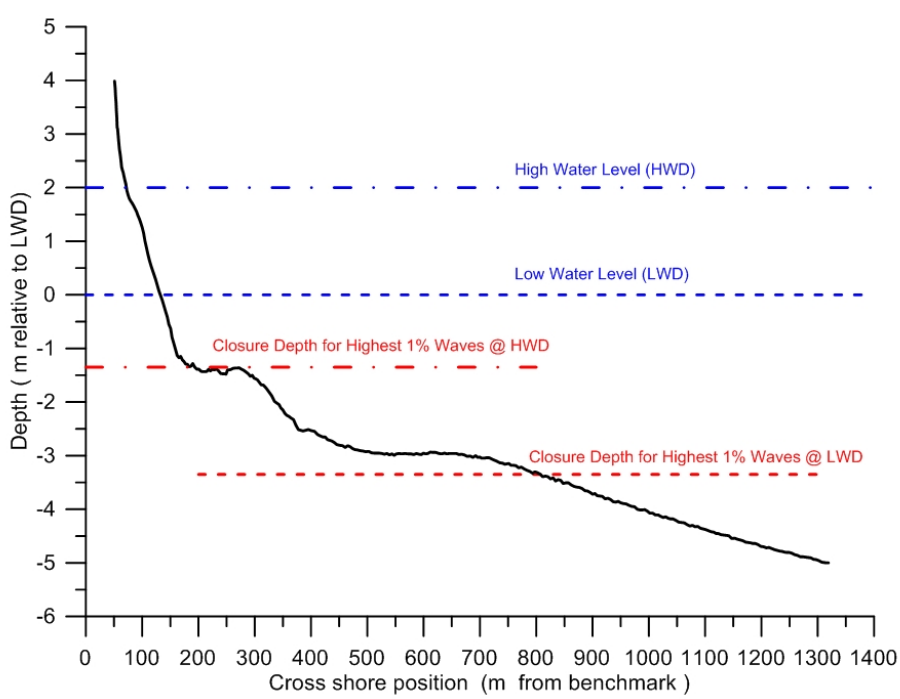

Figure 26. Beach profile variation due to lake water level variation, Camp Perry FUDS Beach, based on low water survey at Rangeline 10579, June 1990.
Vertical elevation shown in meters relative to the LWD at about 174 m msl.

The measured FUDS Beach profiles (Figure 26) were used to calibrate the parameters (e, b) in equations (1) and (2) using a best fitting process that minimizes the mean squared error between the type-b cycloids of the bar berm (red) and shore rise (orange) versus the measured profile (grey). Profile elevations are expressed in terms of LWD that is approximately 174 m above msl. General characteristics of the Camp Perry profiles of note are: the relatively shallow (by ocean standards) shore parallel break point sand bar located at the intersection of the bar-berm and shore-rise cycloids at a depth of about -1.3 m LWD, about 270m offshore; the low-steepness shore rise profile with a slope of about 1:300; and the relatively high berm crest that includes several beach ridges formed by wave over-wash during extreme event storms, many of which are crested by scrubs and trees.

An interesting feature of these calibrated cycloid profiles is that the closure depth was only $h_c \cong 3.35$ m LWD based on the highest 1% waves (Figure 30). In open ocean environments, closure depth is normally about twice that value (Jenkins and Inman, 2006). This difference reflects the fetch-limited characteristics of the lake environment, limiting wave periods to typically 3 sec to 6 sec, and thereby reducing the depths at which wave orbital velocities exceed transport thresholds. Because of this fact, the critical mass of sediment in which UXO are likely to be exposed due to beach profile changes, is limited to a relatively narrow band near shore, shoreward of the -3.35 LWD depth contour (see Section 9.0).

Wave and current forcing are derived from NOAA Bouy #45005 (Figures 27 and 28). Spatial variation in wave forcing passing through the Catawaba and Bass Island complexes is derived from REF/DIF analysis over the far field grid as shown in Figures 29 and 30, based on directional wave measurements from NOAA Buoy #45005 in the western basin of Lake Erie. Figures 29 and 30 use the directional wave buoy data to specify the deep water boundary conditions north of the island complexes in the calculation of the shoaling wave field across the Toussaint River/FUDS Beach Littoral Cell. This calculation is based on REF/DIF analysis as detailed in Dalrymple et al. (1984). Figure 29 provides spatial detail of the shoaling waves from the extreme event storm (maximum design wave) from the 28 year long period of record of NOAA Buoy data. This was a late winter *northeaster* occurring April 10, 1998. In Figure 29, it is apparent how the offshore island complexes break up the incoming northerly waves into a series of directional beams along the Toussaint River/FUDS Beach Littoral Cell. Figure 30 shows the corresponding shoaling response to a set of wave height, period and direction combinations that statistically represent the highest 1% waves occurring in the west Lake Erie basin according to the probability density functions appearing in Figure 28. In either case, directional beams induced by the offshore islands and hummock features from glacial till outcrops produce a pronounced pattern in the nearshore of shadows (regions of locally smaller waves) and bright spots (regions of locally higher waves).

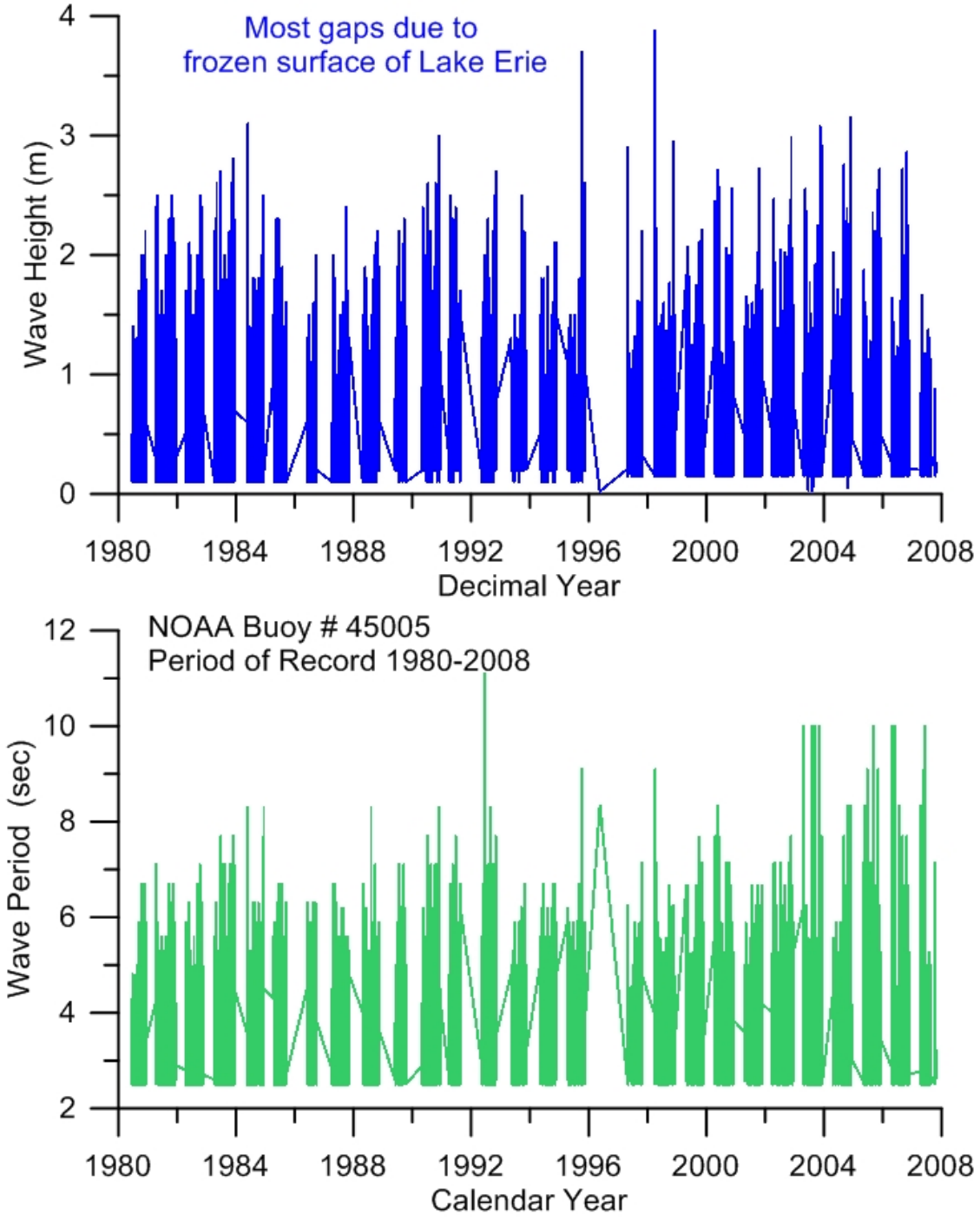

Figure 27. Deep water wave heights (upper) and periods (lower) in western Lake Erie for entire period of record for NOAA Buoy #45005, 1980-2008.
Data gaps due to winter icing of lake surface.

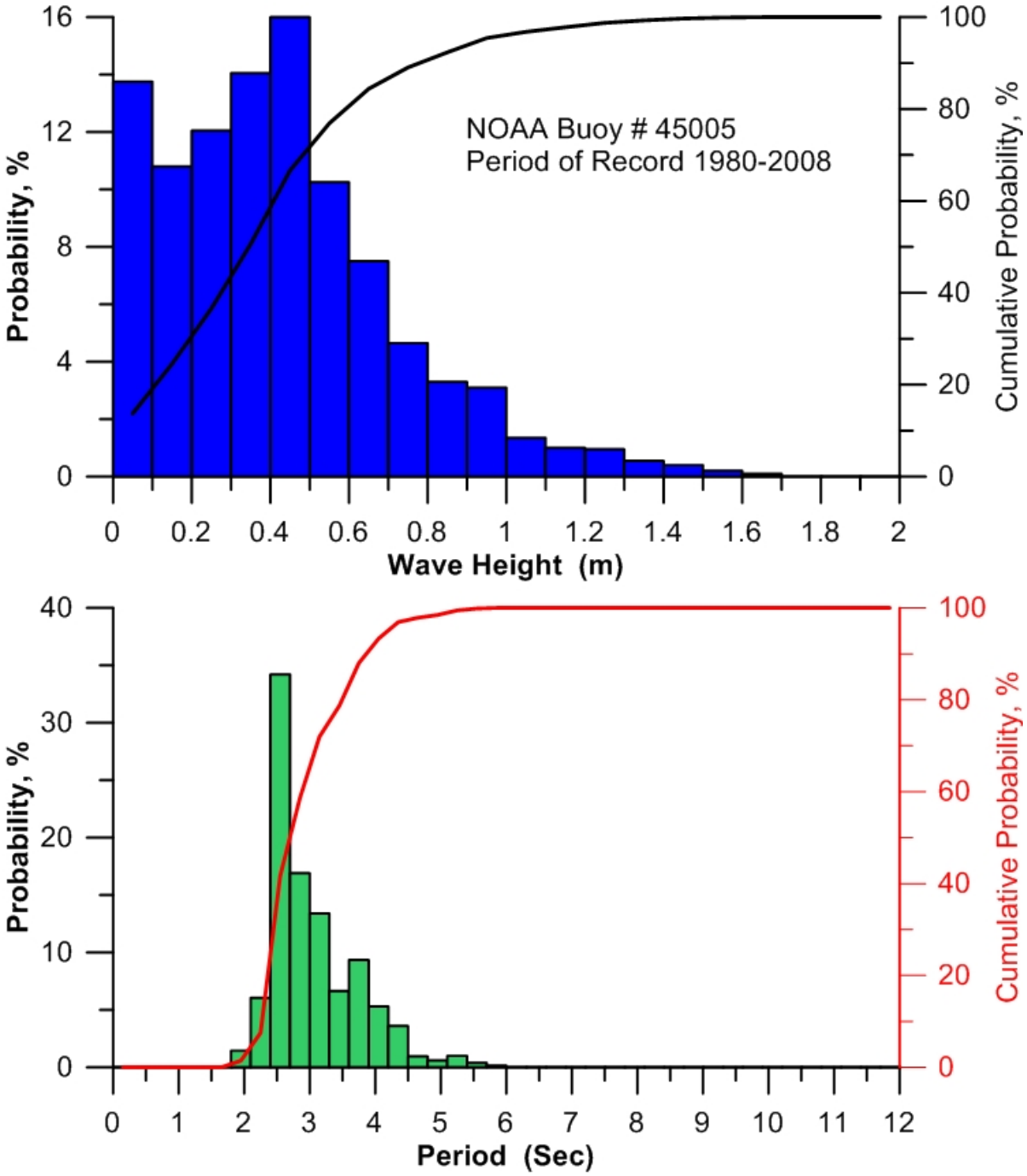

Figure 28. Probability density functions of deep water wave heights (upper) and periods (lower) in western Lake Erie for entire period of record for NOAA Buoy #45005, 1980-2008.

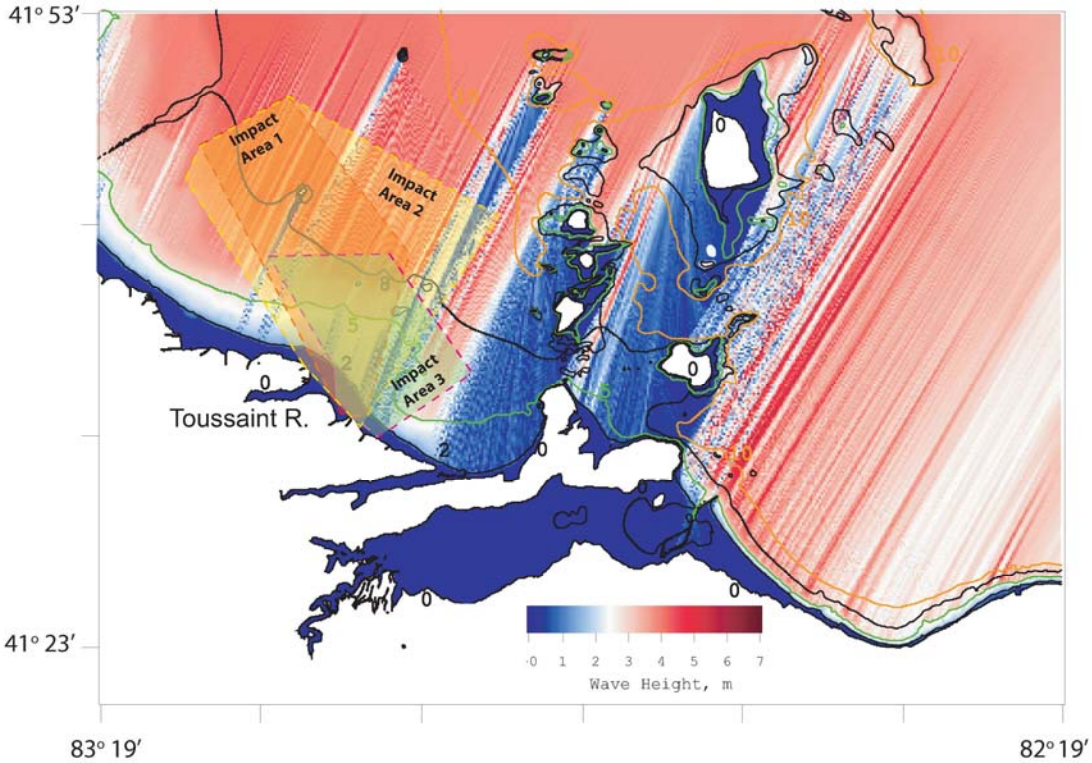

Figure 29. Extreme event REF/DIF pattern, Camp Perry, 10 April 1998, deep water wave height = 3.58 m, period = 9.09 sec, direction = 80 degrees (true).

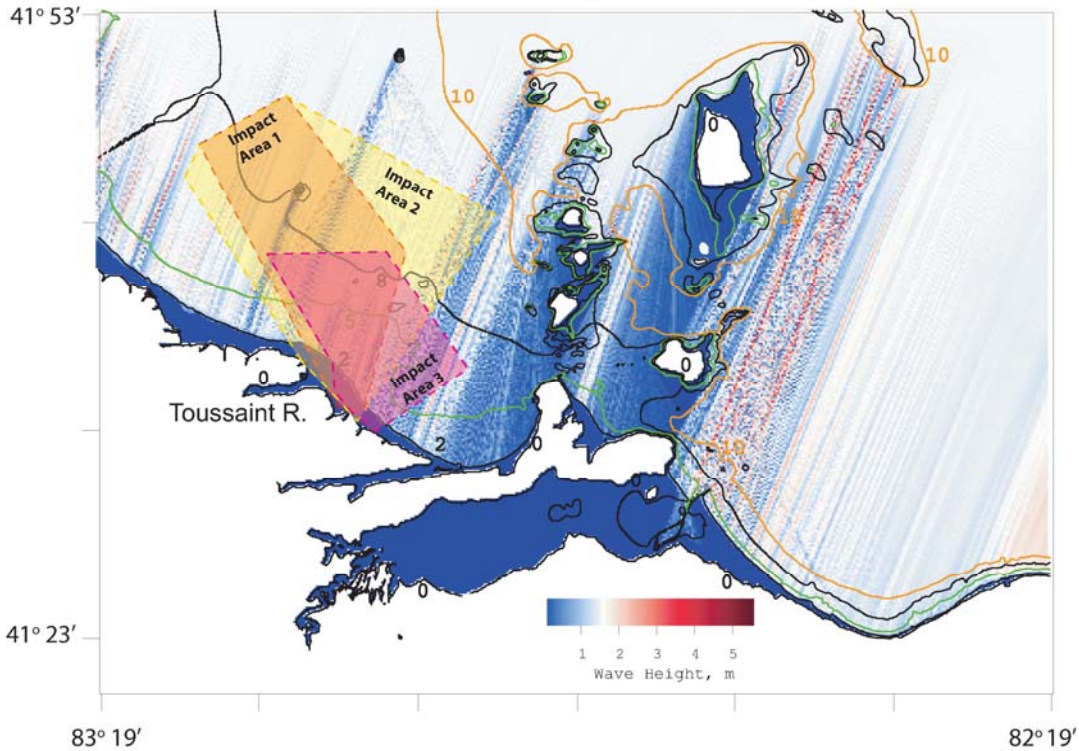

Figure 30. REF/DIF pattern due to highest 1% of Lake Erie wind waves at Camp Perry, deep water wave height = 1.5 m, period = 5 sec, direction = 45 degrees (true).

Wave-driven nearshore currents flow away from bright spots and converge on shadows. Consequently, the predominate longshore current in the Toussaint River/FUDS Beach Littoral Cell flows from northwest towards the south east, away from the Toussaint River mouth and towards Camp Perry. The REF/DIF patterns typical of Figures 29 and 30 also produce a negative divergence of drift along FUDS Beach, which in combination with sediment trapping by the channel and shoals at the mouth of the Toussaint River (Hardman, 1984; Boyd, 1989; DeWillie, 2000) result in long term progressive shoreline recession at FUDS Beach (Pope et al, 1996). The northerly waves are also found to produce considerable banding between shadows and bright spots long the reach of coast between the Toussaint River and the FUDS Beach at Camp Perry. The along shore variation in wave height between these localized shadows and bright spots produces considerable divergence of drift with associated rip cells and complex transient bar formations of the type shown in the Figure 26 beach profile. The evolution of these ephemeral sedimentary bedforms provide one set of dynamics for exposing or burying UXO in the nearshore in the zone between closure depth and the beach berm.

Repeated wave shoaling computations with the buoy data (#45005) as shown in Figures 27 and 28, allow simulations of continuous long term shore rise and bar berm profile evolution typical of Figure 26, spanning a 28 year period of record. However, both the wave shoaling and profile simulations will be sensitive to lake water levels, which can vary significantly over time.

The project team specifies lake water level variations in the forcing function module of the VORTEX (Figure 1), based on historic water level measurements by the NOAA gage station #9063085 that is located in the western basin of Lake Erie at Toledo, OH (NOAA, 2008). Figure 31 gives water level variations over the entire period of record in the upper panel and the inter-annual variations of the last 11 years in the lower panel. The mean water level for the period of record is 174 m relative to the International Great Lakes Datum (IGLD). Lake water levels can vary by as much as 1 m above and below that elevation, which can cause as much as 600 m variation in the width of the beach and the critical mass zone shoreward of closure depth when superimposed on shore rise and bar berm profiles having the slopes typical of those measured at FUDS Beach in Figure 26. As we consider in later sections of this report, such variations can have a profound effect on the exposure and burial of UXO through the adjustments these water levels impose on the equilibrium profile. The lake water level variations have a much stronger effect than tides have on beach equilibrium because the lake water level changes are more persistent and longer lasting than tidal variations. Lake water levels respond to both seasonal and longer term climate variations. The snow melt and runoff in spring typically causes inter annual maximums in lake water levels, while El Nino Southern Oscillation (ENSO) climate oscillations can produce large scale flooding through the Midwest in spring and summer. The lake level maximums in 1997 and 1998, apparent in the lower panel of Figure 31, are a result of ENSO induced floods and extreme snow cover. Because of the large gap in the period of record, the lake water level data can be folded backward in time to 1980 to provide inter-annual water level variation concurrent with the early portion of the wave record in Figure 27.

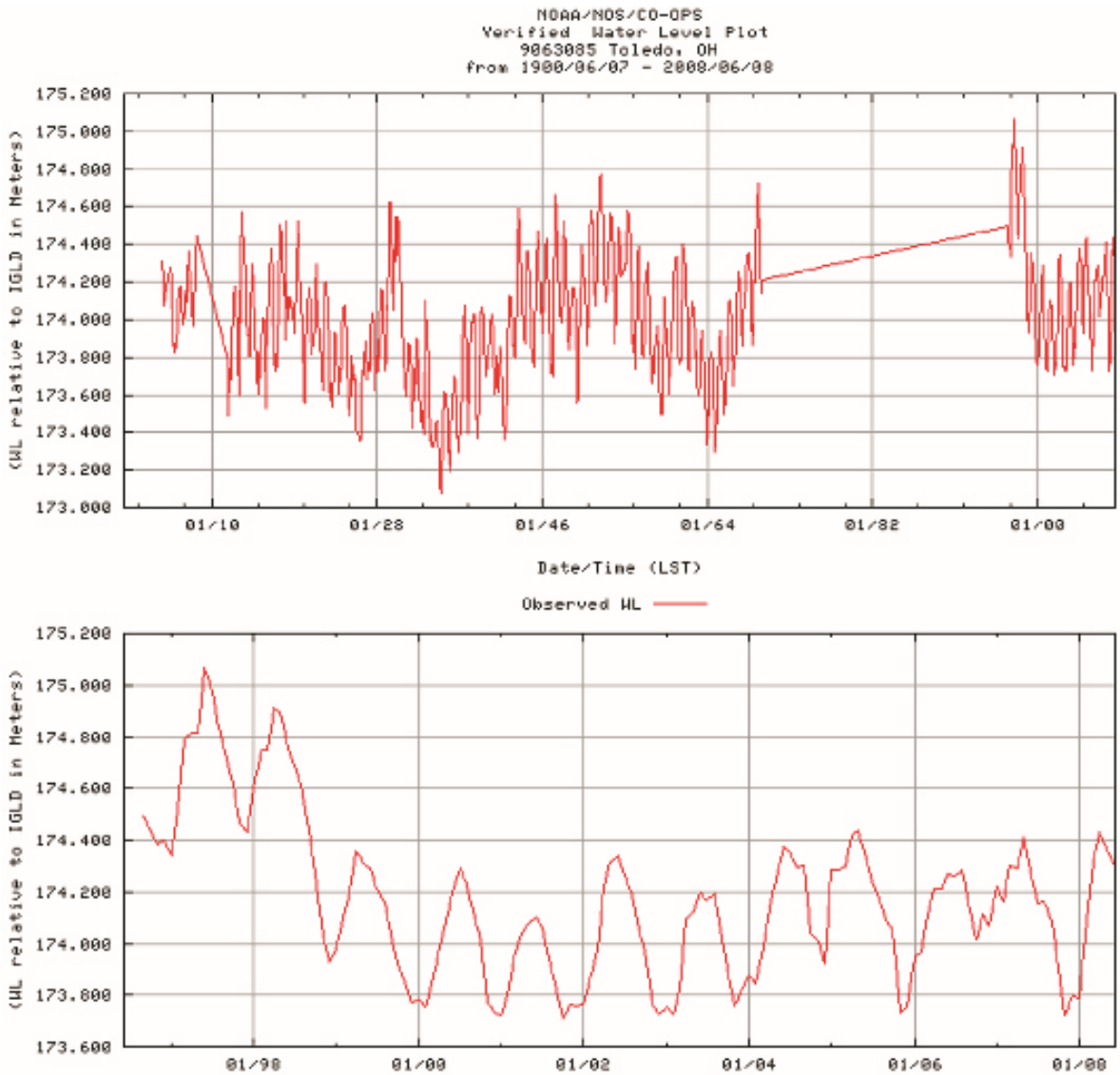

Figure 31. Historic water level variation, Lake Erie from NOAA Station 9063085, Toledo, Ohio.

Period of record (upper), inter-annual variations (lower).

6.2 TARGET SELECTION FOR DETECTION

To provide a systematic and manageable set of inputs for shape-specific calibration parameters, the model simulations concentrated on four basic classes of U.S. Army artillery rounds fired into the Camp Perry Impact Areas I-III. This ensemble of rounds spans the basic range of calibers used on The Range, including: 60 mm M49A2; 81 mm M43A1; and 106 mm M344 rounds. These rounds have the same general body geometries, but vary somewhat in fin configuration, the most complex being the 106 mm M344 round shown in Figure 14, which was the predominant *"large contact"* found by the 1996 electromagnetic (EM)-survey (SAIC, 2006). These shapes were approximated by an elliptic frustrum revolved about the major axis of the round, say the y-axis, taken for example as the transverse axis to the mean flow. For this orientation, the generalized shape of the round can be represented by the analytic expression:

$$R(y) = a - a\left(\frac{y}{S}\right)^{\beta} \tag{8}$$

Here, $a = D/2$ is the basal radius and D is the basal diameter of the round; $R(y)$ is the local radius at any arbitrary location y along the major axis of the round; S is the total length of the round as measured along the y-axis; and β is a constant that adjusts the *taper* of the round. A best fit of Equation (8) to the 60 mm M49A2 round results in a β = 2.51; the 81 mm M43A1 round has a $\beta = 2.87$; and the 106 mm M344 round has a $\beta = 3.47$. These values contrast with the Navy 5"/38 round from previous model studies (Jenkins and Wasyl, 2007; 2008) that used $\beta = 3.5$. =3.5. To accommodate these dimensions and the small radius curves of the shape, the VORTEX shape lattice files for all U.S. Army rounds studied was gridded for 1 mm grid cells, as compared to 3 mm grid cells for the Naval rounds modeled in Jenkins and Wasyl (2007; 2008).

6.3 PARAMETER ESTIMATION

Using the analytical statistical approach to error assessment, the predictive skill factor of the UXO migration distance is computed, ξ, and burial depth, h, as quantified by an estimator adapted from the mean squared error. For burial depth, the skill factor, R_h is of the following form (adapted from Jenkins et al., 2007):

$$R_h = 1 - \frac{1}{N\hat{\sigma}_i}\left\{\sum_{1}^{i=N}\left[\hat{h}(i) - h(i)\right]^2\right\}^{1/2} \tag{9}$$

where $\hat{h}(i)$ is the measured burial depth for i = 1, 2..., N observations, $h(i)$ is the predicted burial depth for the ith observation, and $\hat{\sigma}_i$ is the standard deviation of all observations over the period of record. For migration distance, the skill factor, $R_>$, has a similar form:

$$R_\xi = 1 - \frac{1}{N\hat{\sigma}_i}\left\{\sum_{1}^{i=N}\left[\hat{\xi}(i) - \xi(i)\right]^2\right\}^{1/2} \tag{10}$$

where $\hat{\xi}(i)$ is the measured migration distance for i = 1, 2..., N observations, and $\xi(i)$ is the predicted migration distance for the ith observation.

6.4 TRAINING

The technical lead for the overall analysis must be an engineer whose technical background includes a familiarity with ocean processes and the general principles of computer modeling, as well as the general principles of data collection on the types and amounts of human activity in coastal areas. This lead engineer also needs to be experienced in basic project management and be a liaison with the site UXO manager as well. In order to conduct the entire risk analysis, the lead engineer must be able to use Esri ArcGIS software and the Microsoft Excel spreadsheet program, and be familiar with the overall processes described in Garood (2008).

The lead oceanographer/coastal scientist must be skilled in locating the sources of environmental data (e.g., waves, currents, bottom types, etc.), acquiring those data sets for the time periods of interest, and formatting those data to serve as inputs to the UXO IMM. The lead scientist also

needs a general understanding of coastal processes, basic hydrodynamics, and related ocean engineering technologies in order to assist in setting up the model inputs and understanding its outputs.

Finally, the UXO IMM itself needs to be run by a person skilled in the using basic Fortran programs for computer modeling purposes. The UXO IMM is a Fortran program than will run on a variety of professional-grade laptop or desktop computers, so the user must be capable of compiling and running Fortran programs.

Of course, the above list of skills and abilities may be provided by various possible combinations of individuals. During various stages of the UXO IMM development effort, the analysis work was conducted by as few as two and as many as four to six people.

The detailed requirements for software, computer hardware, and user skills are described in the User's Manual by Garood (2008).

6.5 CLASSIFICATION

Unclassified.

6.6 DATA PRODUCTS

Prior to considering the influence of the local bathymetry and forcing history on the burial and migration response of the UXO, the model is tested in Mode 1 using the UXO shape lattice files resting on a flat planar bed with the Camp Perry grain size distribution (Figure 25) and wave forcing equivalent to the highest 1% waves (Figure 30). Figures 32 and 33 present the modeled instantaneous vortex and scour field produced from a 106 mm M344 UXO round resting proud on the bed with the major axis aligned transverse to a train of 1.5 m high monochromatic waves with 5 second period propagating from right to left. This orientation provides the worst-case assessment for UXO migration (Jenkins et al., 2007). Figure 32 shows the instantaneous streamlines in a plane at the top of the wave bottom boundary layer parallel to the bed plane, whereas Figure 33 shows the same flow field as viewed by instantaneous streamlines in a plane orthogonal to the bed plane and intersecting the UXO in the region of its tail fins. The wave oscillatory velocity amplitude at the top of the bottom boundary layer is 105 cm/sec. This velocity amplitude corresponds to the super-critical transport regime (Jenkins et al., 2007) for the grain size distribution in Figure 25. In this regime, flow separation with a basal vortex is observed on the down-wave (shoreward) side of the UXO, particularly around the tail fins. These strong vortices induce scour and local erosion of the bed around the UXO, forming a pronounced scour hole (Figure 33). As the scour hole deepens, the round slips or rolls into the hole, resulting in migration and burial through what is known either as a *scour and slip* or *scour and roll* burial sequence (Jenkins et al., 2007; Inman and Jenkins, 2002). Unlike previous simulations of this type using Naval rounds, the tail fins of the Army rounds dig into the bed sediments and act like *shear-plate anchors*, thereby resisting tendencies of the round to roll or slip into its scour hole. For this reason, our Mode 1 simulations generally find reduced migration of Army UXO relative to Naval UXO of equivalent size and weight under equivalent forcing (Jenkins and Wasyl, 2007; 2008).

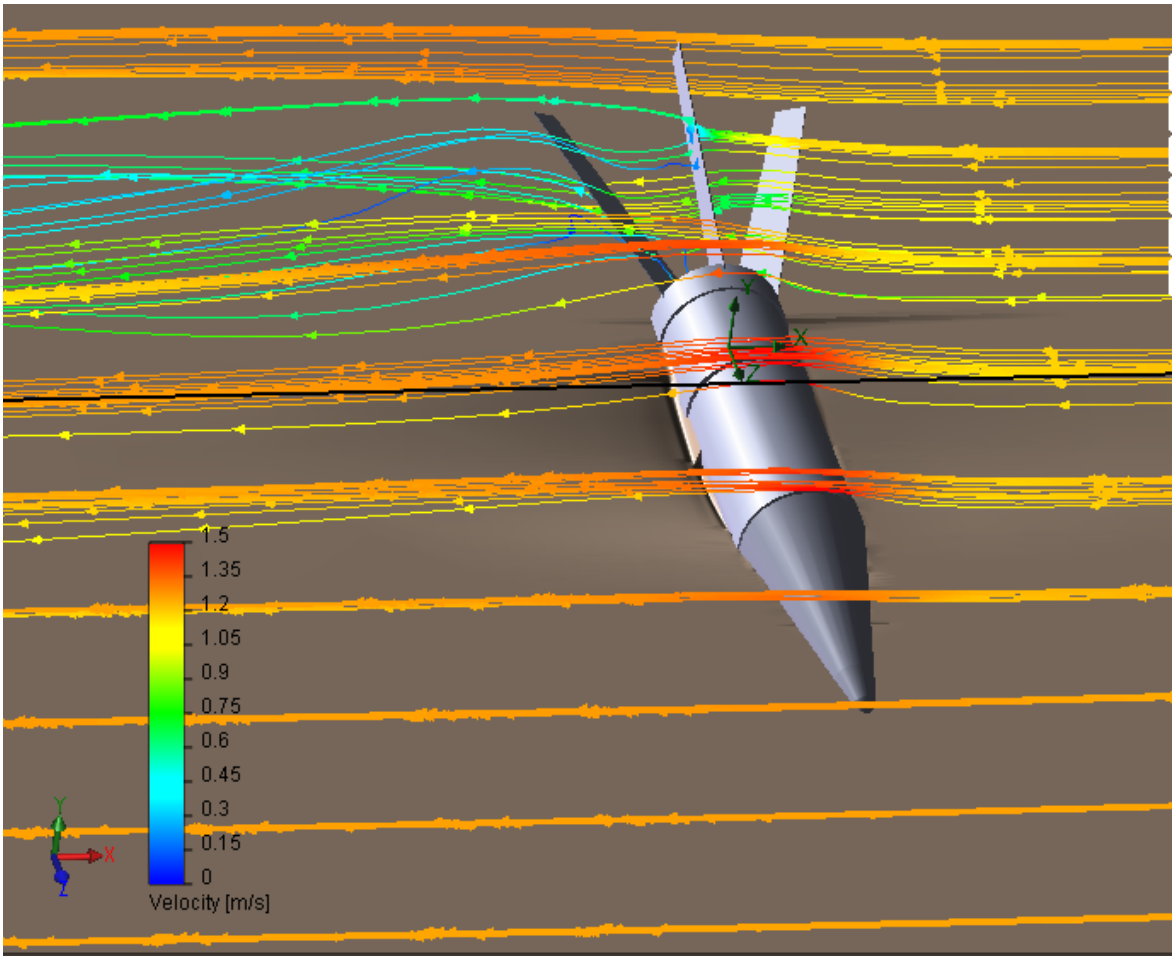

Figure 32. Simulation of vortex and scour field from a Mode 1 simulation of the 106 mm M344 round after an oblique-skip entry mode.

Streamlines are shown in the bed-parallel plane at the top of the wave boundary layer. The UXO round is shown 52% buried in a medium-coarse sand bottom (cf. Figure 25) under a wave crest propagating from right to left at super-critical velocity amplitude.

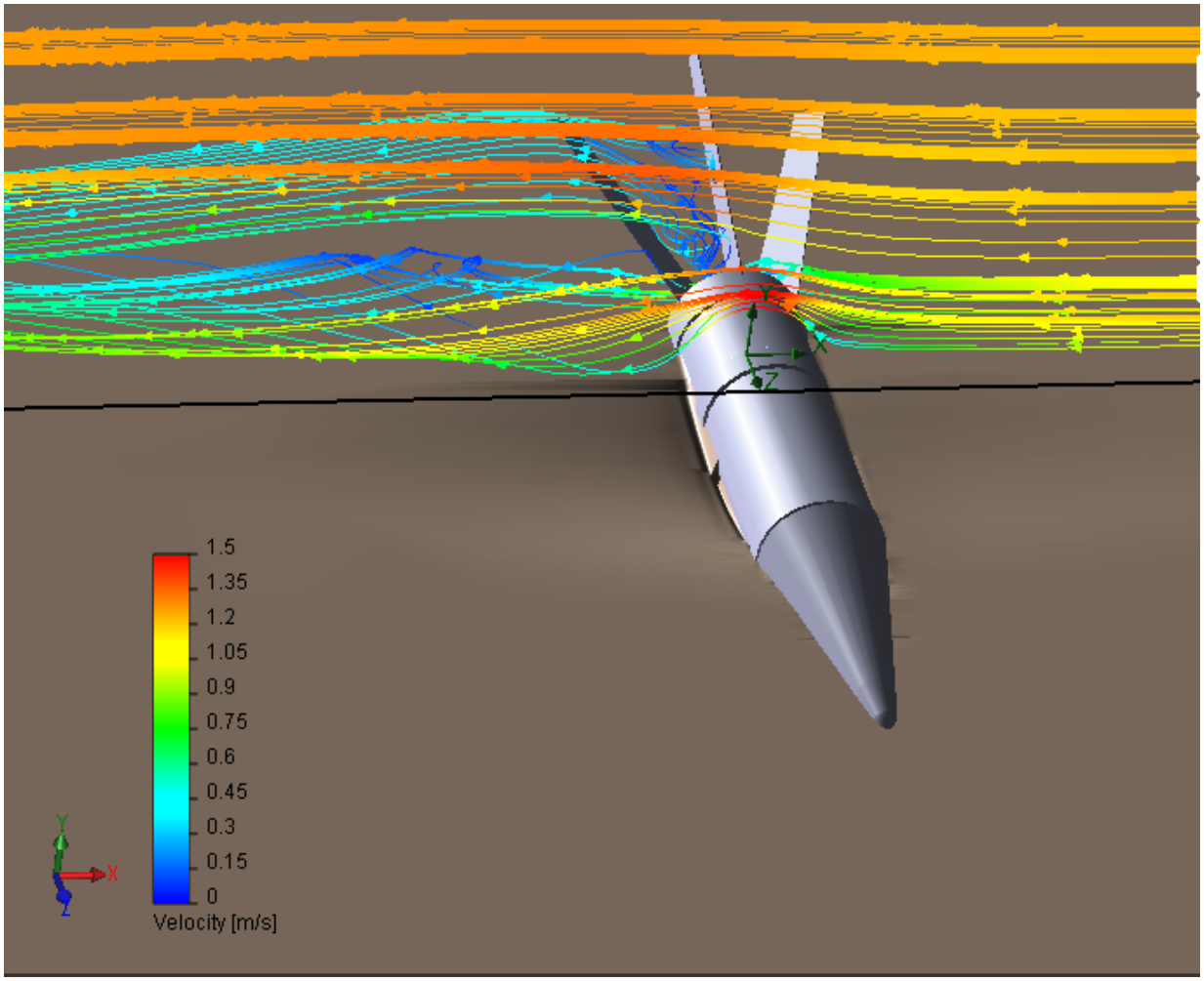

Figure 33. Simulation of vortex and scour field from a Mode 1 simulation of the 106 mm M344 round after an oblique-skip entry mode.

Streamlines are shown in the bed-normal plane at the aft section of the round. The UXO round is shown 52% buried in a medium-coarse sand bottom (Figure 25) under a wave crest propagating from left to right at super-critical velocity amplitude. Note scour hole on down-wave (shoreward) side of the round.

At the instant the flow field in Figures 32 and 33 was calculated, the burial/migration progression of the UXO had advanced to a state of 52% burial. At more advanced stages in the burial/migration progression referred to as *lock-down*, burial becomes sufficiently extensive that migration is no longer possible (Jenkins et al., 2007). For excitation by monochromatic waves of various periods and heights, the distance a Naval UXO migrates before lock-down occurs usually has a monotonic dependence on a parameter of dynamic similitude referred to as the Shield's parameter (Jenkins and Wasyl, 2007; 2008). However, because of the *shear-plate anchoring effect* of the tail fins on an Army UXO, this parametric dependence of migration distance on Shields parameter was generally found to be intractable. Orientation of the Army round relative to the flow was more important. The greatest migration distances of Army rounds prior to burial lock-down occurs when the axis of the round at its tail fins is orthogonal to the mean flow, while the least migration occurs when the axis of the round is parallel to the mean flow.

For shallow water waves in the typical Toussaint River/FUDS Beach Littoral Cell period band of 3 sec to 7 sec, Mode 1 analysis shows that little burial or migration of the Army UXO occurs for wave heights less than 1.0 m (sub-critical regime), (Jenkins et al., 2007; Wilson et al., 2008). Inspection of the historic wave height histogram in Figure 28 indicates that even an exposed or newly laid UXO would have no more than a 4.5% probability of migration, since 95.5% of the time, waves at Camp Perry are less than 1 m high. Thus, the relatively simplistic Mode 1 analysis concludes that UXO migration at Camp Perry can only be the result of relatively rare super-critical wave events, and only some of those events would actually move the UXO because super-critical waves would have to occur concurrently with beach profile shifts that re-expose the UXO and release them from burial lock-down. However, the temporal interplay of beach profile shifts, UXO exposure events, and super-critical wave events cannot be resolved by the simple Mode 1 analysis. We investigate those temporal relationships and their statistics of recurrence in the following section.

The ballistic impact burial model that is embedded into the UXO MM architecture (Figure 1, dark blue Module #12 in lower left) is STRIKE35, a 6-DOF ballistics model developed by Chu, Bushnell and Watson, 2010). It contains physics that describe four independent processes: 1) aerodynamic trajectory through the atmosphere (Hume, 2007, and Hale, 2009); 2) impact with the air-water interface (Chu and Ray, 2006); 3) free-fall through the water column (Chu and Ray, 2006); and 4) impact with a sedimentary seabed (Chu and Fan, 2007). The computational sequence proceeds round by round, starting with the historical range firing records. The firing records provide date, firing pit (firing location), weapon type, ammunition type and loading, number of rounds fired, and azimuth and inclination angles for each firing. The physics of the four aforementioned processes then are applied in order, resulting in a round-by-round prediction of both depth of impact burial and final orientation of the round. Ballistics inputs for these predictions are derived from Camp Perry Firing Logs (Baj, 2008). Simulated trajectories for 106 mm M344 rounds fired from the Camp Perry Firing pits are shown in Figure 34 impacting into the offshore regions of Impact Areas 1, 2, and 3.

STRIKE 35 was validated during controlled impact studies in two test ponds at NAWC/WD, Indian Wells CA (Chu, Bushnell and Watson, 2010)). STRIKE 35 is an evolution from the mine impact burial model IMPACT35 that was validated during ONR's Mine Burial Program (Chu and Fan, 2007). The MBES (predecessor expert system to the UnMES) was validated during ONR's Mine Burial Program (Rennie et al., 2007).

As shown in the following figures, the resulting distributions of ballistic impact provide a significantly more realistic estimate of the initial state of the UXO, thereby providing more accurate predictions of the ultimate fate of the UXO than obtained from previous approaches. The predicted initial UXO burial depth and orientation distributions are used as the input initial UXO population distribution to the UXO MM for subsequent evolution of the burial, scour, and migration properties of the UXO field. The ballistic impact simulations identified two basic types of impact that produce significantly different impact burial characteristics and round orientation. These differences result from the obliquity of the ballistic trajectory as the round enters the water column. This is referred to as "javelin entry mode," and the "oblique-skip entry mode." The javelin entry mode occurs with high apex trajectories from high firing angles (greater than 70o) and near-normal incidence as the round strikes the water surface (e.g., the first trajectory on the left hand

side of Figure 34). With these high apex trajectories and javelin entry mode, the round travels through the water column in a stable nose-down attitude preceded by a pressure wave with no cavitation occurring behind the round (e.g., Figure 35). The round impacts the bottom while maintaining its nose down attitude (Figure 36), and typically penetrates the bottom sediment cover. In the Lake Erie sandy bottom deposits, the javelin entry mode was found to cause burial depths of as much as a meter or more, with penetration into the sediment cover halted by the basement layer of Lake Erie clays. If these clays extend to the surficial layers of the sediment cover, then the javelin entry mode with an inert 106 mm M344 round will result in an impact burial state looking very much like an arrow sticking out of the bottom with its tail fins protruding into the near-bottom flow, exerting high hydrodynamic loads on the round from drag forces acting on the fin section of the round (Figure 37).

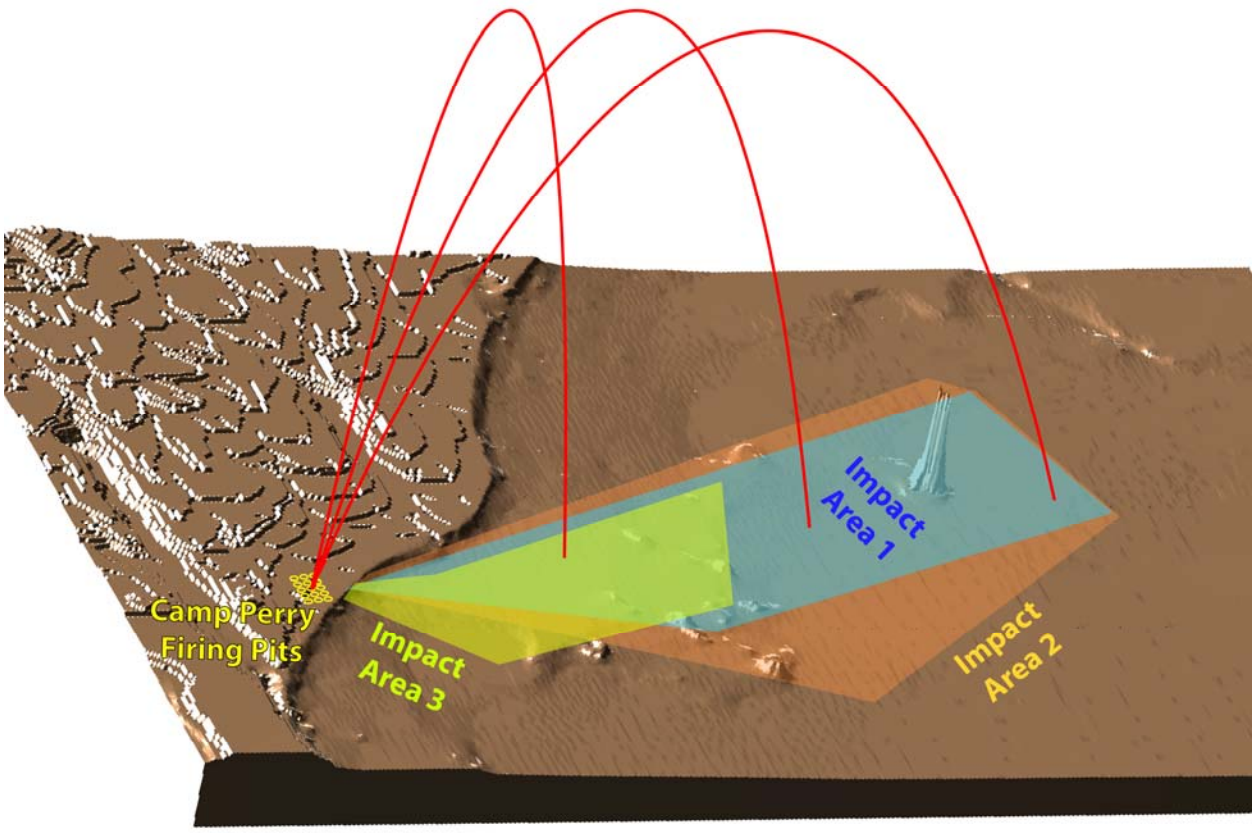

Figure 34. Integrated ballistics/ Impact burial Vortex Lattice UXO IMM Fortran code tested end-to-end for Camp Perry Impact Areas 1, 2, and 3.
Simulated trajectories fired from the Camp Perry firing pits are shown for 106 mm M344 rounds impacting into the offshore regions of Impact Areas 1, 2, and 3.

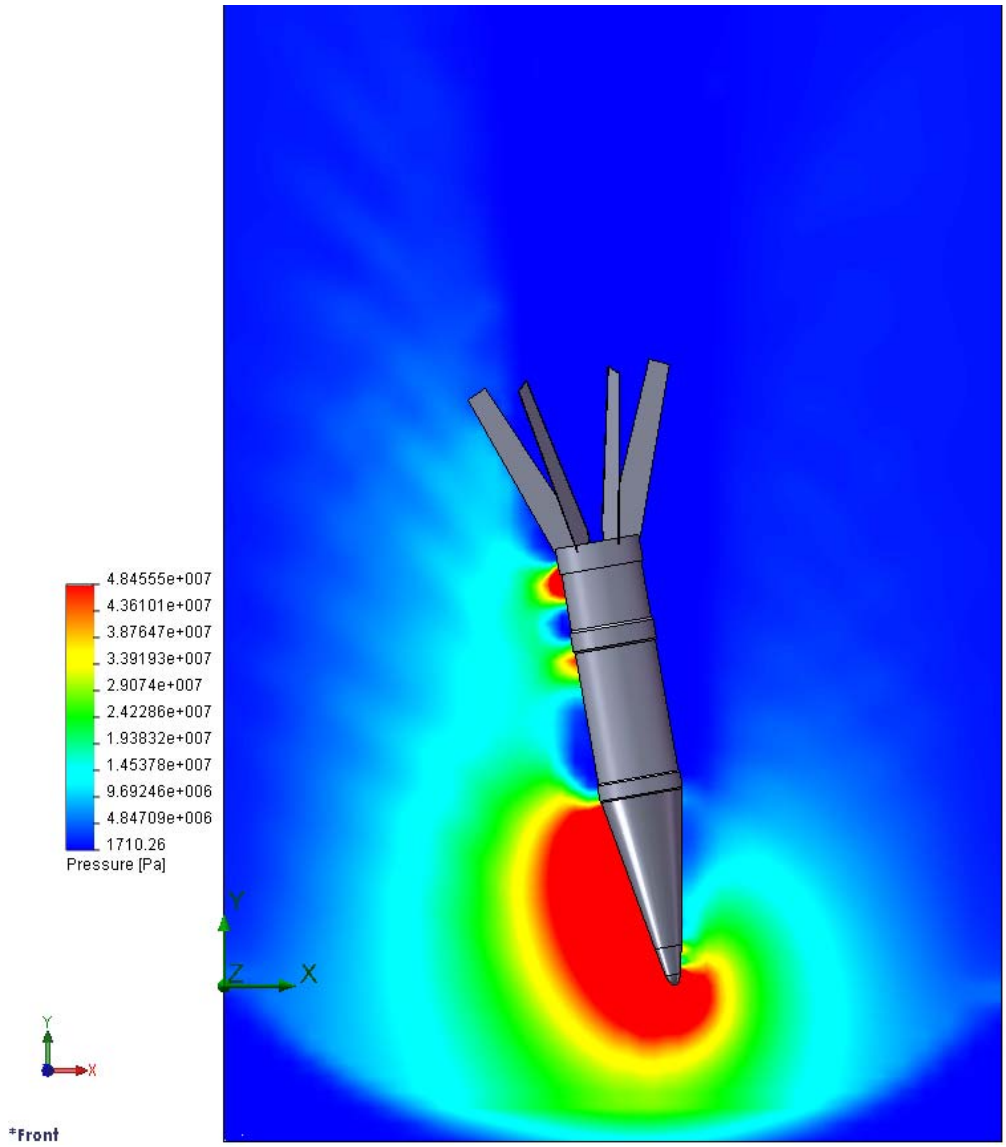

Figure 35. A simulation using the 6-DOF ballistics algorithms lifted from the STRIKE 35 MatLab code and transposed into Vortex Lattice UXO IMM Fortran code.
Simulation shows a 106 mm M344 round (typical of Camp Perry firings) entering the water column from an 85 degree ballistic trajectory angle with pressure wave and no cavitation (javelin entry mode).

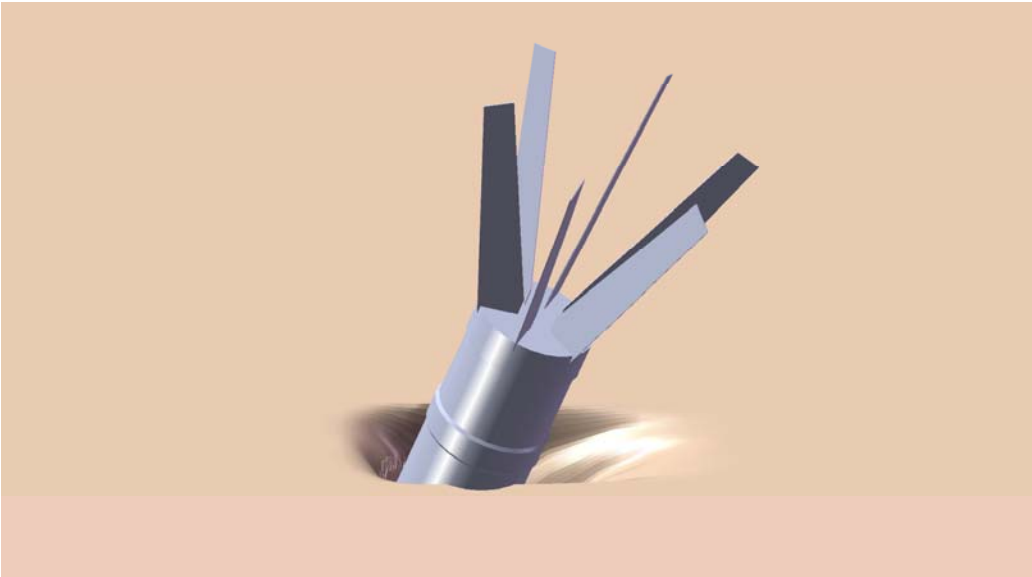

Figure 36. Ballistics impact-burial simulation of a 106 mm M344 round due to javelin entry into Lake Erie clay.

Bearing pressure of clay is taken as 410 kPa (after Safinus, Hossain, and Randolph, 2013).

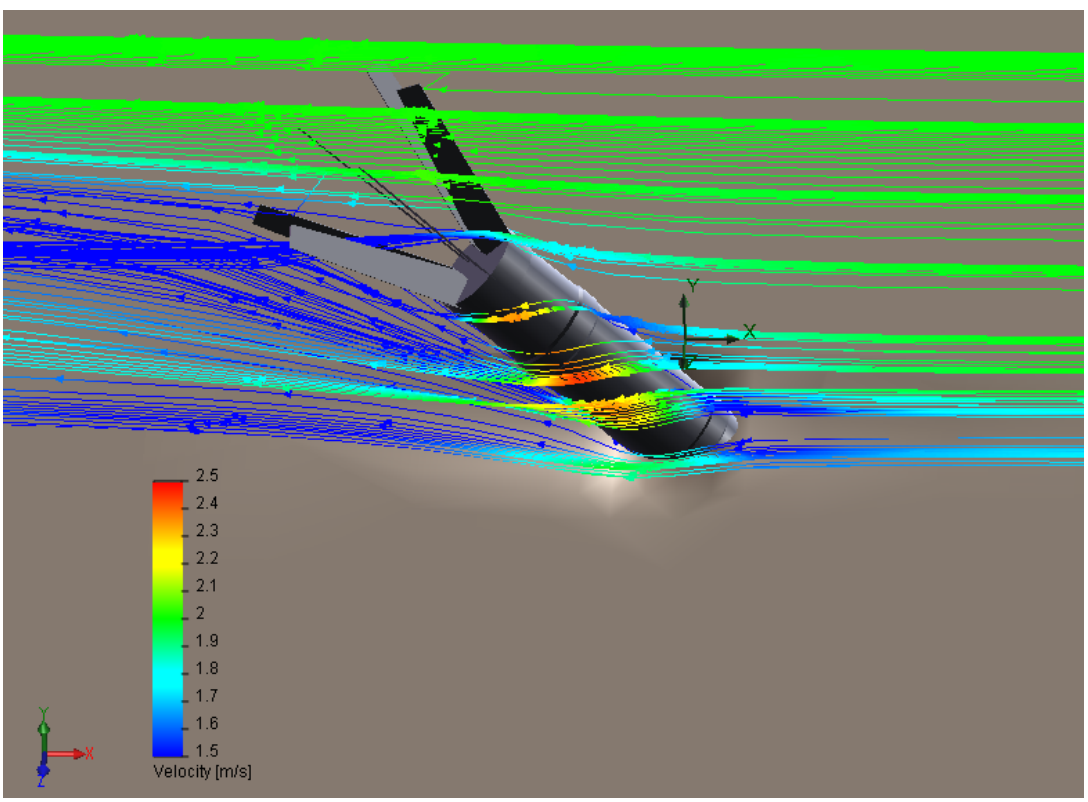

Figure 37. Functional test of the mobility algorithms performed with the UXO IMM Fortran code for Camp Perry Impact Areas 1-3.

Figure shows flow around a 106 mm M344 round after impacting a layer of Lake Erie clay, causing partial burial due to javelin entry. Bearing pressure of the clay was assumed to be 410 kPa (after Safinus, Hossain, and Randolph, 2013).For more oblique impacts with the water surface due to low apex trajectories

from lower firing angles (less than 70E), the round travels through the water column at a high incidence angle producing a cavitation bubble that often breaks off the fin section when the fins make contact with the sides of the cavitation bubble (Figure 38). This action in combination with the large rotational moments exerted by the high incidence angle causes the round to become unstable as it passes through the water column. The flight path through the water column typically develops a large horizontal component as the round rotates with passage through the water column, resulting in an oblique impact with the bottom that may even result in the round skipping along the bottom in the horizontal direction; hence, the term oblique-skip entry mode. Impact burial depth is typically very shallow as a result of an oblique-skip entry, and the round often ends up in a prone attitude on the sedimentary bottom, as shown in Figures 32 and 33. Because of the shallow impact burial depth and prone attitude, the UXO rounds are significantly more likely to become mobile after oblique-skip entries following low apex trajectories and low firing angles.

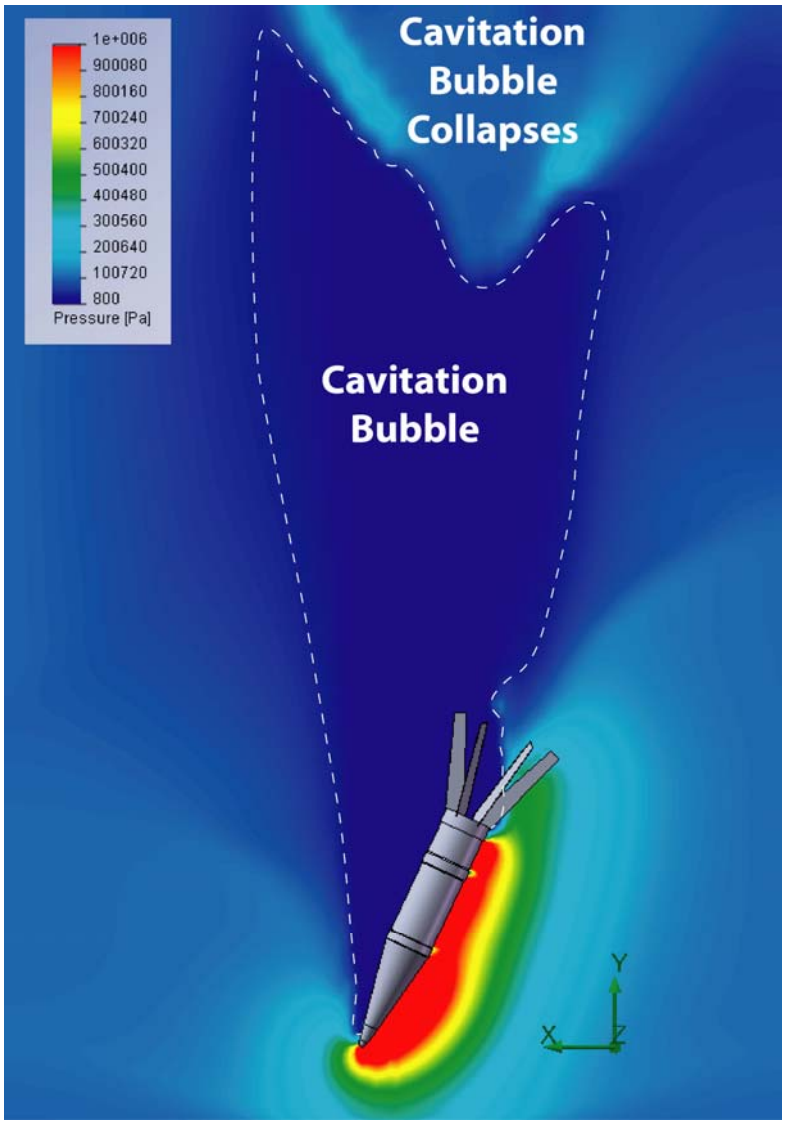

Figure 38. UXO IMM simulation of a 106 mm M344 round entering the water column from a 60E ballistic trajectory angle with cavitation bubble (oblique-skip entry mode).

Camp Perry once had as many as 15 firing pits located approximately 1 kilometer (km) inland from the Lake Erie shoreline. Firing records indicate that the heavy artillery (principally the 106 mm smooth bore howitzers) primarily used pits # 1, 3, 4, 6, and 7, while the smaller mortar rounds M43A1 81 mm and M49A2 60 mm were fired from pits # 9, 11, 13, and 14. The firing records have some data gaps, but using a moving average interpolation across the data gaps suggests that over 3.9 million rounds have been fired since 1941, impacting the offshore regions of Impact Areas 1-3 (Figures 18 and 34). Documented firing activity with the fewest data gaps was logged during the Viet Nam War era (1964-1972), and during the period immediately before and after Desert Storm (1990-1991) (Baj, 2008). Figure 39a shows a direct comparison of UXO "targets" found by underwater magnetometer survey conducted by SAIC (2006) versus an UXO IMM simulated impact site of a 106 mm M344 round. A statistical comparison of the actual UXO locations and simulated distributions based on a "nearest neighbor" approach was performed in order to create a pairing between the known target locations, obtained from the WES (1993) electromagnetic surveys and the SAIC (2006) towed array surveys, and the predictions. The predictions are made by the STRIKE35 ballistics algorithms integrated into UXO IMM; 98,613 firing trajectories were simulated using the documented firing log information giving firing pit location, weapon type, ammunition type, number of rounds fired, and azimuth and inclination angles for each firing. These simulations assumed that all weapons types fired straight, so that the logged azimuth gave the true direction of the trajectory from the firing pit. Therefore, the range to impact from the firing pit output from the STRIKE 35 algorithms, and the logged azimuth angle allowed the impact point of each simulated firing to be co-registered on the Lake Erie bathymetry. Approximately 6,000 "large contacts" (35-50 nano Teslas) and "small contacts" (10-35 nano Teslas) from the WES (1993) electromagnetic surveys and the SAIC (2006) towed array surveys also were co-registered on the Lake Erie bathymetry. The statistics-based nearest neighbor search was performed to find the closest match between the approximately 6000 known large and small EM contacts and the 98,613 simulated impact points, resulting in 2,135 matches with a distance from simulated position to known UXO location within a specified tolerance. This pairing did not allow a given known UXO contact to be matched with more than one simulated trajectory. Figure 39b gives a regression analysis of the range from the Camp Perry firing pits to the impact location simulated by the UXO IMM (vertical axis) versus the range from the firing pits to the electromagnetic contact locations discovered by the SAIC (2006) underwater magnetometer surveys (horizontal axis). This regression analysis gives a predictive skill of R-squared = 0.868 as measured by the coefficient of determination for ranges out to 12 km from the firing pits. This demonstration of predictive skill was taken as validation of the ability of the UXO IMM to predict impact locations from the Camp Perry firing logs.

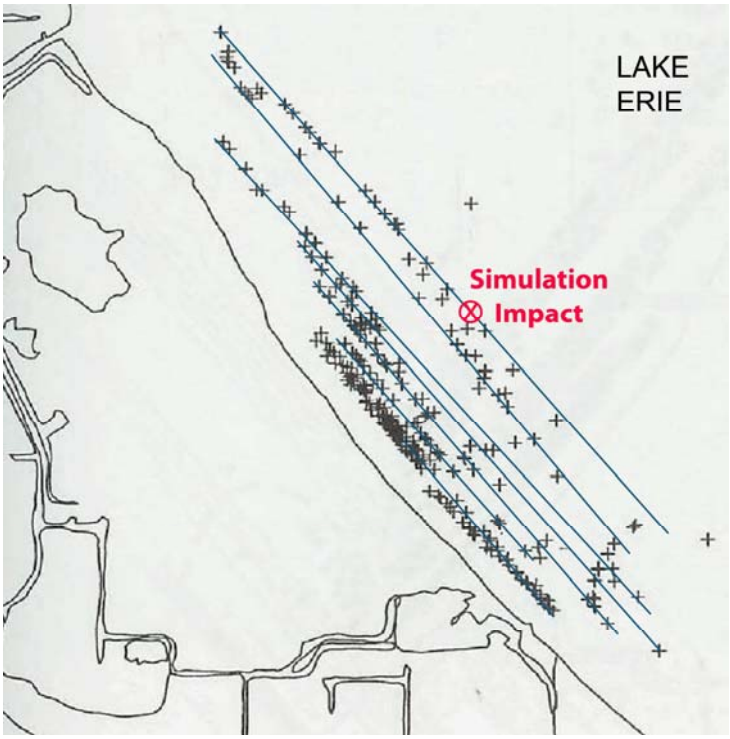

Figure 39a. UXO IMM simulation of a 106 mm M344 impact in Impact Area 3 as compared against known UXO target locations.

Large contacts (crosses) from 1996 electromagnetic survey of UXO at Camp Perry/FUDS Beach (from Pope et al., 1996).

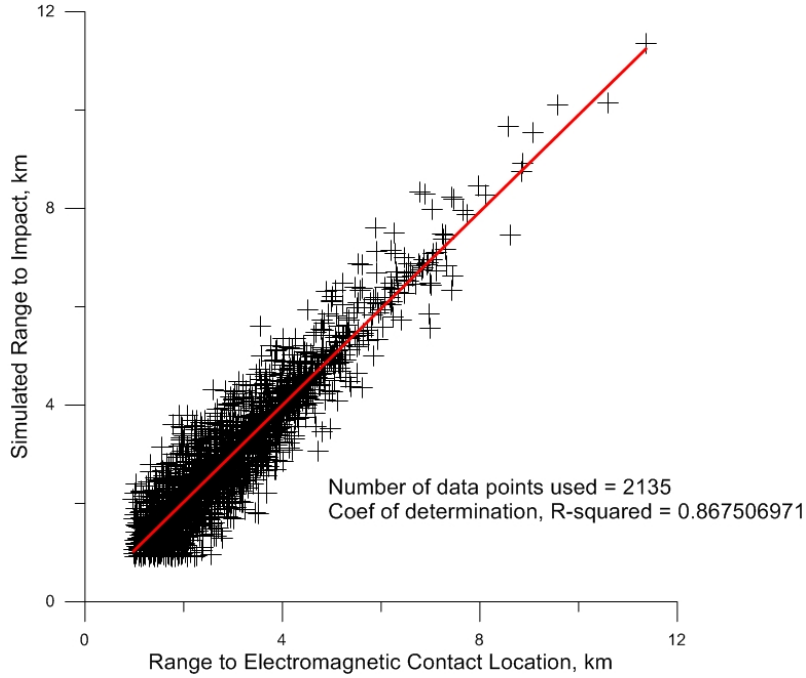

Figure 39b. Regression analysis of the range of trajectories from the Camp Perry firing pits to impact locations simulated by the UXO IMM versus the range distance from the firing pits to the electromagnetic contact locations discovered by the SAIC (2006) underwater magnetometer survey.

In the main range fan, 92% of the targets checked by the SAIC divers were actually UXO, while the remaining 8% were other metal objects. The size of the UXO varies from small caliber bullets to as large as the 106 mm rounds. However, the dominant UXO types are the Army 106 mm M344 round artillery shells, the 60 mm M49A2, and 81 mm M43A1 mortars. Figure 40 gives the probability distribution of the impact burial depth of the 2,135 validated impacts simulated by the UXO IMM from the firing logs, while Figure 41 shows a cross section through the sediment cover in the nearshore of Figure 39 impacts (the ranges of the simulated impacts along the vertical axis in Figure 39b correspond to the ranges of the UXO along the horizontal axis in Figure 41). The vertical bearing pressure assumed for these impact burial simulations was 240 kilopascal (kPa) for the surficial layers of fine sand typical of the grain size distribution in Figure 25, and 410 kPa for the basement layer of Lake Erie clays (Ahmad et al., 2011; Safinus, Hossain, and Randolph,2013).. The impact burial probability distribution in Figure 40 is clearly bi-modal, with the majority being deep impacts on the order of 60 cm to 120 cm resulting from high apex trajectories with javelin entry modes. The UXO rounds associated with these deep impacts are likely not subject to subsequent mobility due to the fetch limited wave heights and wave periods along the southwest shores of Lake Erie (Figure 27). However, the smaller peak in the bi-modal distribution of Figure 40 is attributable to shallow impacts associated with oblique trajectories and oblique skip entries. These shallow impacts (burial depths about 15 cm) amount to 2.53% of the firings in the Camp Perry firing logs, and account for about 98,613 of the UXO targets in Impact Areas 1-3. Due to these shallow burial depths, the targets from oblique skip entries become the focus of our UXO mobility analysis in Section 7.

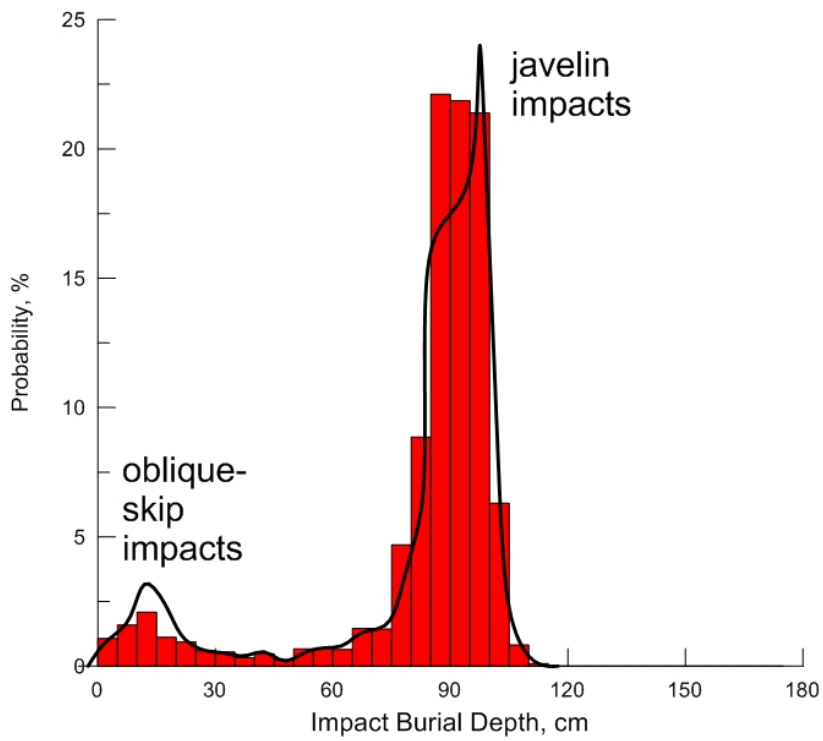

Figure 40. UXO IMM predicted bi-modal impact burial probability distribution for Camp Perry Impact Areas 1-3.

Based on 2,135 impact locations (cf. Figure 39b). Bearing pressure is assumed to be 240 kPa for the surficial layers of fine sand and 410 kPa for the basement layer of Lake Erie clays (Ahmad et al., 2011; Safinus, Hossain, and Randolph,2013).

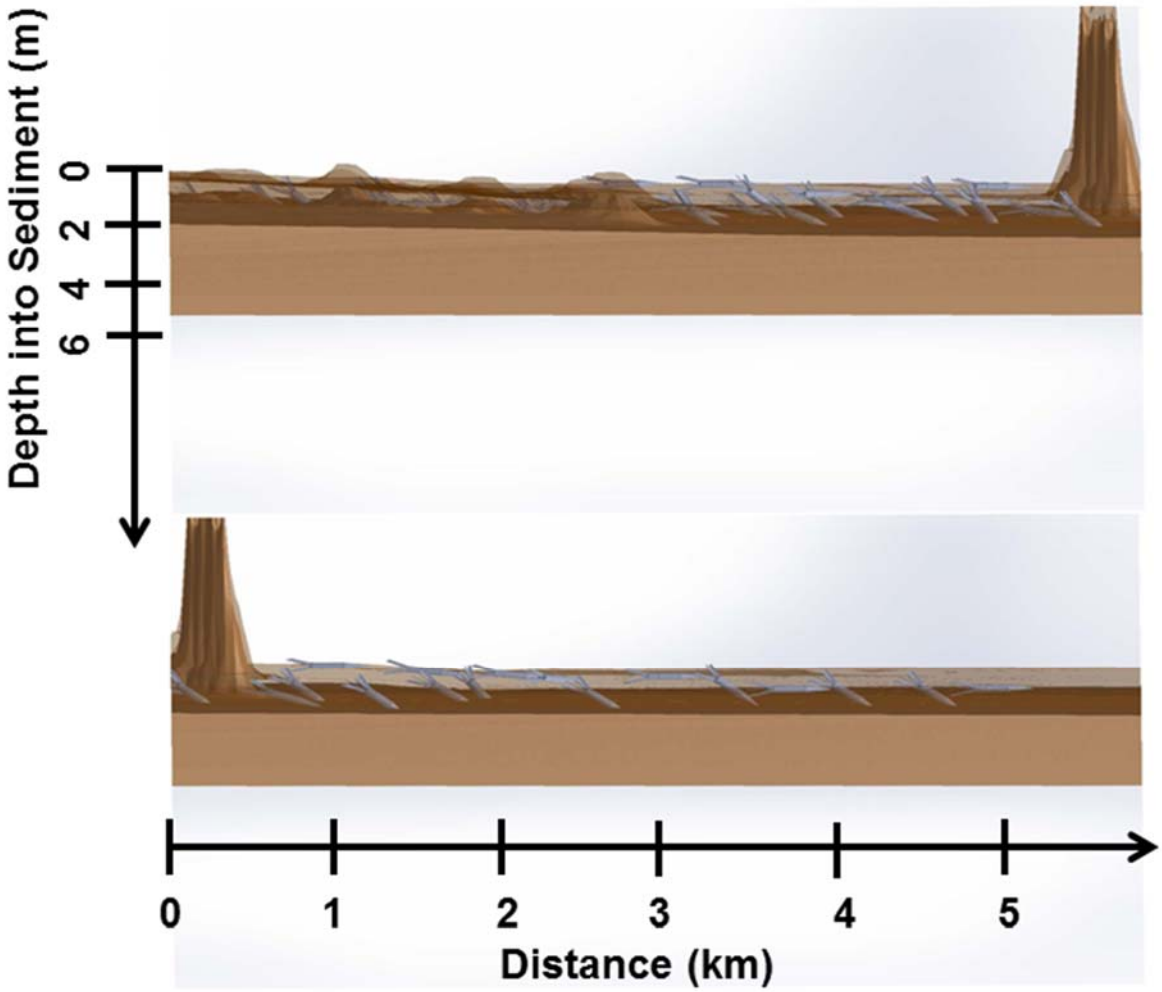

Figure 41. UXO IMM predicted spatial (range and depth) distribution of the 106 mm impacts in the Lake Erie sediment cover taken from the 2,135 simulated impact locations that give rise to the bi-modal impact burial probability distribution in Figure 40.

The Lake Erie sediment cross section shown in this figure is taken along the eastern shoreline-intersecting boundary of Impact Area 1 between the 3 m and 8 m depth contours in Figure 17. The upper panel shows the vertical cross section through the sediment cover between the 3 m depth contour on the left and the rocky outcrop near the 5 m depth contour on the right, and the lower panel shows vertical cross section through the sediment cover between the 5 m outcrop on the left and the 8 m depth contour on the right. The javelin impacts are those UXO that appear in the dark brown intermediate layer, whereas the oblique-skip impacts are illustrated by the UXO that are oriented nearly horizontally in the uppermost sediment cover (plotted as light brown and on the order of 1 meter thick) overlying the Great Lakes Bedrock formation. Note that the UXO shapes are not plotted to scale so they can be seen more easily in the figure.

This page left blank intentionally.

7.0 PERFORMANCE ASSESSMENT

The Camp Perry firing logs (Baj, 2008) indicate that 3.9 million rounds have been fired into three impact areas (Figure 17) totaling 388.27 km^2 area of southwest Lake Erie. Applying the impact burial probability density function from Figure 40 to a total of 3.9 million impacts, it was concluded that 98,613 UXO targets in Impact Areas 1-3 resulted from oblique skip entries with shallow burial depths. This subset has the highest subsequent mobility potential as a consequence of the shallow impact burial. The UXO IMM was applied to this subset for subsequent exposure and migration simulations using wave forcing from Figure 27, fine-scale bathymetry from Figure 17; initial beach profiles per Figure 26; and the grain size distribution in Figure 25. The UXO population was divided among three types of UXO rounds in a two-to-one split (small rounds to large rounds) with 1 each of the 60 mm M49A2 and 81 mm M43A1 rounds for every 106 mm M344 round. Initial burial for these subset simulations was based on the oblique skip peak in the impact burial probability density function in Figure 40 that resulted from UXO IMM ballistics simulations of the 2,135 validated targets. The initial orientation of each round was parallel to the bottom plane, consistent with the oblique skip entry mode (Figures 32 and 33). The model computed exposure, migration, and subsequent burial at time step intervals of $\Delta t = 52.6$ minutes over a 28-year long simulation period as dictated by the period of record for forcing data (Figure 27). Model simulations were arrested during the periods of ice cover each winter as indicated by the gaps in the wave forcing data in Figure 27.

Because of the great length of the wave forcing record, these data were treated as representative in order to apply them synchronously with other data that had larger gaps. In particular, the lake water level data possesses a large gap in the first half of the wave record, between 1980 and 1997, and no beach profile data were available before or after 1990. The gap in the water level data was filled by folding the lake water level data backward in time to 1980 to provide inter annual water level variation concurrent with the early portion of the wave record. The 1990 beach profile was treated as the initial $t = 0$ shoreline boundary condition, and the UXO model simulation was run forward in time from that point using the waves and (partly-proxy) water level data from 1990 to 2008. To complete the 28 year long simulation, the front end of the wave forcing and water level data from 1980 to 1990 were folded forward in time, extending the simulation another 10 years beyond 1997 to 2008. These procedures demonstrate a vulnerability of the UXO IMM process-based model to gaps in important input data.

Figure 42 gives a UXO IMM VORTEX model simulation of time evolutions of burial and migration for one of the 106 mm M344 rounds during the high energy, extreme event portion of the period of record. Historically, this period corresponded to the ice-free period between 27 March 1998 and 5 December 1998. In Figure 42, migration distance (blue) and burial depth (red) represent scalar lengths relative to the initial position at the start of the simulation. The migration distance is read from the outer left-hand vertical axis; burial depth is read from the outer right-hand vertical axis; and wave height is plotted in gray according to the inner left-hand vertical axis. Migration was primarily on/off shore with the convention that transport off shore is taken as positive, while movement onshore is negative. Burial depth is measured from the bottom of the round at its basal end. The time axis in Figure 42 is given in terms of Julian Day relative to the start of year 1998. During the Figure 42 time-stepped simulation of a buried 106 mm M344 round, waves reached heights of 3.88 m on 10 April 1998 (Figure 29), but also exceeded 2.2 m in May 1998 and exceeded

2.6 m in November 1998. Concurrent with the spring episode of high waves, lake water levels were near historic maxima (about 174.9 m LWD). The combination of high waves and high water levels provides the necessary forcing to erode the beach profile and expose buried UXO inshore of closure depth. The simulation begins with the round buried 27 cm beneath the lake bottom, about the average burial depth in Figure 43. The location of this particular 106 mm M344 round is inshore of closure depth at a cross-shore location of X = 350 m on Range 10579 (Figure 26). The project team found that with the onset of the extreme waves and high lake water levels in April (circa Julian Day 100) that the106 mm M344 round rapidly un-buries and becomes 85% exposed (burial depth approaches 1.5 cm) as the beach profile erodes and retreats landward. As this retreat happens, the round is released from burial lock-down and is free to migrate, rolling down slope and off shore about 44.7 cm from its initial position. By 10 May 1998 (Julian Day 125), the last of the big wave events has ended and the round remains in a mostly exposed condition, free to move, but lacking persistence of super-critical wave forcing (H > 1 m) to move the round significantly further. During the following 189 days (Julian Day 125 to 314), the round moves shoreward about 10 cm in a series of very small incremental steps concurrent with the relatively few super-critical waves that briefly exceed 1 m heights. This shoreward movement of the UXO also coincides with the shoreward migration of beach sands that re-establish the summer equilibrium profile, following the erosion resulting from the preceding winter/early-spring storms. With the summer accretion along the bar-berm profile, the UXO almost totally re-buries by November 1998 (Julian Day 314), to a burial depth of 10 cm. An early winter storm on 10-14 November 1998, including a 2.7 m high wave, abruptly erodes the beach and re-exposes the UXO, moving it again in the down slope, offshore direction a net distance of 50.8 cm from its initial starting point. After 14 November 1998, a milder wave climate sets in and persists to the end of the simulation period on 5 December 1998, where the simulation is halted due to the onset of icing. During the last 3 weeks of the simulation (Julian Day 318 to 339), the UXO repeats behavior typical of the preceding the mild summer period, and begins to re-bury with slight incremental shoreward movement, concurrent with shifts in the beach profile.

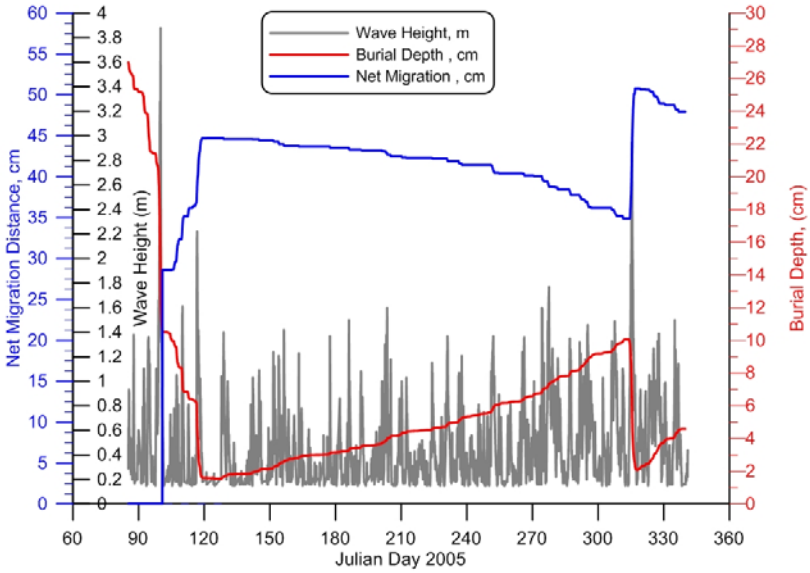

Figure 42. UXO MM simulation of migration and burial sequence, Lake Erie, 27 March, 1998 to 05 December, 1998.

To quantify the statistical spread of burial, exposure, and migration over all three impact areas at Camp Perry, daily estimates of burial, exposure, and migration were simulated for 98,613 oblique-skip entry targets representing three types of UXO. From these daily outcomes, probability density functions of burial, exposure, and predicted UXO movement were constructed. Figure 43 presents the probability density function (histogram) of UXO burial depth based on 98,613 modeled outcomes of the three UXO types. Ninety-seven percent of the modeled outcomes predicted fully buried UXO. The mean burial depth was found to be 27 cm and the maximum burial depth was calculated at 79 cm. Any UXO buried deeper than 79 cm were buried that deep via a javelin impact (Figure 40) and not from wave forcing over the 28 year period under consideration. Therefore, they are not subjected to dynamic burial and exposure, and remain permanently entombed below the critical mass as a consequence of impact burial. Thirty-nine percent of the modeled outcomes predicted burial depths in the range of 5 cm to 24 cm, which was consistent with the range observed in the USACE burial field tests (Evans-Hamilton, 2003) conducted at Camp Perry FUDS Beach in 2001-2003. However, the field tests were relatively brief compared to the 28 year long model simulations and the field tests did not capture some of the more energetic conditions found earlier in the period of record. Also, the model predictions cover all three Camp Perry impact areas, whereas the field tests were confined to the northern reach of FUDS Beach adjacent the Toussaint River where beach retreat is somewhat more pronounced and would tend to mask burial. Generally, however, the mean outcome of the model burial (about 27 cm) is close to the mean range of the 2001-2003 field tests (19 cm to 20 cm).

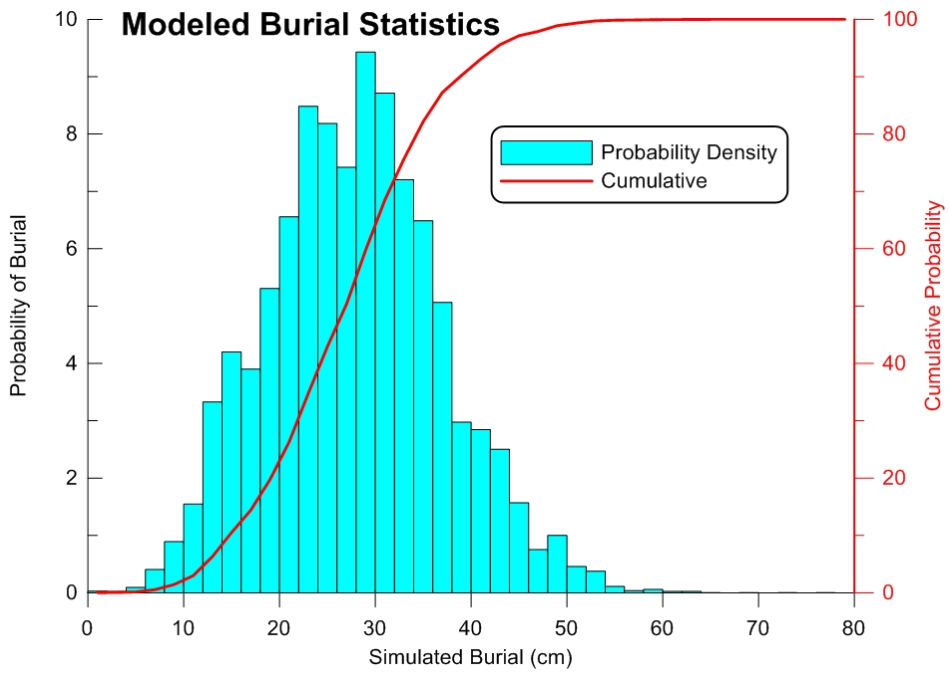

Figure 43. Probability density (blue) and cumulative probability (red) of UXO burial depths at Camp Perry Impact Areas 1-3 from UXO MM simulations using wave forcing, 1980-2008.

Probability distributions based on 98,613 modeled outcomes.

Exposure is a critical mechanism in the UXO mobility problem, as only those rounds that become sufficiently exposed to be released from burial lock-down are subject to migration. Exposure

consequently sets an upper bound on the quantifiable risk assessment. Figure 44 gives the probability density function (histogram) of UXO exposure based on 98,613 modeled outcomes of the shallow oblique-skip impacts in three Camp Perry Impact areas. Because of the variable caliber of the 3 types of UXO, exposure is expressed in terms of percent of the silhouette of the round that is exposed. The project team found that only 98.6% of the shallow oblique-skip impacts of the UXO in the offshore impact areas at Camp Perry (or about 97,000 rounds) will exhibit some degree of exposure in a 28 year period. However, the UXO IMM calculations show that only 4.5% of the shallow oblique impacts of UXO will become sufficiently exposed (more than 50% exposed) to be released from burial lock-down and have a potential to move. This result means that out of 3.9 million buried UXO rounds in the three offshore impact areas at Camp Perry, of which 98,613 UXO are shallow impacts due to oblique-skip entries, only 4,485 UXO rounds have the potential to migrate from their point of impact due to storms and lake water level changes, and nearly all of those are in the nearshore between the beach and the -3.35 m LWD depth contour (extending about 700 m offshore of the beach berm). Moreover, only 1% of those shallow impacts (about 1,000 rounds) will become exposed 80% or more, and thus have likelihood of movement over significant distances.

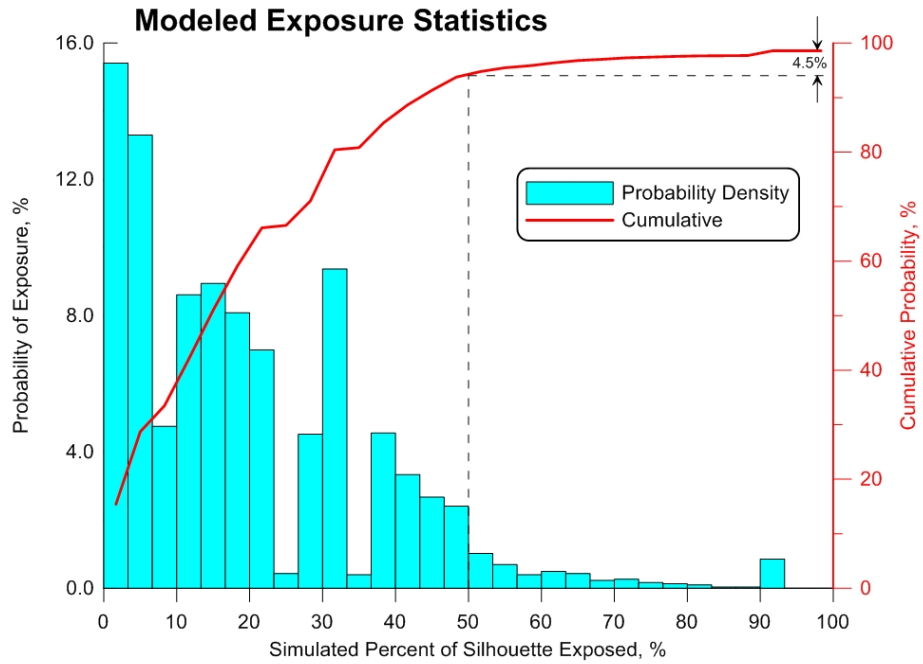

Figure 44. Probability density (cyan) and cumulative probability (red) of UXO exposure at Camp Perry Impact Areas 1-3 from UXO MM simulations using wave forcing, 1980-2008.
Probability distributions based on 98,613 modeled outcomes.

The UXO IMM results of UXO exposure were used to quantify the statistical likelihood of UXO movement at Camp Perry due to coastal processes. A probability density function was constructed of net migration distance from a subset of the exposure results made up of the 4,485 UXO in the nearshore that are sufficiently exposed (50% exposed or more) to be released from burial lock-down. Figure 45 gives those probability distributions, revealing that 70% of the 4,485 exposed UXO will move less than 19 cm over a 28 year period. In fact, the mean net migration distance is only 15 cm. Only 10 % of the exposed UXO (about 450 rounds) move a net distance of 0.5 m, and

only 5% (about 225 rounds) exhibit a net movement of more than 1 m away from their point of impact; 0.1% (5 rounds) have a net migration of 2.9 m or more; while the largest net movement of any of the 4,485 exposed rounds was 3.7 m. These results are fully consistent with the 2001-2003 migration studies of UXO surrogates at Camp Perry conducted by the USACE (Evans-Hamilton, 2003; Welp et al., 2004). However, these model results and field observations of migration involve significantly smaller movement than found in previous UXO studies conducted in ocean environments on exposed coastlines (Jenkins and Wasyl, 2008; Wilson et al., 2008). While the relatively low-energy, fetch-limited environment of Lake Erie may contribute to that outcome, the shear plate anchoring effect of the stabilizer fins of Army rounds also limit migration by inhibiting the scour-and-roll progression that is the dominant mechanism behind the migration process for Navy rifle rounds. Also, as noted in the Figure 42 time progression, the rounds at Lake Erie tend to migrate back and forth with the sand movement associated with erosion of winter beach profiles and re-building of summer beach profiles. The histogram in Figure 45 only tracks the net migration, while the gross movement may actually be greater, as in Figure 42 where the gross migration was found to be 35% greater than the net migration.

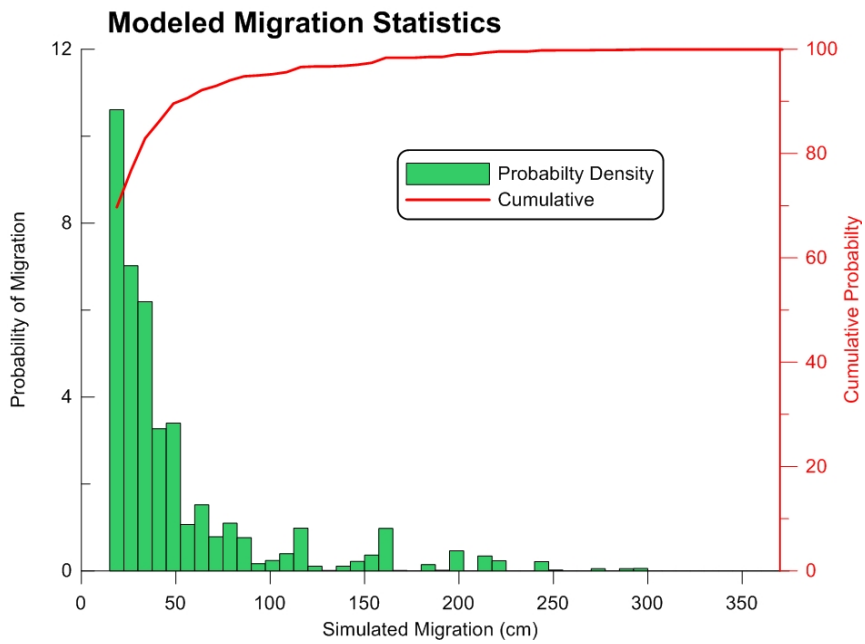

Figure 45. Probability density (green) and cumulative probability (red) of UXO migration distances at Camp Perry Impact Areas 1-3 from UXO IMM simulations using wave forcing, 1980-2008.

Probability distributions based on 4,485 modeled outcomes.

The skill factor predicted by the UXO IMM at Camp Perry was calculated at $R_h = 0.86$ for impact burial and $R_> = 0.95$ for subsequent migration. The impact burial skill factor calculation of $R_h = 0.86$ was based on the observed burial depth of EM targets recovered by divers during the SAIC (2006) surveys. Those targets are represented by the small colored dots in Figure 23. The skill factor $R_> = 0.95$ for subsequent migration is based on comparison of UXO IMM simulation with observations from the UXO migration study at Camp Perry conducted by WES in 2001-2003 (Evans-Hamilton, Inc., 2003). Those studies recorded single event migration distances predominantly in the range of 25 cm to 50 cm for 106 mm surrogates, consistent with Figure 45.

To track the gross movement, and to assess the stability of the UXO field in the offshore regions of Impact Areas 1-3, the cumulative departure, K_R, was computed from initial impact position X_i due to subsequent migration as:

$$K_R = \sum_{i=1}^{N} |X_i = \eta_i|, \tag{11}$$

where η_i is the migration distance over i =1, …, N numbers of modeled outcomes. This statistic is plotted in Figure 46 and represents the combined gross movement over time of the 4,485 UXO in the nearshore that are sufficiently exposed (50% exposed or more) to be released from burial lock-down, out of a total of 98,613 rounds modeled for shallow oblique-skip impacts. Figure 46 shows the combined gross movement is 2700 m to 3000 m over a 28 year period of wave forcing (Figure 27) for the 4,485 potentially mobile UXO targets, or an average gross movement of 0.6 m to 0.66 m for each mobile target. In summary, the UXO do not appear to be very mobile in the nearshore of Camp Perry. However, of greater importance to the long term monitoring of this site is the time response of the cumulative residual in Figure 46. It shows that gross movement of UXO in the offshore waters of Impact Areas 1-3 is episodic, occurring in response to a handful of large storm wave events (6 severe weather events over 28 years) and is not continuous or gradually in response to seasonal changes. Figure 46 also shows that very little gross movement of the UXO occurs after 9,000 to 10,000 days, and consequently the UXO can be considered stable after periods of time on the order of 25 to 30 years in this environment.

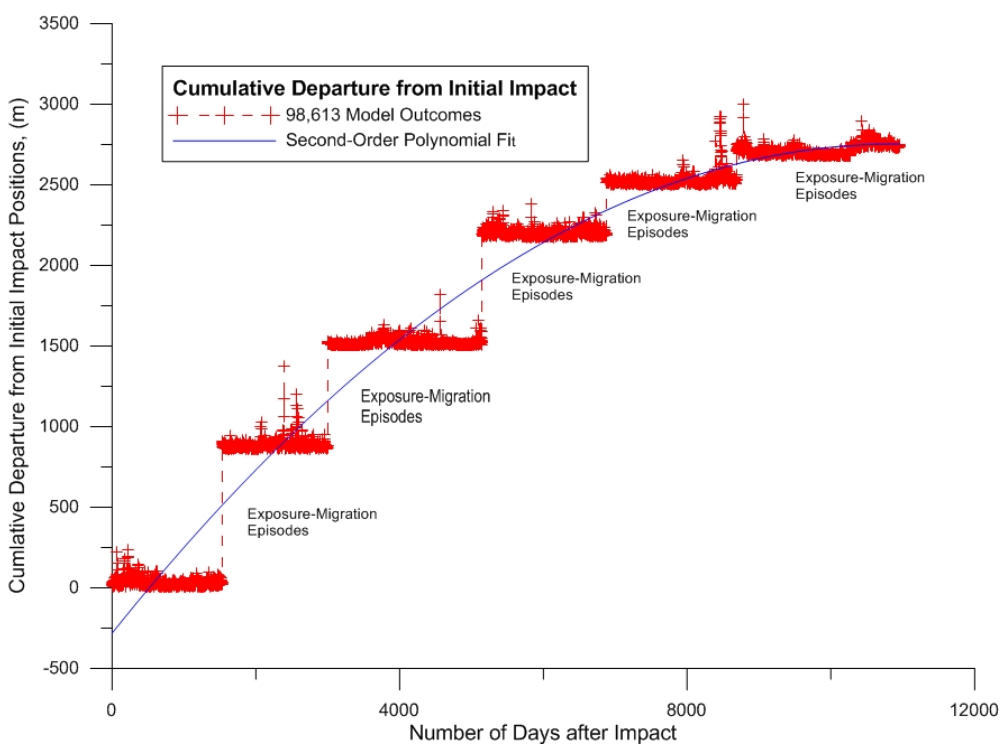

Figure 46. Cumulative departure from initial impact positions for UXO in offshore Impact Areas 1-3, based on 98,613 modeled outcomes with 4,485 mobile targets using wave forcing 1980-2008.

Cumulative departure, K_R, from initial impact position X_i due to subsequent migration is calculated as: $K_R = \sum_{i=1}^{N} |X_i = \eta_i|$, where η_i is the migration distance over i = 1, …, N numbers of modeled outcomes.

With these statistics, the Mode skill comparisons were used at the Camp Perry Lake Erie setting. Although this setting has a complex bathymetry, that bathymetry is manipulating a much lower level of incident energy than previous validation sites at Field Research Facility (FRF), Duck, North Carolina, and Pacific Missile Range Facility (PMRF), Hawaii (Wilson et al., 2008). Also, those lower energies are working on an Army-grade UXO shape that is more resistant to movement than the Naval rounds tested at Duck, NC. Nonetheless, the Camp Perry site is a good proxy for a marginal sea coastline, which is another one of the five generic coastal types in the Geomorphic Coastal Classification System (Jenkins et al., 2007) and the third most abundant coastal type where UXO are found. The skill level of the lower modes to the Mode 3 baseline predictions at Camp Perry were compared, although the predictive skill of those Mode 3 predictions have only been verified by anecdotal evidence from the 2001-2003 ordnance mobility studies (Evans-Hamilton, 2003; Welp et al., 2004).

Figure 47 gives the regression plot of Mode 1 predictions of UXO migration at FUDS Beach, Camp Perry as compared against the Mode 3 baseline predictions. The Mode 1 migration predictions are surprisingly good, with *R-squared* = 0.900. However, the probabilities per meter of migration in Figure 47 for the fetch-limited environment are much smaller than the probabilities per meter of migration in a high energy environment. For example, at Duck, NC, the average migration distance was observed to be in the range of 2-12 m over an 8-month period (June 22, 2005 to February 15, 2006), and 1-3 m during the winter of 2007 (February 13 to May 31, 2007) at the PMRF, Hawaii test site (Wilson, et al., 2008). Clearly, the relatively high coefficients of determination obtained from Mode 1 predictions at Camp Perry in Figure 47 are the result of differences in very small migrations due to the low energy environment. In other words, a relatively crude prediction is doing quite well because it is predicting small numbers, and higher order predictions are only going to be able to make small differences in what are already very small numbers. Recall that 70% of the Mode 3 migration distances in Figure 45 were less than 19 cm. This conclusion is born out in the regression plots of migration from Mode 2 predictions in Figure 48. The addition of the complex bathymetry (Figure 17) into the model improves the coefficient of determination for migration predictions by little more than 4%, yielding *R-squared* = 0.945 for Mode 2 relative to Mode 3.

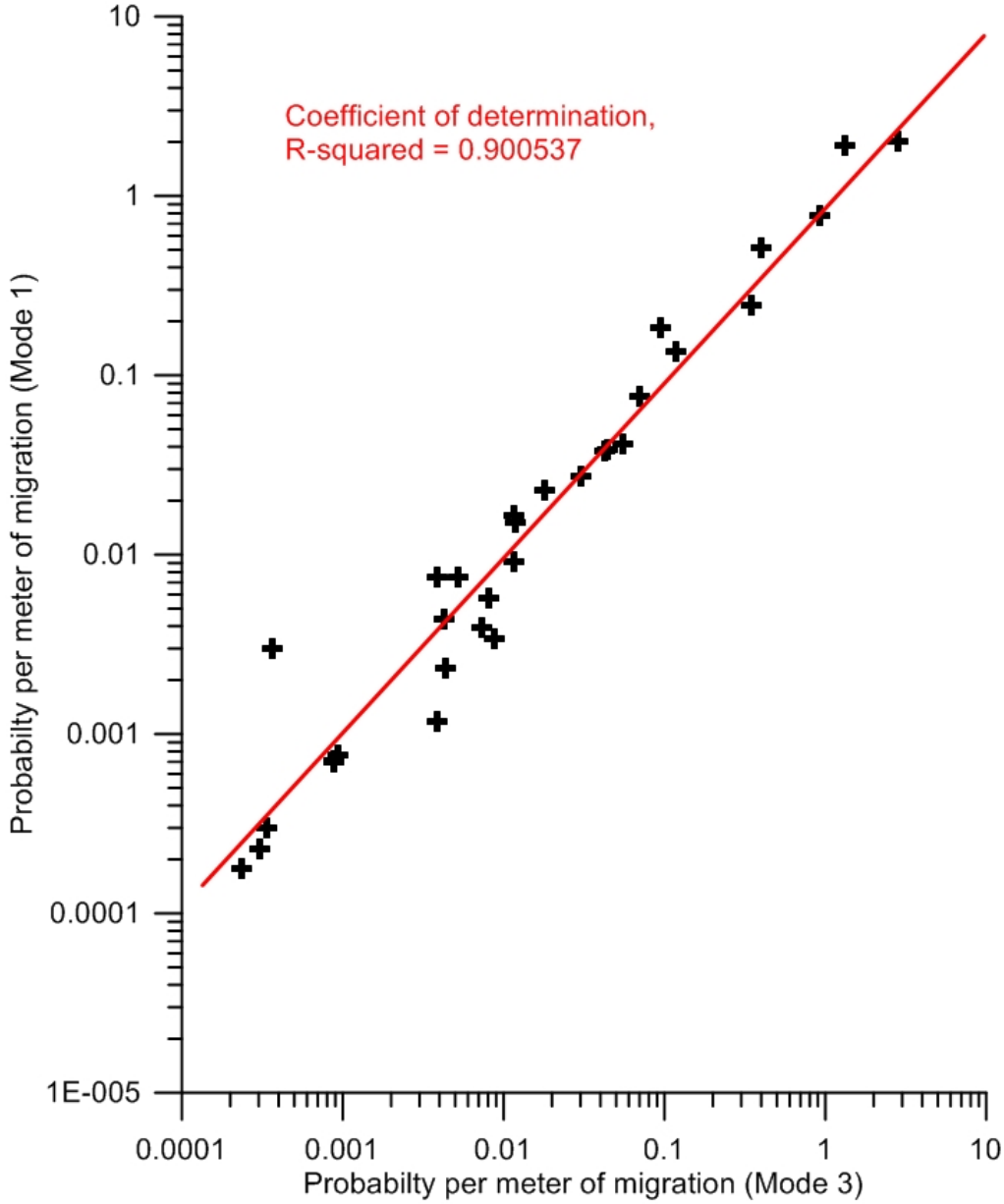

Figure 47. Regression analysis of Mode 1 versus Mode 3 predictions of UXO migration at Camp Perry, Lake Erie, OH, based on M344 106 mm rounds.

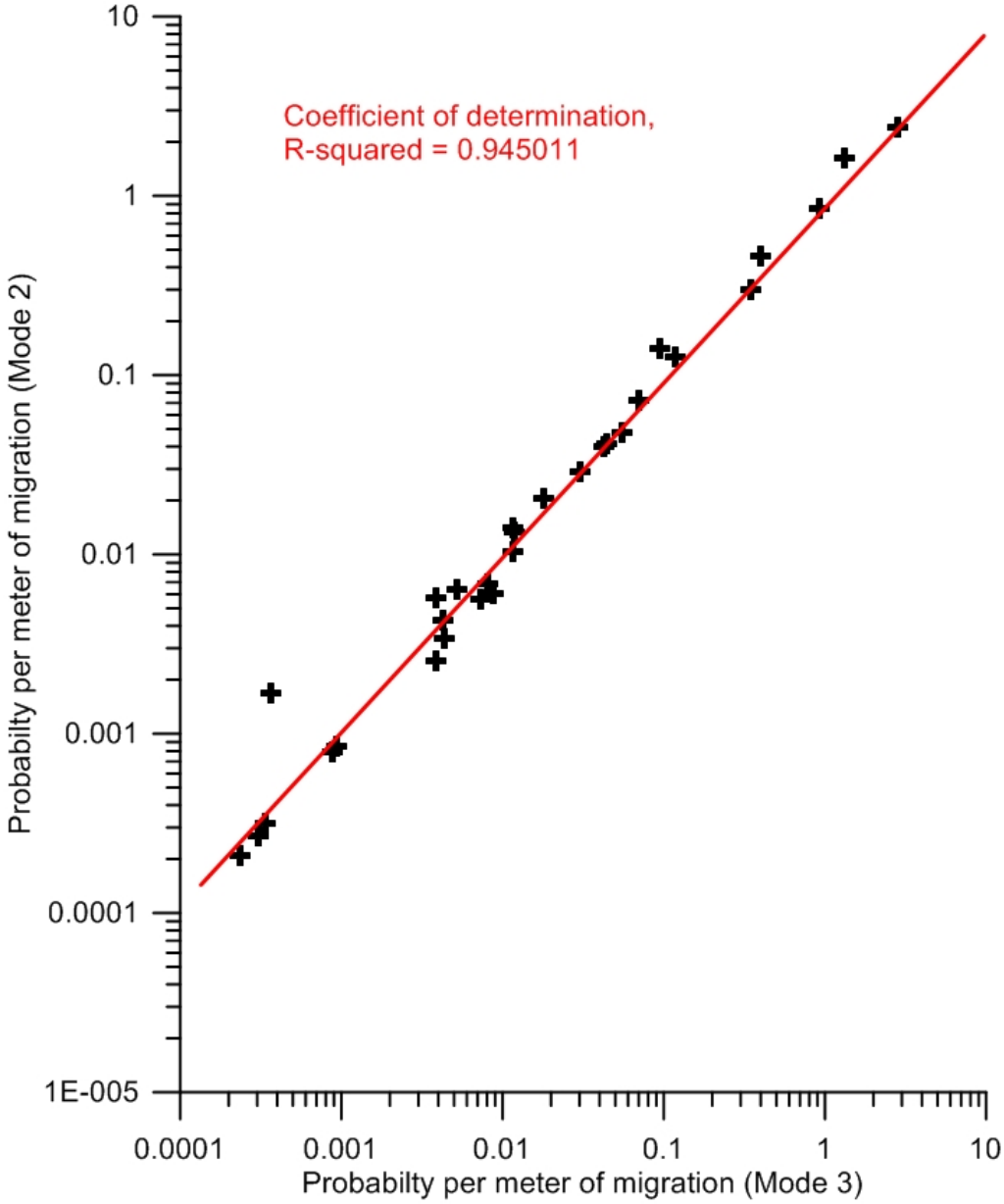

Figure 48. Regression analysis of Mode 2 versus Mode 3 predictions of UXO migration at Camp Perry, Lake Erie, OH, based on M344 106 mm rounds.

The low energy argument does not apply to the burial skill results in Figures 49 and 50. Here, probability per cm of burial at Lake Erie is on par with those values found at Duck, NC. The coefficient of determination for Mode 1 burial estimates at Lake Erie is *R-squared* = 0.947 (Figure 49), while Mode 2 gave *R-squared* = 0.986. The project team believes the lower Mode burial predictions did so well at Lake Erie because the stabilizer fins of the Army rounds cause vigorous scour burial (Figure 42) and the Mode 1 critical mass gave a fairly accurate assessment of the exposures of the buried UXO populations.

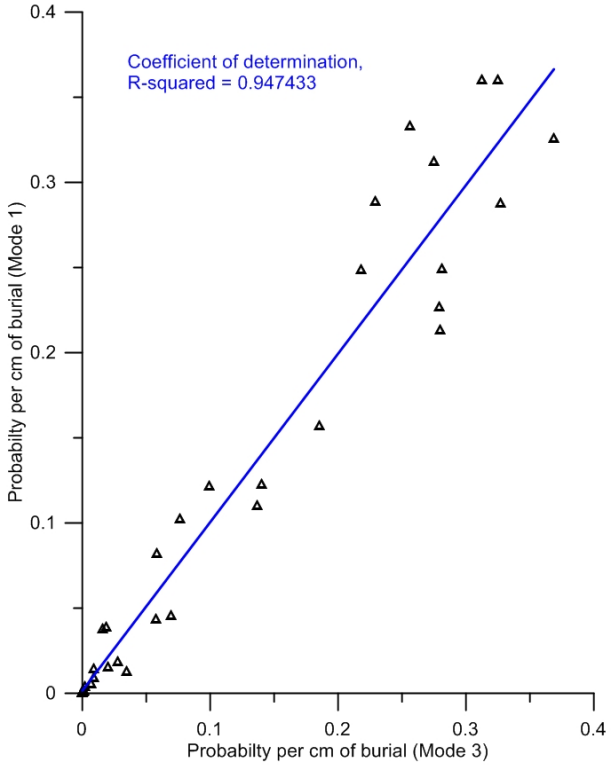

Figure 49. Regression analysis of Mode 1 versus Mode 3 predictions of UXO burial at Camp Perry, Lake Erie, OH, based on M344 106 mm rounds.

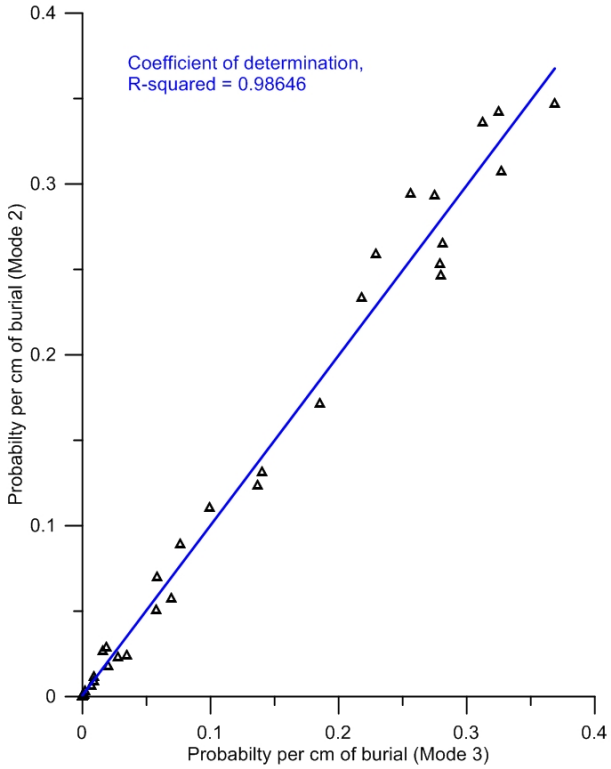

Figure 50. Regression analysis of Mode 1 versus Mode 3 predictions of UXO burial at Camp Perry, Lake Erie, OH, based on M344 106 mm rounds.

8.0 COST ASSESSMENT

8.1 COST MODEL

Per the Federal Remediation Technologies Roundtable (FRTR) *Guide to Documenting and Managing Cost and Performance Information for Remediation Projects (EPA 542B 98-007, Oct 98*), "the total cost for an application should not include other project phases/activities, such as preliminary assessment/site investigation, remedial investigation/feasibility study, remedial design, or post-closure surveillance and long-term monitoring." Since the UXO MM is a basic tool to support all of the "other project phases/activities," the cost structure of this section will not include most of the items in the standard format that pertain to the actual remediation process.

The operational costs of using the UXO IMM and associated IM are substantially less than the costs that were required to develop and validate the two models. The primary cost elements for using the UXO IMM, in generally descending order, are:

- Data acquisition (climatology, bathymetry, seafloor conditions, human use activities, UXO history and distribution). The costs can be minimal if the site is already well documented, but can be as much as several hundred thousand dollars for each small site if in situ surveys are required.
- Data formatting and processing for use (gridding bathymetry, deriving UXO population – can be as much as a few months of labor).
- UXO IMM computer operations (typically less than a few weeks of labor).
- Report development.
- Customer liaison.

The UXO IMM is applied in steps (Mode 1, 2, 3 as required), therefore, the total cost of using the UXO IMM is controlled by the level of detail required, and by the site-specific results obtained as the analysis proceeds. The actual costs of the UXO IMM development and validation are provided on the next page for reference. Example estimates of costs for various levels of site analysis are then provided.

The Navy program that developed the UXO MM and provided the initial limited validation started in December 2002, and concluded in December 2005. The entire ESTCP UXO MM validation program started in June 2004, and concluded in June 2008. The program spanned 5 years and the total expenditure was approximately $1,795,750. The ESTCP investment was approximately $1,278,000.

Table 6 summarizes the program costs. The investment was divided between the UXO IMM development work (28%) and the field validation effort (72%).

Table 6. UXO MM program cost summary.

	Navy	ESTCP	Total
Mobility Model Development			**$498,375**
FY02-FY04	$143,375		
FY05-FY08		$355,000	
Mobility Model Validation			**$1,297,375**
Pt. Mugu Test	$119,188		
Measurement Method Field Test	$255,188		
FRF Duck, NC Demonstration		$404,320	
PMRF Kauai, HI, Demonstration		$433,320	
Example Application Analysis		$85,360	
	$517,750	$1,278,000	$1,795,750

FY=fiscal year

8.2 COST DRIVERS

As discussed above, the main cost drivers on the use of the UXO IMM are the acquisition and processing of the environmental data required as inputs to the models. The best way to illustrate the range of those costs is by example.

The costs to apply the UXO IMM at full-scale sites are separated into three phases of analysis. The detailed process of applying the UXO IMM to a full-scale site is described in Wilson et al. (2008e).

Mode 1 Screening Analysis

The first phase uses only Mode 1 of the UXO IMM. All of the inputs for this phase are composed of existing data available from a "desk-top" study. Default values are used for many of the UXO IMM inputs, based on the general coastal type. The primary purpose of the Mode 1 analysis is to determine areas that are *not* at risk of human exposure to UXO. Therefore, these are areas where either (a) there are no UXO of concern; or (b) the UXO is permanently entombed—buried at depths below any known or forecast human activities (i.e., fishing, dredging, etc.). The term "permanently" is limited by the worst-case storm activity ever recorded or forecast for the site. Table 7 shows an example cost estimate for a basic Mode 1 screening analysis of a typical UXO "site."

Table 7. Nominal cost of Mode 1 screening analysis of a single UXO site.

Mode 1 Screening Analysis	Cost ($)
Initial contact, problem definition, liaison	20,000
Preliminary screening (set up ARCGIS, plot areas of use, define closure depth)	20,000
Mode 1 analysis of UXO movement at selected points in risk areas (no Model modifications)	30,000
Preliminary analysis of risk of human interaction	8000
Initial report and recommendations	8000
Program management	10,000
Mode 1 Total	**96,000**

The assumptions made in this cost estimate are as follows:

- UXO site manager liaison is provided via NAVFAC;
- Analysis performed by support contractors (e.g., engineers/computer analysts);
- UXO site managers have Mode 1 level data available, including:
  - general estimate of history of UXO type and distribution;
  - basic bathymetry (NOAA charts or past local surveys);
  - defined areas of responsibility (boundaries);
  - summary of type and location of human use (e.g., fishing, recreation, dredge, etc.);
- Initial analysis performed without travel (no site visits);
- Baseline "site" is a single section of coastline (e.g., small bay, offshore from firing range, etc.); and
- Duration of Mode 1 phase is approximately 3-6 months.

Note that the word, "site," in this context refers to a relatively small, contiguous area of UXO with dimensions on the order of a few kilometers, such as a small bay, firing range, etc. Estimates for larger "sites" such as an entire island, or a major coastline, etc., are developed as multiples of single sites.

Unless either (a) the desktop data for the Mode 1 are unusually complete and detailed, or (b) the Mode 1 analysis clearly shows that even conservative estimates place virtually all the UXO at the site at very low risk of human interaction, it will be necessary to conduct a more detailed analysis, using additional site-specific data inputs (Mode 2).

Mode 2 Detailed Analysis

The Mode 2 analysis is only conducted on those parts of the site that are not clearly shown to be low risk by the Mode 1 analysis. Mode 2 requires input data for the local environmental conditions that are not normally available for UXO sites. However, the Mode 2 analysis does not involve any direct surveys of the UXO distribution itself. The assumptions for the Mode 2 Detailed Analysis phase are as follows:

- Mode 1 was previously completed;
- UXO site manager liaison is provided via NAVFAC;
- Analysis performed by support contractors (e.g., engineers/computer analysts);
- Environmental site surveys required (though a UXO survey is not):
  - bathymetry (LIDAR or multibeam backscatter [MBBS] for details of depth at 2-5m spacing, less than 1 m resolution);
  - bottom samples to determine sediment properties;
  - on-site wave measurements are necessary to refine the REF/DIF model;

- on-site human use surveys are conducted to obtain fishing data, etc;
- Climate and human use studies cover one annual cycle; and
- Mode 2 phase lasts about 18 months after Mode 1.

Mode 2 will likely meet the analysis needs for most sites.

The costs to apply the UXO IMM at full-scale sites varies considerably with the size and location of the site (e.g., area to be modeled, cost of data to be collected), complexity of the bathymetry, level of human use, etc. The size of UXO sites ranges from as little as a square kilometer to the offshore area of Camp Perry on Lake Erie, about 150 km^2 (Figure 17). This area could be surveyed in a single day by aircraft at approximately $50,000 per day, plus mobilization costs. The subsequent post-processing of the data costs approximately $1000/$km^2$. Therefore, the total price for LIDAR survey of typical UXO sites range from about $90,000 for Impact Area 1 to as much as ≈ $310,000 for the entire far field of southwestern Lake Erie around Camp Perry. For an example mid-sized site, the estimated cost is shown in Table 8. Note again that the dominant costs are associated with the site surveys.

Table 8. Estimated Cost of Mode 2 detailed analysis.

Mode 2 Detailed Analysis	Cost
Detailed Mode 2 phase program plan	10,000
Bathymetry survey (LIDAR or MBBS)	200,000
On-site sediment sampling and ADCP (four seasons)	95,000
Human use surveys (fishing, boating, diving, etc.	30,000
Update Mode 1 ARCGIS and data sets	15,000
Mode 2 Analysis of UXO movement at selected points in risk areas.	50,000
Updated analysis of risk of human interaction	12,000
Mode 2 report	12,000
Program management	35,000
Total	**459,000**

Mode 3 Enhanced Analysis

Mode 3 adds the final input detail of enhanced estimates of the UXO initial distribution. Since obtaining this type of information is the most expensive, and potentially dangerous data to collect, it is only added to the process when the desk-top data on UXO distributions are not credible due to such issues as age, inconsistencies, and either (a) clear evidence exists of substantial risk of human interaction, or (b) large-scale UXO movements are predicted that require more accurate estimates. The development of enhanced UXO distribution estimates involves several possible technologies and considerable on-site effort and cost. It begins with additional analysis of historical data to convert recorded UXO entry (e.g., air drops, gunnery, etc.) into expected impact with the seafloor and initial burial. These data are matched against more refined on-site surveys of the seafloor itself to locate and identify UXO that are not entirely buried. The final step is to locate buried UXO using sub-bottom profilers, magnetometers, diver, checks, etc.

The assumptions for a Mode 3 enhanced analysis cost estimate are as follows:

- Mode 1 and 2 were previously completed;
- Mode 3 is only used for cases of high risk, or if UXO data are questionable;
- UXO site manager liaison is provided via NAVFAC;
- Analysis performed by support contractors (e.g., engineers/computer analysts);
- Mixture of means used to develop UXO distribution baseline:
  - impact analysis (historical firing records and physics of impact);
  - analysis of previous bottom imagery to detect surface UXO;
  - new visual searches of seafloor (e.g., ROV, towed fish, divers);
  - new acoustic surveys (e.g., imagery, sub-bottom);
  - magnetometer surveys;
- Costs vary considerably with size and location of site and type of UXO; and
- Mode 3 phase spans approximately 12 months beyond Mode 2 phase (6 months survey, 6 months analysis).

Table 9 shows an example estimate of the costs of this additional Mode 3 Enhanced Analysis phase.

Table 9. Mode 3 Enhanced Analysis Cost Estimate.

Mode 3 Detailed Analysis	Cost
Detailed Mode 3 phase program plan	5000
Impact analysis (historical firing records plus physics of impact)	8000
Analysis of previous bottom imagery (for surface UXO)	10,000
New visual searches of seafloor (ROV, towed fish, divers)	200,000
New acoustic surveys (imagery, sub-bottom)	200,000
Magnetometer surveys	50,000
Run Mode 3 simulations (updates Mode 2 results at key points). Estimate half-life of UXO survey data versus remediation schedule	30,000
Updated analysis of risk of human interaction	12,000
Mode 3 report	12,000
Program management	50,000
Total	**577,000**

8.3 COST BENEFIT

No other available computer models exist where the UXO IMM can be compared to determine competitiveness. The most instructive comparison is the cost of applying the UXO IMM versus the potential savings in remediation efforts.

In any event, the cost of using the UXO IMM to define areas of high risk will be small compared to alternative approaches such as sweeping the total area of possible UXO contamination, which can easily cost many tens of millions of dollars per site. As of this report, the UXO IMM is also the only tool that allows credible analysis of sites to be conducted to verify that risk either is already at an acceptably low level, and therefore does not require comprehensive clean up costs; or, to set

the depth and area of cleanup so that it covers the entire risk area and avoids the need to sweep the area again later, if adjacent UXO migrate into the swept area after cleanup. Also, analysis at the Mode 1 level reduces the need for Mode 2 data collection, and, in turn, Mode 2 reduces need for Mode 3 to be conducted.

One way to quantify the value and compare the cost of using the UXO IMM is to estimate the Return on Investment (ROI). That is, compare the cost savings produced by the UXO IMM, less the investment costs, as a fraction of the investment costs. The equation for ROI is:

$$\text{ROI} = (\text{Savings} - \text{Investment})/\text{Investment}$$

An ROI of 0 is the break-even point where the savings equals the investment.

Of course there are other non-economic benefits associated with using the UXO IMM, such as reducing risk, demonstrating good faith efforts, etc. However, this analysis solely focuses on cost benefits.

The primary cost benefit from the UXO MM is to reduce the size of the area requiring cleanup and remediation. The UXO IMM shows where UXO are permanently entombed deeper than any human interaction will occur. It also provides the limits of UXO movement, so it bounds the need for "preventative" clearance measures.

The actual ROI depends heavily on the derived percent reduction in required cleanup, which will not be known until the UXO IMM is applied to specific sites. However, it is possible to bound the ROI.

For example, in 2004, the approximation of "best-possible" ROI was determined as follows:

- The estimated cost to clean up three major underwater UXO sites (Mare Island, Vieques, Kaho'olawe) was ≈ $2,764M.
- The estimated cost of the UXO MM development and validation program was $1.32M (note that no estimates for operational use were available at that time).
- If the UXO IMM program showed that no cleanup was required at those three sites, which is unlikely, but a "best case" scenario, the ROI would then be equivalent to

$$\frac{(\$2764 - \$1.32)}{\$1.32} = 2092$$

This value translates into savings that are 2092 times the cost of using the UXO IMM—a significant ROI.

Now that the development program is concluded, it is possible to develop a more realistic estimate of the ROI.

- First, there is now a better estimate of the cost to use the UXO IMM. A Mode 1 screening analysis can be performed for a single site for approximately $200k. However, if detailed

in situ surveys of the UXO baseline population are required, it could cost as much as $1M per site. These two estimates range from $0.6M (minimum) to $3.0M (maximum) for the three sites. Also, the cost correction for inflation makes the three-site total cleanup cost equal to ≈ $3,233M.

- Second, the analysis can consider the example sites and how much cleanup area might actually be reduced by using the UXO IMM analysis to better estimate of savings.
- As a final step, the minimum amount of cleanup reduction required to equal the future investment costs, the break-even point, can be determined.

Note that the $1.5M development costs are sunk and not part ROI for future investments.

For the updated "best case" scenario (parallels the 2004 approach),

$$ROI = (\$3233M - \$3M)/\$3M = 1077$$

which translates into savings = 1077 x UXO IMM use costs.

This page left blank intentionally.

9.0 IMPLEMENTATION ISSUES

Beach clearances of UXO were conducted along the 5 km of FUDS Beach at Camp Perry in 1992 (EOD, 1992) and again in 2002 (American Technologies, 2002). UXO were also cleared from the Toussaint River channel during the dredge demonstration project in 1998 (Welp et al., 1998). After all these clearance exercises, anecdotal reports of UXO reappearing in the cleared areas still occurred. These reports are contrary to the observational data of UXO movement from the 2001-2003 ordnance migrations studies (Welp, et al., 2004) and the results of the model simulations studies herein find that the UXO at Camp Perry simply do not move much further than their own length. The notional argument is that UXO reappear on the beach by being transported onshore after storms. However, the project team will use the far-field mechanisms of the UXO IMM to provide more likely explanations for the reappearance of UXO, which involve lake water level variations and shoreline retreat. These mechanisms are entirely consistent with the observational data and are based on two large scale characteristics of the western basin of Lake Erie and the Toussaint River/FUDS Beach Littoral Cell.

It is true that neither the 1992 nor the 2002 clearance exercises went sufficiently far off shore to reach closure depth, and thus un-cleared ordnance still exists offshore at depths where profile changes can re-expose these items. The 1992 exercise cleared to a depth of -2 ft LWD and the 2003 exercise cleared to a depth of -3 ft LWD; whereas closure depth is at -3.35 m (-11.0 ft) LWD. Consequently, at low lake water levels, these un-cleared areas may be subject to wave erosion and exposure of the UXO. However, high lake water levels may have an even greater effect, particularly when it comes to exposing formerly buried UXO on the higher portions of the beach profile that are subject to wetting and drying by wave run-up and where people generally traffic the beach. Figure 51 shows how the equilibrium cycloids of the FUDS Beach profile at Range line #10579 would readjust to a rise in lake water level as occurred in 1997 and in 1998. While closure depth adjusts upward to higher elevations in response to a lake water level rise, the equilibrium profiles re-adjust both upward and landward, cutting into the barrier beach ridge and possibly exposing UXO buried by impact in the former back-beach regions. In essence, a rise in lake water level shifts the critical mass landward and to higher elevations, allowing waves to erode areas not subjected to prior erosion; thereby exposing some of the more deeply buried UXO. Unlike the action of high tides, high lake levels can persist for many months, thereby increasing the duration of wave erosion in back-beach areas formerly un-worked by waves, and increasing the likelihood of large storm waves occurring concurrent with those high water levels. Sometimes this concurrent action results in over-wash and breaching of the barrier beach, potentially exposing additional UXO. While beach clearances have worked these back beach areas, the critical mass thickness can increase to several meters once the equilibrium bar-berm profile fully recedes landward with the high water crest (Figure 51). Consequently, deeply buried UXO that were possibly undetected by prior beach clearance activity may be exposed. The appealing aspect of the high water level theory is that it does not require heavy immobile UXO with fins to roll upslope and onshore in order to appear on the beach; but rather broad scale changes in the equilibrium beach profiles in response to high lake water levels will dig up some of the more deeply impacted UXO in regions of the beach and shoreline that normally (or only rarely) do not erode. By the latter explanation, the UXO did not move onto the beach, but rather they were always there, just buried.

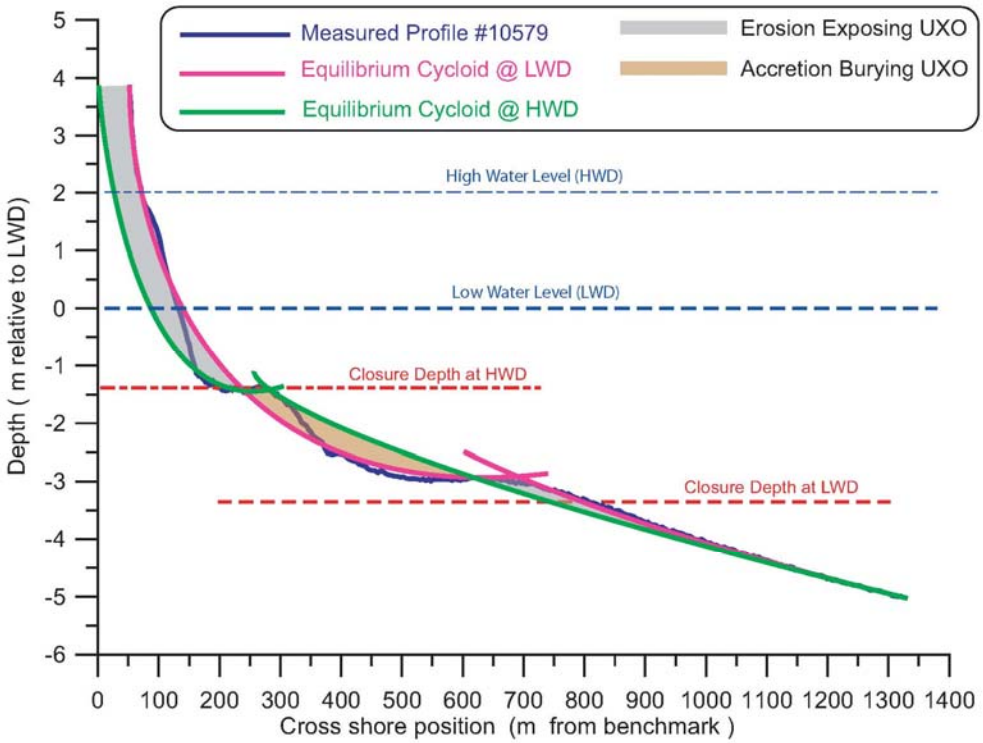

Figure 51. Beach profile change due to lake water level variation, Camp Perry FUDS Beach, based on low water survey at Range-line 10579, June 1990.
Vertical elevation shown in meters relative to the LWD at about 174 m msl.

The second explanation for the reappearance of UXO on FUDS Beach is somewhat similar to the high water level theory but involves long term shoreline retreat (Figure 52). It is an historic fact that the shoreline south east of the Toussaint River has been progressively retreating landward since at least 1877 (Pope et al., 1996). Here the shoreline has experienced long-term recession rates, ranging from as little as 0.27 m/year (0.9 ft/year) on the updrift side of the stone stick-out feature located near the Camp Perry border at profile range line #10625 (Figure 53), to as much as 1.1 m/year (3.6 ft/year) at profile range line #10695. The average retreat rate for the study area is between 0.61 and 0.91 m/year (2 and 3 ft/year), or a total of 68.9 to 103.3 m (226 to 339 ft) since 1877 (cf. USGS, Ohio Division, 1993).

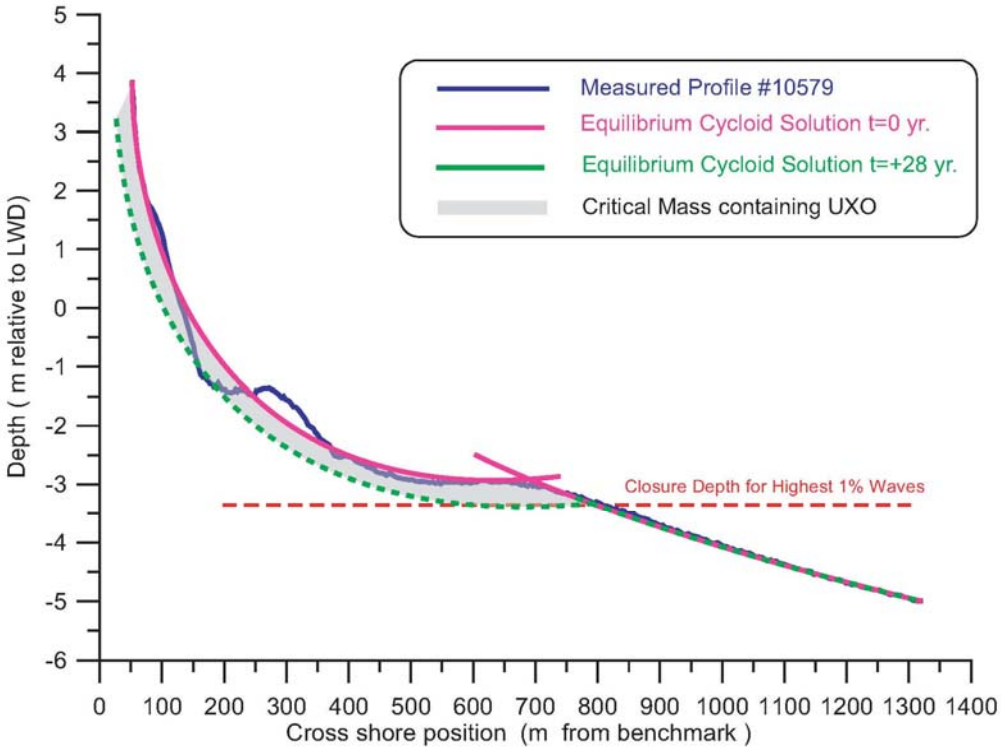

Figure 52. Beach Profile recession (green-dashed) computed by far-field mechanics of UXO IMM over 28 year period at Camp Perry FUDS Beach, Range-line 10579.
Measured profile (blue) from June 1990, used as initial profile for best fit cycloid at t=0 (red). UXO impact burial in shaded area subject to re-exposure.

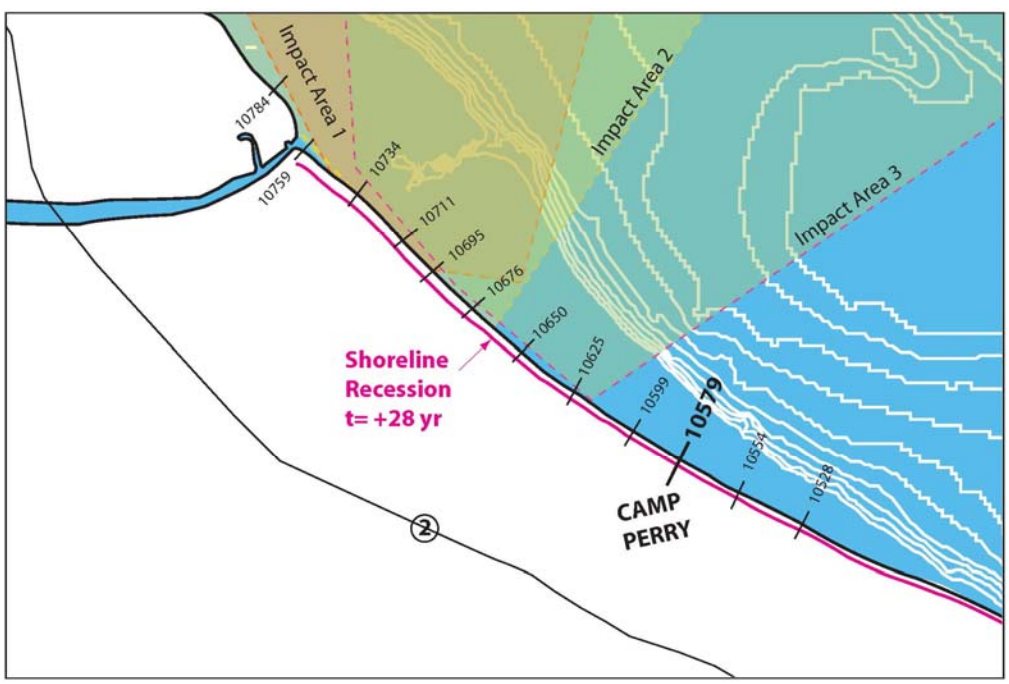

Figure 53. Shoreline recession computed at Camp Perry (FUDS Beach) from 28 years of wave forcing (Figures 27 and 28) using far-field module of the UXO IMM.

The cause of the historic shoreline recession is twofold. One mechanism involved is the systematic negative divergence of drift along the reach of coast between the Toussaint River and Camp Perry, as a consequence of arrangement of shadows and bright spots in the REF/DIF pattern. This wave shoaling pattern is set up by the sheltering effects of the offshore island complexes, and causes longshore currents flowing out of the Toussaint River/FUDS Beach Littoral Cell toward the south east to be stronger than those flowing into the cell from the northwest, resulting in a net outflow of littoral sediment from the cell. That net outflow occurs at the expense of the sand supply stored in the FUDS Beach barrier system. The other causal mechanism for FUDS Beach recession is a lack of sand inflow from the Toussaint River updrift of the beach. The dredged channel at the Toussaint River, with its adjacent sand shoal functions as a sediment trap to littoral drift that would otherwise proceed downcoast and replace the sands that are eroded from the FUDS Beach barrier system to feed the negative divergence of drift. This situation is a classic sediment budget problem that the coupled control cell architecture of the far-field modules in the VORTEX model are well suited to handle (Jenkins et al., 2007).

Figure 52 shows the landward shift in the cycloid solutions for the beach profile at Camp Perry computed by the VORTEX model for 28 years of shoreline recession at constant lake water level, as forced by the shoaling patterns of the historic wave record from Figure 27. The profile shift in Figure 52 does not conserve sediment mass, unlike that for the lake water level rise in Figure 51. In Figure 51, areas of erosion that expose UXO (gray shaded areas) are balanced by adjacent areas of accretion that bury UXO (brown shaded areas). Instead, in Figures 52 and 53, the beach sediment mass is progressively diminished at a rate equal to the net (negative) flux in the divergence of the drift inside the control cell for FUDS Beach. The rate of change of volume flux through the control cell, q, causes the equilibrium profile to shift landward in time (recession), $\Delta x(t)$, as:

$$\Delta x(t) = \frac{1}{\Delta y(Z_1 + h_c)} \int \left(\frac{\partial}{\partial y}\left(\varepsilon \frac{\partial q}{\partial y}\right) - V \frac{\partial q}{\partial y} + J(t) \right) dt \tag{12}$$

where γ now is the mass diffusivity, V is the longshore drift computed from longshore variations in wave height from the REF/DIF analysis, J is the flux of sediment from river sources, Δy is the alongshore length of the control cell, h_c is the closure depth, and Z_1 is the maximum run-up elevation from Hunt's formula (Jenkins and Inman, 2006). Sediment yield from the Toussaint River, J, is calculated from streamflow, Q, based on the power law formulation of that river's sediment rating curve (Welp and Clausner, 1998):

$$J = \gamma Q^{\omega} \tag{13}$$

where γ, ω are empirically derived power law coefficients of the sediment rating curve from best fit (regression) analysis (Jenkins and Inman, 2006). Application of Equation 12 to the position of the equilibrium cycloids produces the receded beach profile indicated in green after 28 years of wave forcing shown in Figure 52. The model result finds the profile at range #10579 recedes at a rate of about 1 m/yr, consistent with the survey literature (Pope et al., 1996; USGS, 1993; Benson, 1998). The receded shoreline position computed by the model after 28 years of wave forcing is shown in red on Figure 53. The recession at other range lines indicated is also comparable to aerial photo observations in Pope et al. (1996). While the closure depth does not change with progressive

shoreline retreat, the critical mass progressively grows at an average annual rate of $dV_c/dt = 19.6\ m^3$ per meter of beach per year. A UXO population density of 1 round per 100 m^3 implies that progressive shoreline recession at Camp Perry will expose about 1 new round every 5 years per meter of beach. Along the 5 km reach of FUDS Beach, shoreline recession would therefore expose about 980 rounds per year (both above and below the waterline) in the 700 m wide near-shore zone between closure depth and the berm crest, or about 27,000 rounds over the entire 28 year-long simulation. Along the 5 km reach of FUDS Beach, shoreline recession would expose about 980 rounds per year (both above and below the waterline), or about 27,000 rounds over the entire 28 year-long simulation. Thus, about one-quarter of the 98,613 rounds predicted to become exposed in 28 years by the UXO IMM simulation are due to shoreline retreat. The fundamental distinction here, however, is that shoreline retreat is progressive, not episodic like extreme storm events or lake water level variation and not periodic like seasonal beach profile variation. Therefore, those 980 rounds per year exposed by shoreline retreat are new rounds, not previously subjected to visual detection or beach clean-up. That number will continue to grow over time until shoreline recession exhumes all of the deepest impact burials.

This page left blank intentionally.

10.0 REFERENCES

Ahmad, M., et al., 2011. "The critical shear stress for sand and mud mixture," *Appl. Math., Sc.*, vol 5, no. 2, pp 53-71.

Allen, J., 1984. *Sedimentary Structures, Their Character and Physical Basis*. Amsterdam: Elsevier.

American Technologies, Inc., 2002. "Draft Site Specific Final Report, Time Critical Ordnance and Explosive (OE) Removal Action Former Erie Army Depot (Beach Area), Carroll Township, Ohio," prepared for U.S. Army Corps of Engineers, Louisville District, American Technologies, Inc., Task Order 0002, 30 September 2002.

Assel, R.A. and J.M. Ratkos, 1991. A computer tutorial and animation of the normal ice cycle of the Laurentian Great Lakes of North America for 1960-1979. NOAA Technical Memorandum ERL GLERL-76, Great Lakes Environmental Research Laboratory, Ann Arbor, MI (PB92-129949/XAB), 31 pp.

Baj, S., 2008. "Camp Perry Firing Logs," U.S. Army Corps of Engineers, Buffalo District, 64 pp.

Bagnold, R.A., 1956. "The flow of cohesionless grains in fluids," *Philos. Trans. R. Soc. London Ser. A*, 249(964), 235-297, 1956.

Bagnold, R.A., 1963. "Mechanics of marine sedimentation," In *The Sea, Ideas and Observations on Progress in the Study of the Seas, vol. 3, The Earth Beneath the Sea, History*, edited by M.N. Hill, pp. 507-528, Wiley, New York, 1963.

Batchelor, G.K., 1970. *An Introduction to Fluid Mechanics*. Cambridge: Cambridge University Press.

Bennet, J.R., 1974. *On the dynamics of wind-driven lake dynamics*. J. Phys. Oceanogr. 4, 400-414.

Benson, D.J., Unpublished report. "Lake Erie Shore Erosion and Flooding, Ottawa County, Ohio." Ohio, Division of Geological Survey.

Bolsenga, S.J., G.M. Green, and K.M. Hinkel, 1988. Nearshore Great Lakes ice statistics.

Bowen, A.J., 1980. "Simple models of nearshore sedimentation: beach profiles and longshore bars," in *The Coastline of Canada: Littoral Processes and Shore Morphology*, Paper 80-10, edited by S.B. McCann, pp. 1-11, Geologic Survey of Canada, Ottawa, Ontario,1980.

Boyd, H.F., 1989. "Detailed Project Report and Environmental Assessment of Proposed Navigation Improvements at the Mouth of the Toussaint River," Army Corps of Engineers, Buffalo District, Corps of Engineers, 23 pp, plus appendices.

Burt, W., M.C. Powers, and D.W. Pritchard, 1952. "Operation Mud – Results of Studies of Mine Penetration in the York River," Chesapeake Bay Institute: Johns Hopkins University, Ref. No. 52-25.

Coastal Data Iinformation Program, 2013. "Coastal data information program," http://cdip.ucsd.edu/.

Collins, T.J., 1980. "Investigating bridge scour," *Railway Track and Structure*.

Chiew, Y. and B.W. Melville, 1987. "Local scour around bridge piers," *J. Hydraulic Res*, vol. 25, pp. 15-26, 1987.

Chu, P.C., A.F. Gilles, C. Fan, and P. Fleischer, 2002. "Hydrodynamics of Falling Mine in Water Column," *J. Counter-Ordnance Tech. (5th Int. Symposium on Tech. and Mine Problem)*, pp. 100-108, 2002. Available: http://www.demine.org/SCOT/Papers/pdfpapers.html.

Chu, P.C., J.M. Bushnell, and K.P. Watson, 2010. "Tail Separation and Surface Impact Effects on the Underwater Trajectory of the JDAM." *9th International Symposium on Technology and Mine Problem*, NPS, Monterey, California, 17-20 May 2010, 10 pp.

Chu, P.C., 2009. "Mine impact burial prediction from one to three dimensions." *ASME Appl. Mech. Rev.*, 62 (1), 010802 (25 pages), DOI: 1115/1.3013823.

Chu, P.C. and C.W. Fan, 2007. "Mine impact burial model (IMPACT35) verification and improvement using sediment bearing factor method." *IEEE J. Ocean. Eng.*, 32 (1), pp. 34-48.

Chu, P.C., and G. Ray, 2006. "Prediction of High Speed Rigid Body Maneuvering in Air-Water Sediment Columns," *Adv. Fluid Mech.*, Vol 6, pp. 123-132.

Dalrymple, R.A., et al., 1984. "Wave diffraction due to areas of energy dissipation," *J. Waterway Port, Coast, and Ocean Engineering*, vol. 110, p. 67-79, 1984.

DeWillie, G.R., 2000. "Finding of no Significant Impact and Environmental Assessment, Operations and Maintenance (Channel Dredging and Side-Casting) Toussaint River, Ottawa County, Ohio," U.S. Army Corps of Engineers, Buffalo District, Corps of Engineers, 3 pp, plus appendices.

DeVisser, A., 2004. "Environmental Security Technology Certification Program (ESTCP) Demonstration Plan 200417 Predicting the Mobility and Burial of Underwater Unexploded Ordnance (UXO) using the Modified VORTEX Model," October 2004 through April 2006, 16 November 2004.

Dill, R., 1958. "The Burial and Scouring of Ground Mines on a Sandy Bottom," San Diego, CA: U. S. Navy Electronics Laboratory, Research Report NEL 861.

Donohue, J., and L.E. Garrison, 1954. "An Evaluation of Mine Behavior Observations in Four Test Areas," Narragansett Marine Laboratory: Univ. Rhode Island, Reference 54-13, 1954.

EOD Technology, Inc., 1992. "Draft Final Report for the Interim Removal Action of UXO at the Former U.S. Army Erie Ordnance Depot, Ohio," EOD Technology, Inc., Oak Ridge, Tennessee, DACA87-92-D-0125 Delivery Order 0001, December.

Evans-Hamilton, Inc., 2003. "Final Data Report, Toussaint River Ordnance Mobility Study," U.S. Army Corps of Engineers Waterways Experiment Station Coastal and Hydraulics Lab, Evans-Hamilton, Inc. File: 7000 – 01, July.

Foxwell, D.,1991. "New technology Takes on the Sea Mine," Int. Defense Review, pp. 1097-99/1101-1102, Oct. 1991.

Frazier, D., and C.E. Miller, 1955. "Geological and Engineering Characteristics at Mine Behavior Test Sites," Narragansett Marine Laboratory: Univ. Rhode Island, Reference 55-16, 1955.

Fujisaki, A., J. Wang, H. Hu, D.J. Schwab, N. Hawley, and Y.R. Rao, 2012. A modeling study of ice–water processes for Lake Erie applying coupled ice-circulation models, Journal of Great Lakes Research, 38, p. 585–599.

Gallagher, E.L., S. Elgar, and R.T. Guza, 1998. "Observations of sand bar evolution on a natural beach," *J. Geophys. Res.*, 103(C2), 3203-3215.

Garrood, D., 2008. "UXO Mobility Model Users' Manual," NAVFAC ESC Technical Report, Revision 8.4, ESTCP 200417, 2 June 2008, 79pp.

Hale, J.S., 2009. "Stand-off Assault Breaching Weapon Fuze Improvement (SOABWFI) Underwater Trajectory Test - 1 (UTT-1)." Boeing Report, No. 09J0059, pp. 33.

Hardiman R., 1984. "Initial Appraisal Report on Improvements to Navigation at the Toussaint River in Carroll Township, OH," letter report to Department of the Army, Buffalo District, Corps of Engineers, 22 pp, plus appendices.

Havelock, T.H., 1940. "The pressure of water waves upon a fixed obstacle," *Proc. Roy. Soc. London*, Ser. A, vol. 175, p. 409-421, 1940.

Havelock, T.H., 1952. "The moment on a submerged solid of revolution moving horizontally," *Quarterly Journal of Mechanics and Applied Mathematics*, vol. 5, p. 129-136, 1952.

Humes, G., 2007. Technology Transition Agreement, EC SHD-FYO6-03 FNC Product: Standoff Assault Breaching Weapon Fuse Improvement.

Hunt, I., Jr., 1959. "Design of seawalls and breakwaters," *J. of Waterways, Harbors and Coastal Engineering Division*, 85, 123-152.

Inman, D.L. and A.J. Bowen, 1962. "Flume Experiments on Sand Transport by Waves and Currents," in *Proc. 8th Conf. on Coastal Engin.*, Council on Wave Research, Univ. of California, San Diego, pp. 137-150.

Inman, D.L. and T.K. Chamberlain, 1955. "Particle size distribution in nearshore sediments," Finding Ancient Shorelines: *Society of Economic Paleontologists and Mineralogists*, Special Publication 3, pp. 106-129.

Inman, D.L. M.H.S. Elwany, and S.A. Jenkins, 1993. "Shore-rise and Bar-Berm Profiles on Ocean Beaches," *J. Geophysical Res.* vol. 98, no. C10, pp. 18,181□18,199, Oct. Available: http://repositories.cdlib.org/sio/cmg/11/

Inman, D.L. and S.A. Jenkins, 1996. "A Chronology of Ground Mine Studies and Scour Modeling in the Vicinity of La Jolla," Scripps Institution of Oceanography: University of California, San Diego, SIO Reference Series 96-13.

Inman, D.L. and S.A. Jenkins, 1999. "Climate Change and the Episodicity of Sediment Flux of Small California Rivers," *J. Geology* vol. 107, no. 3, pp. 251-270, May 1999. Available: http://repositories.cdlib.org/sio/cmg/2/.

Inman, D.L., and S.A. Jenkins, 2002. "Scour and Burial of Bottom Mines, A Primer for Fleet Use," Scripps Institution of Oceanography: Univ. of California, San Diego, SIO Reference Series 02-8, 2002. Available: http://repositories.cdlib.org/sio/reference/02-8/

Inman, D.L., and S.A. Jenkins, 2005. "Accretion and Erosion Waves on Beaches," in *Encyclopedia of Coastal Science*, M. Schwartz, Ed. Dordrecht, Netherlands: Springer, pp. 1-4, 2005. Available: http://repositories.cdlib.org/sio/cmg/6/

Jarrah, D.H., 2001. "Predicting Underwater Corrosion Rates of Unexploded Ordnance (UXO) – Definition and Governing Parameters," NAVFAC ESC, Nov.

Jenkins, S.A. and D.L. Inman, 1985. "On a submerged sphere in a viscous fluid excited by small-amplitude periodic motions," *J. Fluid Mechanics* vol. 157, pp. 199-224.

Jenkins, S.A. and D.L. Inman, 2002. "Model for Mine Scour and Burial: An Illustrated Abstract with Technical Appendix," Scripps Institution of Oceanography: University of California, San Diego, SIO Reference Series 02-2.

Jenkins, S.A. and D.L. Inman, 2006. "Thermodynamic solutions for equilibrium beach profiles," *J. of Geophysical Res.* vol. 111, C02003, doi:10.1029/2005JC002899, 21 pp.

Jenkins, S.A. and J. Wasyl, 1990. "Resuspension of estuarial fine sediments by tethered wings," *J. Coastal Res.* vol. 6, no. 4, p. 961-980.

Jenkins, S.A. and J. Wasyl, 2005. "Model for Prediction and Updates for UXO Transport during MMFT 1 & 2, Ocean Shores, WA," submitted to Sound and Sea Technologies, 170 pp, December.

Jenkins, S.A. et al., 2007. "Scour and Burial Mechanics of Objects in the Nearshore," *IEEE Jour Oc Eng*, vol. 32, no. 1, pp78-90, Jan.

Jenkins, S.A. and J. Wasyl, 2007. "Model for Prediction of UXO Transport and Burial during Field Tests at PMRF, Kauai, HI," submitted to Sound and Sea Technologies, 48 pp, November.

Jenkins, S.A. and J. Wasyl, 2008. "Model for Prediction of UXO Transport and Burial during Field Tests at Field Research Facility (FRF), Duck, NC," submitted to Sound and Sea Technologies, 58 pp, January.

Johnson, C.J., B. Sugiyama, B. Wild, S. Lin, and A. Pedersen, 2002. "Environmental effects of underwater ordnance," Navy Internal Tech Report, SPAWAR, San Diego Code D362 and NAVFAC ESC Point Hueneme, EV45, January, 302 pp.

Jonsson, I. and N.A. Carlsen, 1976. "Experimental and Theoretical Investigations in an Oscillatory Turbulent Boundary Layer," *J. Hydraulic Res*, vol. 14, no. 1, pp. 45-60.

Kajiura, K., 1968. "A Model of the Bottom Boundary Layer in Water Waves," *Bull. of the Earthquake Res. Institute (Tokyo)*, vol. 46, pp. 75-123.

Kirby, J.T., 1986. "Higher-order approximations in the parabolic equation method for water-waves," *J. Geophysical Res.*, vol. 91, no. C1, p. 933-952.

Lamoure, J. and C.C. Mei, 1977. "Effects of horizontally 2-dimensional bodies on mass transport near sea bottom," *Journal of Fluid Mech.*, vol. 83, no. 3, pp. 415-433.

Liebeck, R.H., 1973. "A Class of Airfoils Designed for High Lift in Incompressible Flow." AIAA Paper No. 73-86, Jan. 1973; *J. Aircraft* vol. 10, Oct., pp. 610-17.

Longuet-Higgins, M.S., 1953. "Mass transport in water waves," *Phil. Trans.*, Ser. A, vol. 245, p. 535-581.

Longuet-Higgins, M.S., 1970. "Steady currents induced by oscillations around islands," *J. Fluid Mech.*. vol. 42, no. 4, p. 701-720.

McCormick, B., 1979. *Aerodynamics, Aeronautics, and Flight Mechanics*. New York: John Wiley and Sons.

McMaster, R., L.E. Garrison, and S.D. Hicks, 1955. "Marine Sedimentation Project; Mine Behavior Studies," Narragansett Marine Laboratory: Univ. Rhode Island, Reference 55-15.

Mulhearn, P., 1993. "Experiment on Mine Burial by Scour," Maribyrnong, Victoria 3032, Australia: Materials Research Laboratory, MRL-TN-632.

National Geophysical Data Center, 2008. http://www.ngdc.noaa.gov/mgg/gdas/gd_designagrid.html.

National Oceanic and Atmospheric Association (NOAA), 2008. National Data Buoy Center, http://www.ndbc.noaa.gov/station_page.php?station=45005.

NOAA, 2008. Lake Erie Current Water Levels, Great Lakes on Line, http://glakesonline.nos.noaa.gov/glin.shtml?station_info=9063085+Toledo,+OH.

NOAA TM ERL GLERL-69. Great Lakes Environmental Research Laboratory, 2205 Commonwealth, Ann Arbor, MI.

Naval Facilities Engineering Service Center, 2008. "Applications Guidance Document: Predicting the Mobility and Burial of Underwater Unexploded Ordnance (UXO) using the UXO Mobility Model," Naval Facilities Engineering Service Center, Ocean Engineering Division, OP51Port Hueneme CA, ESTCP Project 200417, Contract N62473-06-D-3005, 82pp.

Oceanographic and Atmospheric Master Library, 2004. Available: http://navy.ncdc.noaa.gov/products/oaml.html

Ohio Division of Geological Survey, 1993. "Lake Erie Erosion Hazard Area Preliminary baseline survey," September.

Peace, A. and N. Riley, 1983. "A Viscous Vortex Pair in Ground Effect," *J. Fluid Mech.* vol. 129, pp. 409-426, April.

Pettijohn, F. and P.E. Potter, 1964. *Atlas and Glossary of Primary Sedimentary Structures*. New York: Springer-Verlag.

Pope, J., et al., 1996. Beach and Underwater Occurrences of Ordnance at a Former Defense Site: Erie Army Depot, Ohio," U.S. Army Corps of Engineers, Waterways Experiment Station, 119 pp., plus appendices.

Pope, J., R.D. Lewis, and T. Welp, 1996. *"Beach and Underwater Occurrences of Ordnance at a Former Defense Site: Erie Army Depot, Ohio,"* U.S. Army Engineer Waterways Experiment Station, Vicksburg, MS.

Raudkivi, A., 1990. *Loose Boundary Hydraulics*. Oxford: Pergamon Press.

Reineck, H. and I.B. Singh, 1975. *Depositional Sedimentary Environments*. New York: Springer-Verlag.

Rennie, S.E., and A. Brandt, 2011. "Underwater Munitions Expert System to Predict Mobility and Burial," SERDP pre-proposal #12 MR02-005, 7 pp.

Safinus, S., M. Hossain, and M. Randolph, 2013. "Comparison of stress-strain behavior of carbonate and silicate sediments," *Proc. 18th International Conf. Soil Mech. and Geotech. Eng.*, Paris, pp 267- 270.

Science Applications International Corporation, 2006. "*The MTA UXO Survey and Target Recovery on Lake Erie at the Former Erie Army Depot*," ESTCP Project MM 2003-24, Jim R. McDonald.

Saylor, J.H. and G.S. Miller, 1987. Studies of large-scale currents in Lake Erie, 1979–80.J. Great Lakes Res. 13 (4), 487–514.

Smith, A.M.O., 1972. "Aerodynamics of High-Lift Airfoil Systems." AGARD CP 102.

Stauble, D.K., 1992. "Long-term profile morphodynamics: field research facility case history," U. S. Army Corps of Engineers: Coastal Engineering Research Center Technical Report CERC-92-7.

Stauble, D., 2002. "A review of the role of grain size in beach nourishment projects," U.S. Army Engineer Research and Development Center, Coastal and Hydraulics Laboratory.

Stratford, B.S., 1959. "The Prediction of Separation of the Turbulent Boundary Layer," *J. Fluid. Mech.*, Vol. 5, Jan. 1959, pp. 1-16.

Taylor, G.I., 1946. "Note on R.A. Bagnold's Empirical Formula for the Critical Water Motion Corresponding with the First Disturbance of Grains on a Flat Surface," *Proceedings of the Royal Society of London Series A*, vol. 187, no. 1008, pp. 16-18.

Toussaint River Investigation, 1999, Summary Report for Erie Ordnance Depot. Prepared by Rock Island Corps of Engineers for Huntsville Engineering and Support Center Corps of Engineers, 100 pp.

Tucker, L., 2003. "UXO clearance, Jackson Park, exNAD," April.

Tunstall, E.B. and D.L. Inman, 1975. "Vortex Generation by Oscillatory Flow over Rippled Surfaces," *J. Geophysical Res.*, vol. 80, no. 24, pp. 3475-3484, Aug.

United States Army Engineering and Support Center, 2009. "Ordnance and Explosives Program Fact Sheets," www.hnd.usace.army.mil/oew/factshts.

U.S. Coast Guard, 1977. Joint U.S. Coast Guard - Canadian Coast Guard guide to Great Lakes ice navigation. U.S. Coast Guard, Ninth District, 1240 East 9th Street, Cleveland, OH.

U.S. Environmental Protection Agency (U.S.EPA), 2000. Office of Solid Waste and Emergency Response, "Used or Fired Munitions and Unexploded Ordnance at Closed, Transferred, and Transferring Military Ranges - Interim Report and Analysis of EPA Survey Results," EPA 505-R-00-01, April.

United States Geological Survey, 2008. "National Water Information System: Web Interface," http://waterdata.usgs.gov/nwis/.

Van Dyke, M., 1964. "Lifting-Line Theory as a Singular-Perturbation Problem," *J. Applied Mathematics and Mechanics* vol. 28, pp. 90-102.

Van Dyke, M., 1975. *Perturbation Methods in Fluid Mechanics*. Stanford, CA: Parabolic, 271 pp.

Welp, T. and Clausner, J., 1998. *"Toussaint River Unexploded Ordnance (UXO) Demonstration Dredging Project,"* U.S. Army Engineer Waterways Experiment Station CHL-98-6, Vicksburg, MS, August.

Welp, T., et al., 2004. "Toussaint River, Ohio, Ordnance Migration Study," U.S. Army Corps of Engineers, Engineer Research and Development Center, 86 pp., plus appendices.

Wilson, J., 2004. *"UXO Migration Field Test Point Mugu Lagrangian Drifters FINAL REPORT,"* Sound and Sea Technology Report 04-13, 23 September.

Wilson, J.V. and S.A. Jenkins, 2005. "UXO Measurement Method Field Tests (MMFT1&2) and Mobility Model Modification FINAL REPORT," Sound and Sea Technology Report 05-07, 31 December.

Wilson, J.V., A. DeVisser, and B. Sugiyama, 2008a. "(ESTCP) 200417 Predicting the Mobility and Burial of Underwater Unexploded Ordnance (UXO) Using the UXO Mobility Model, FIELD TEST REPORT (FRF Duck, NC)," NAVFAC ESC Technical Report.

Wilson, J.V., A. DeVisser, and B. Sugiyama, 2008b. "(ESTCP) 200417 Predicting the Mobility and Burial of Underwater Unexploded Ordnance (UXO) Using the UXO Mobility Model, FIELD TEST REPORT (PMRF Barking Sands, Kauai, Hawaii)," NAVFAC ESC Technical Report.

Wilson, J.V., A. DeVisser, and B. Sugiyama, 2008c. "(ESTCP) 200417 Predicting the Mobility and Burial of Underwater Unexploded Ordnance (UXO) Using the UXO Mobility Model,FINAL REPORT," NAVFAC ESC Technical Report.

Wilson, J.V., A. DeVisser, and B. Sugiyama, 2008d. "(ESTCP) 200417 Predicting the Mobility and Burial of Underwater Unexploded Ordnance (UXO) Using the UXO Mobility Model, Cost & Performance Report," NAVFAC ESC Technical Report.

Wilson, J.V., A. DeVisser, and B. Sugiyama, 2008e. "TO-2008-09-16-T061, Example Applications Analysis Using the UXO Mobility Model: Lake Erie Impact Range Analysis, NAVFAC ESC Technical Report, 53 pp.

APPENDIX A

POINTS OF CONTACT

Point of Contact	Organization	Phone Fax E-Mail	Role In Project
Gerald D'Spain, Ph. D.	Marine Physical Laboratory Scripps Institution of Oceanography 291 Rosecrans Street San Diego, CA 92106	Phone: (858) 534-5517 Fax: (858) 534-5255 E-Mail: gdspain@ucsd.edu	Principal Scientist
Scott A. Jenkins, Ph. D.	Marine Physical Laboratory Scripps Institution of Oceanography 291 Rosecrans Street San Diego, CA 92106	Phone: (858) 822-4075 Fax: (858) 534-5255 E-Mail: sjenkins@ucsd.edu	Principal Research Engineer
Joseph Wasyl	Marine Physical Laboratory Scripps Institution of Oceanography 291 Rosecrans Street San Diego, CA 92106	Phone: (858) 534-5809 Fax: (858) 534-5255 E-Mail: jwasyl@ucsd.edu	Numerical Scientist Programmer

APPENDIX B

Health and Safety Plan (HASP)

No field work of any kind is required by this demonstration plan. The software modification / validation uses existing data.

ESTCP Office
4800 Mark Center Drive
Suite 17D08
Alexandria, VA 22350-3605

(571) 372-6565 (Phone)

E-mail: estcp@estcp.org
www.serdp-estcp.org